Bosque Soil Evaporation Monitoring and Modeling

Annual Report for Year 1

Dr. John Stormont, Principal Investigator
277-6063 jcstorm@unm.edu

Dr. Julie Coonrod, Principal Investigator
277-1988 jcoonrod@unm.edu

Enrique Farfan, Graduate Student

Dylan Harp, Graduate Student

Department of Civil Engineering
MSC01 1070
1 University of New Mexico
Albuquerque, NM 87131-0001
Fax: 277-1988

October18, 2004

EXECUTIVE SUMMARY

This project addresses the Research Area: Water Depletions and Hydrology, specifically, Task 1 – Quantify and evaluate losses from evaporation and evapotranspiration (ET). We have established field sites to measure/monitor soil evaporation at five sites along the middle Rio Grande. These locations represent different conditions with respect to soil type, water table depth as well as different combinations of sun/shade and cleared/mulched conditions. At these field sites, instrumentation has been installed to measure water content, suction and temperature between the water table and the ground surface. Measurements of surface temperature differences using infrared thermometry have also been initiated. During the first year of the project, the emphasis has been on establishing the field monitoring locations and developing the methodology for estimating evaporation rates from measured data. The evaporation estimates will be used to develop a spatially distributed model that will account for different water table depths, climate parameters, and soil type. It is anticipated that the combination of monitoring and modeling will assist decision makers in bosque restoration strategies.

INTRODUCTION AND BACKGROUND

This project involves monitoring soil water evaporation as a function of different conditions with respect to the distance to the water table, soil type, climatic conditions, river staging, shading, and surface mulch. These data will be used to develop a GIS-based predictive model that will be used to estimate soil water evaporation under different conditions along the Middle Rio Grande. This model may be useful as a river and bosque management tool. For example, clearing and thinning of bosque vegetation necessarily reduces the amount of shaded soil, and increases the exposure of the soil to wind. Thus, an increase in the amount of soil water evaporation is expected. Because surficial detritus and leaf litter effectively insulate the soil surface, removal of this material may also increase soil evaporation. The impact of such activities can be estimated from the results of this proposed effort.

This project has three broad objectives:

1. **Monitor soil water evaporative fluxes at various locations along the Middle Rio Grande Bosque.** We are monitoring soil water content, soil water potential and temperature data at five locations. These data will be used to interpret evaporative fluxes. Most of the locations coincide with sites at which evapotranspiration is being independently monitored, and provide conditions of variable soil types, distances to the ground water table, and surface conditions (shade and/or mulch). We will also utilize a rapid method for estimating soil evaporation based on infrared thermometry.

2. **Derive an empirical predictive model for soil water evaporation**. The field measurements will indicate how evaporation is affected by climate, soil type and layering, water table distance, and the surface condition. Our goal is to develop empirically based estimates of evaporation as a function of these key variables. As part of this process, we will utilize a numerical model of soil moisture movement in the unsaturated zone in connection with the atmosphere.

3. **Develop an integrated GIS-based model for estimating soil water evaporation**. The GIS model will incorporate our predictive model with inputs regarding spatial and temporal

variability of climate, river staging, and soil types to derive a map of the estimated soil water evaporation along the Middle Rio Grande.

We are employing soil water flux measurements and surface temperature measurements for interpreting soil water evaporation. The soil flux measurements involve measuring water content and soil water potential at various depths within the soil and relating these values to soil water fluxes. Soil water potential measurements provide the hydraulic gradient with depth that will indicate which direction the water is moving (up, down, or equilibrium). The water content measurements are used to estimate the net flux between soil water potential measurement locations as well as to estimate the hydraulic conductivity of the soil as a function of depth. For steady-state conditions, the evaporative flux can be determined directly from the constant soil water flux. The method can also be applied to non-steady evaporation by monitoring the upward water flux within the soil as a function of position and time.

The method for estimating evaporation from surface temperature measurements can be considered as a simple energy balance method on a small-scale. All other factors being equal, a wetter soil will have a lower temperature during the day compared to a drier soil because evaporation of soil water consumes some of the net radiation at the surface. This method requires the measurement of the surface temperature of a dried soil, a fully wetted soil and the "ambient" soil. By comparing these temperatures, the evaporative flux from the ambient soil can be estimated.

SUMMARY OF PROGRESS

Task 1.1 – Select and characterize measuring locations

We have established soil water flux monitoring locations at four sites: Albuquerque (Civil Engineering Bosque Laboratory), Belen, Sevilleta, and Bosque del Apache (two sites). These sites were chosen for a number of reasons. It is necessary to have micro-meteorologic equipment to collect information on temperature, rainfall, and wind speed/direction. At the time of installation Belen, Sevilleta and Bosque del Apache had evapotranspiration towers located nearby that include micro-meteorological equipment. The evapotranspiration tower in Belen was vandalized in early summer, 2004. Because of the different conditions at each location, monitoring at these sites will have the benefit of measuring soil water flux under different conditions with respect to groundwater depth, soil type, and canopy and surface layer characteristics.

At each site, up to four locations for monitoring the soil water flux between the ground surface and the water table were selected. Soil samples from each distinct soil layer between the surface and the water table were retrieved for laboratory analyses, including measurement of grain size distribution, plasticity parameters, hydraulic conductivity, and development of moisture characteristic curves. During the sampling activities, the location of the groundwater table was confirmed, and soil layering was identified.

Results from characterization of the field locations are given in Appendix 1.

Task 1.2- Monitor soil water flux and climate

Instrumentation arrays to measure soil water content, temperature and suction were established at the field sites. These instruments are connected to a data acquisition system to permit unattended operation and data collection. Water content is being measured with TDR (time domain reflectometry) probes, soil water suction or potential is measured with a tensiometer system comprised of porous ceramic cups connected to pressure transducers, and temperature measurements will be made with thermocouples. The TDR probes were calibrated in the laboratory prior to field installation, as were the pressure transducers for the tensiometer system. TDRs, tensiometers and thermocouples were placed at regular depth intervals in the soil between the water table and the ground surface.

A total of 68 TDRs, 73 thermocouples and 52 tensiometers have been installed. Data has been periodically downloaded from the data loggers at the field sites. A data analysis program is being developed to reduce the data for plotting and subsequent analysis in terms of evaporation rates.

Details regarding instrumentation installation and calibrations are given in Appendix 1.

Task 1.3 – Measure evaporation with the infrared thermometry method

Efforts have focused on developing the experimental methodology for eventual field measurements. A complete soil energy balance experiment has been established on the roof of Tapy Hall on the campus of the University of New Mexico. The purpose of the energy balance experiment is to measure the complete energy balance, including latent heat flux due to evaporation. In addition, surface temperatures of wetted soil (ambient soil) and a dry reference soil are measured. From these measurements, the soil evaporation rate E can be found by the temperature difference between the ambient (T_o) and completely dry soil (T_d) as

$$E = S\,(T_d - T_o)$$

where S can be derived empirically from the energy balance data, and is expected to be a function of various constants and meteorological conditions including wind speed. The energy balance measurements permit an evaluation of how to derive the "S" term, including methods developed by previously by other researchers for different applications.

A complete description of the energy balance experiment including results and analyses to date is given in Appendix 2.

Task 2 – Develop predictive model for estimating evaporation

The purpose of this task is to develop a simple predictive model of evaporation to permit evaporation at other sites and conditions to be estimated. This evaporation model will be incorporated into a GIS model (Task 3). The model will be empirically based, that is, it will be derived from the database of evaporation we develop. This database will consist of evaporation

as a function of depth to water table, soil type and layering, sun-shade conditions, climate and surface conditions.

The empirically based, simple predictive model will be evaluated with the aid of a computer program that can estimate evaporation under a wide range of conditions. We have selected the computer program UNSAT-H for this task. UNSAT-H includes both liquid and vapor water movement through saturated and unsaturated soils, and includes coupling to climatic conditions. The first step to utilizing this computer program is to configure it to conduct inverse simulations, that is, input measured water content, suction and temperature data and predict evaporation rates. We first converted UNSAT-H to a Linux format, and then linked it to an optimization program. The program now has the capability to estimate evaporation rates through iterative calculations that seek to match the predicted and measured water content, suction and temperature data. A one-dimensional column evaporation test has been initiated on the roof of Tapy Hall to produce a data set for verification of the computer program.

Task 3 – Develop GIS-based model of soil water evaporation

The GIS model will use well data available from the evapotranspiration tower sites combined with USGS stage data in the Rio Grande to create a groundwater surface model based on the stage in the river. Once the model has been created, different scenarios of river flow can be simulated such that potential evapotranspiration can be estimated. The model will be limited due to the spatial variation of wells. However, as more wells are established in the Middle Rio Grande, the model can be improved. We have compiled most of the groundwater data for the evapotranspiration towers. Some very preliminary work on creating a groundwater surface based on river stage has been initiated.

Appendix 1

Progress Report for tasks 1.1 : Select and characterize measuring locations; and Task 1.2: Monitor soil water flux and climate
October 10 , 2004

Field Installation

In order to monitor the soil water evaporative fluxes in the Middle Rio Grande, five monitoring stations were installed at different locations along the river: Bosque del Apache North, Bosque del Apache South, Sevilleta, Belen and the Civil Engineering Bosque Laboratory (Albuquerque) [fig 1]. These locations were selected in order to complement data from the monitoring stations with the micro-meteorological data available from the ET towers.

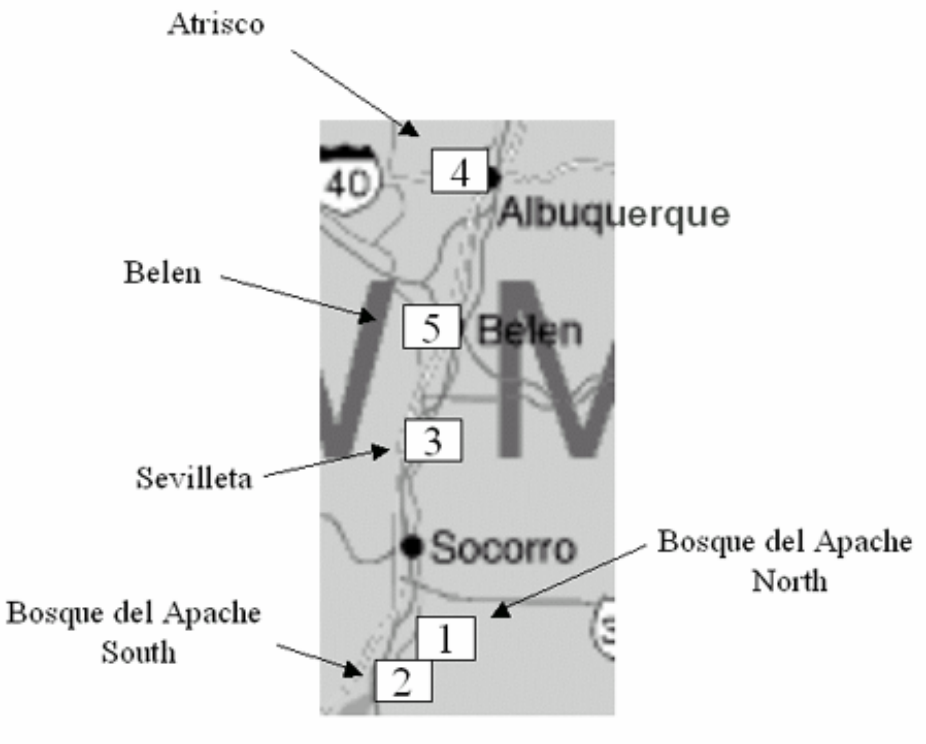

Fig 1. Site locations

Basic configuration

Every site has a defined number of areas that are monitored. These areas can be a combination of: bare soil - sunny, bare soil - shaded, mulched soil - sunny and mulched soil - shaded conditions (figure 2). For each area, the instrumentation arrays to measure soil water content, temperature and soil water potential were placed as shown in figure 3.

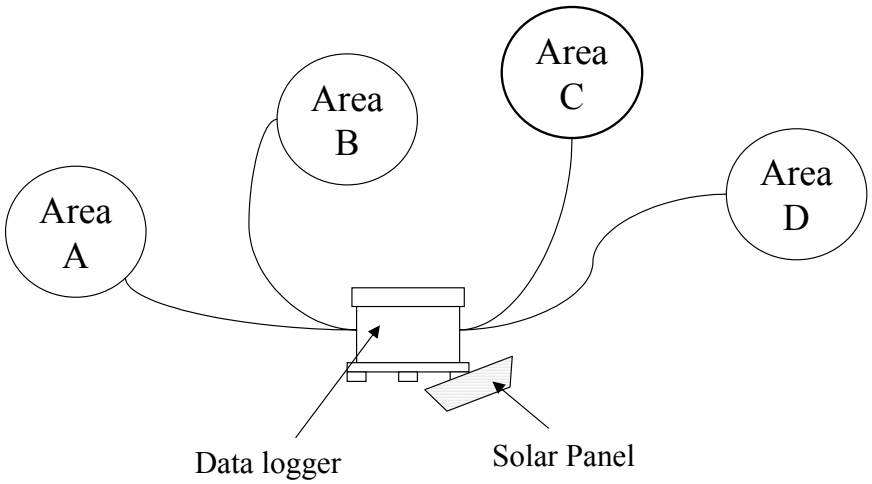

Fig. 2 Simplified plan view of a basic site configuration

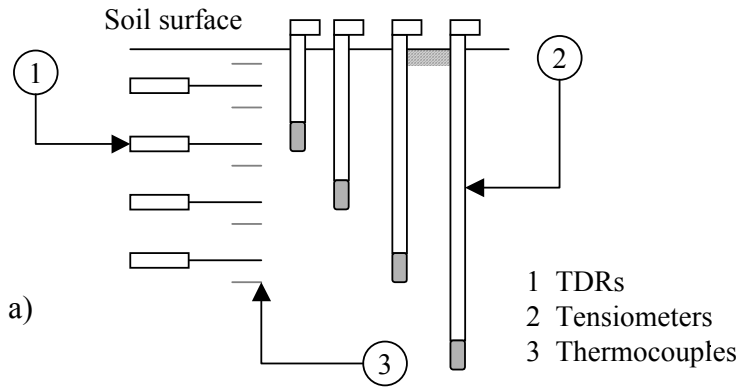

a)

b)

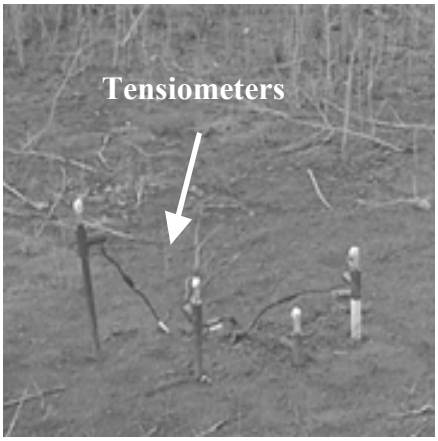

c)

Fig 3. a) Typical soil water flux instrumentation at one monitored area b) TDR installation c) Tensiometers installation.

Each sensor is connected to a data logger (CR10X Campbell Scientific) which records the data provided by monitored areas. The data logger, placed inside an enclosure box, works with a battery that is kept charged by a solar panel placed near the box. The enclosure box is held by fence-posts that are secured into the ground. The boxes are placed at 0.91 m (3 ft) over the ground (see also Appendix A). Electrical cables of 9.14 m (30 ft) long were used to connect each sensor to the data logger.

The following code is used to identify and label the various instruments in the field.

For the site designation, a roman numeral is used for each location:

- Bosque del Apache North (I)
- Bosque del Apache South (II)
- Sevilleta (III)
- Civil Engineering Bosque Laboratory (Atrisco) (IV)
- Belen (V)

Letters are used to designate the areas within each site:

- Area (A)
- Area (B)
- Area (C)
- Area (D)

For the sensor identification a number is used:

- Sensor 1 1
- Sensor 2 2
- Sensor n n

For example, the identification of the second TDR at the Sevilleta in area 2 is: III.B.2

Equipment

The equipment and sensors were chosen according to the environmental condition in the field, requirements and costs. The products manufactured by Campbell Scientific Inc. were selected because their wide use in research, field durability, compatibility sensors and comparative costs. The equipment used is described below (see also Appendix A.)

- **Data logger**

The data logger used at each site is a CR10X unit. This device has a wiring panel where the sensors are connected. The unit is powered by a 12 volt source contains a 128 K flash memory for the operation system and stored programs and a capacity to store 62,280 data points.

- **Multiplexer**

  Since the data logger has a limited number of sensors that can be connected to it, a multiplexer AM 16/32 is used to increase the capacity of the data logger.

- **Temperature reference**

  A temperature reference connected to the data logger is used as a reference to calculate the temperature measured by the thermocouples.

- **Battery**

  A 12 volt battery is used to power the data logger.

- **Solar Panel**

A solar panel (MSX 10) is used to keep the battery charged.

- **Regulator**

A regulator (CT100) is used to connect the data logger, the battery and the solar panel.

- **Enclosure**

  Because the presences of dust, water, sunlight, or environmental pollutants in the field, a protective enclosure for the data logger was required. This enclosure, made by fiberglass-reinforced polyester enclosures, is UV-stabilized and reflects solar radiation. It reduces temperature gradients inside of the box protecting the sensitive equipment.

- **<u>Sensors</u>**

  - **TDR (Time-domain reflectometer)**

The sensor CS-616 from Campbell Scientific is used to measure the soil water content in the field. The CS-616 sends an electromagnetic pulse into the soil, a portion of the signal is reflected to the probe and registered by the sensor, a correlation of the response of the soil to this electromagnetic pulse and the soil water content can be established for the soil.

- **Tensiometers**

The soil suction is measured using a tensiometer device manufactured by Soil Measurement Systems. This sensor is composed of a ceramic porous cup (which acts as an interface between the water in the reservoir and the soil), the reservoir-a plastic tube of the required length to store water, and a pressure transducer placed in the top of the instrument to measure the changes in pressure in the plastic tube.

The water moves through the ceramic cup to the surrounding soil and equilibrium between the tensiometer and the soil is achieved. The pressure transducer registers the change in pressure of the reservoir and the soil suction can be calculated from it.

- **Thermocouples**

A thermocouple type T (constantan and cooper) is used to measure the temperature variation in the soil profile. The cable is manufactured by OMEGA Engineering Inc. Welding the ends of the cable with a high quality solder can create a junction. When the thermocouple circuit is open, a voltage is generated by a difference in temperature between the junctions. For an open circuit where one of the junction temperatures is known (reference temperature), the temperature at the opposite junction can be calculated (measured temperature).

Calibrations

Similar to the TDRs, the pressure transducers used with the tensiometers were calibrated. A calibration was performed for every sensor to establish a relationship between its response as a function of soil moisture content or soil suction.

TDRs Calibration

The TDR response can be affected by many factors such as soil composition, soil density, and temperature. In order to determine the response of the TDRs, a calibration in the laboratory was performed.

Using soil from the Shirk site in the South Valley of Albuquerque, four buckets were prepared at different soil volumetric water contents at 1.25 g/cm^3 dry density equal to the estimated field density. Each TDR was inserted vertically in every bucket and, with a CR10X data logger the TDR response was recorded. The relationship between volumetric moisture content and TDR response was established (see figure 4).

Figure 4 shows that the responses of 16 TDRs, used in this calibration, are homogeneous. In other words, a nearly equal response from the TDRs to the same volumetric water content was found for this soil. This becomes an advantage, because if we can determine the responses for a single TDR, its calibration curve can be use to interpret other instruments.

The probe output response to changing water content for Shirk soil can be described using a quadratic equation

$$\theta_v = 0.0921 * \tau^2 + 2.9534 * \tau + 29.155 \qquad \text{Eq. 1}$$

with R^2 equal to 0.98. The mathematical relationship is shown below.

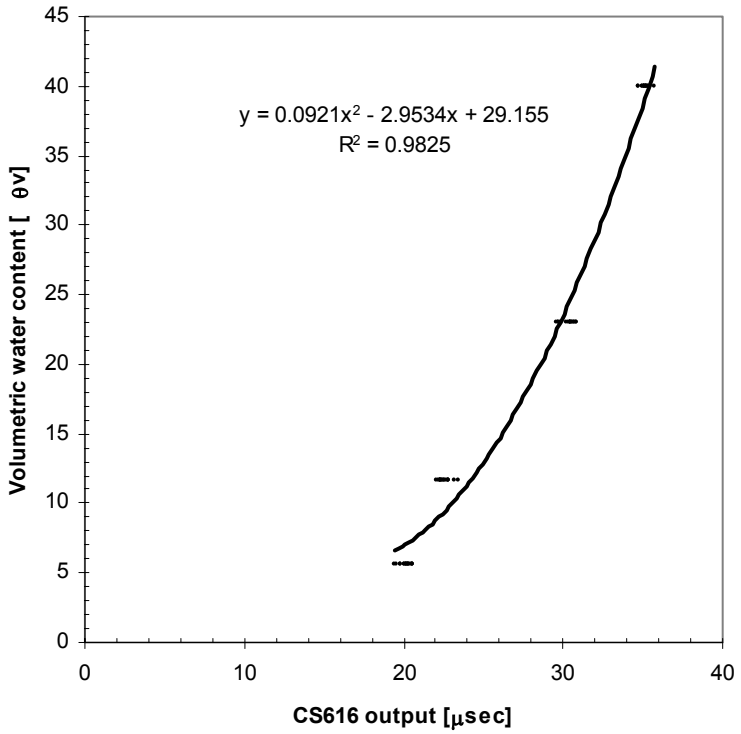

Figure 4 CS616 quadratic calibration curve

To determine the correlation between the TDR output and the soil volumetric water content at the field site, TDRs were calibrated in place as will be described for each site in the next sections.

Tensiometers Calibration

Tensiometers are widely used to determine hydraulic gradients, wetting fronts and soil hydraulic properties. In order to calibrate the tensiometers, the pressure transducers have to be calibrated.

The sensor is plugged to a plastic tube connected to a reservoir with water open to atmospheric pressure. When the water level in the reservoir coincides with the elevation of the pressure transducer the suction is considered zero. To produce a positive pressure in the sensor the reservoir is raised to a known elevation. The difference in height between the sensor and the water level in the reservoir can be interpreted as the pressure or head applied to the sensor. To test the pressure transducer under negative pressure, or suction, the water reservoir is lowered under the pressure transducer level. This produces suction in the sensor, which is registered in the data logger. Again the amount of negative pressure applied can be interpreted as the difference in height between the water level in the reservoir and the sensor.

Figure 5 shows the calibration curves for different tensiometers corresponding to the Location I Area A (Bosque del Apache North). A difference between calibration curves for different pressure transducers is observed in this figure. This difference implies that each sensor has to be calibrated and there is no opportunity to use a common calibration curve between them.

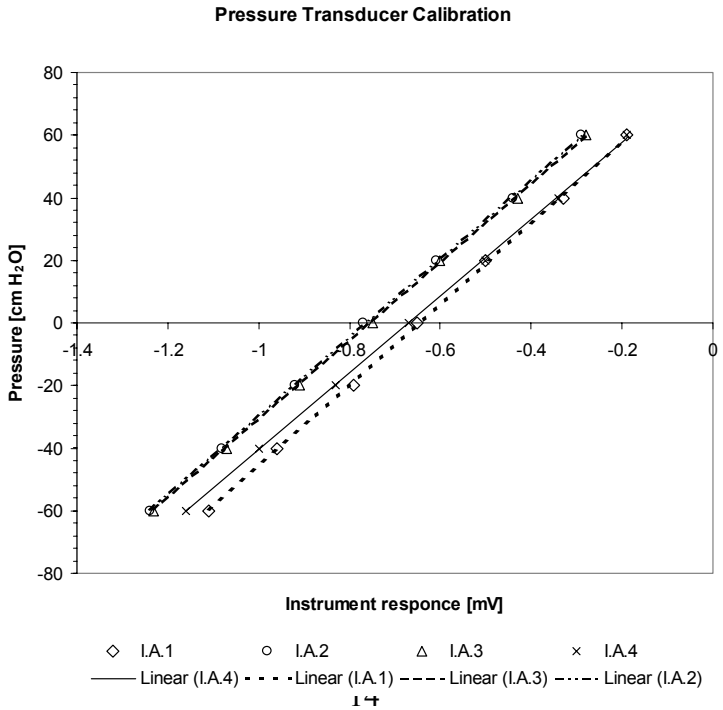

Figure 5 Calibration curves for pressures transducer

Calibration curves for each used pressure transducer are in Appendix B.

Field Installation Bosque del Apache North

Summary of the installation

Date of installation: March 17, 2004
Coordinates: 33º 52' 7.42" N 106º 50' 54.37"W
Water table at time of installation: 92.56 cm (38 in)

As-Built Configuration:

The data logger and instruments were installed on the west side of the river, approximately 30 m (100 ft) from the edge of the river. Areas A and B are approximately 6 m (20 ft) from the data logger on the river side . Areas A and B are about 1.8 m (6 ft) apart. Areas C and D are 3 m (10 ft) from the box toward the access road; the distance between C and D is 4.6 m (15 ft) (see Figure 6).

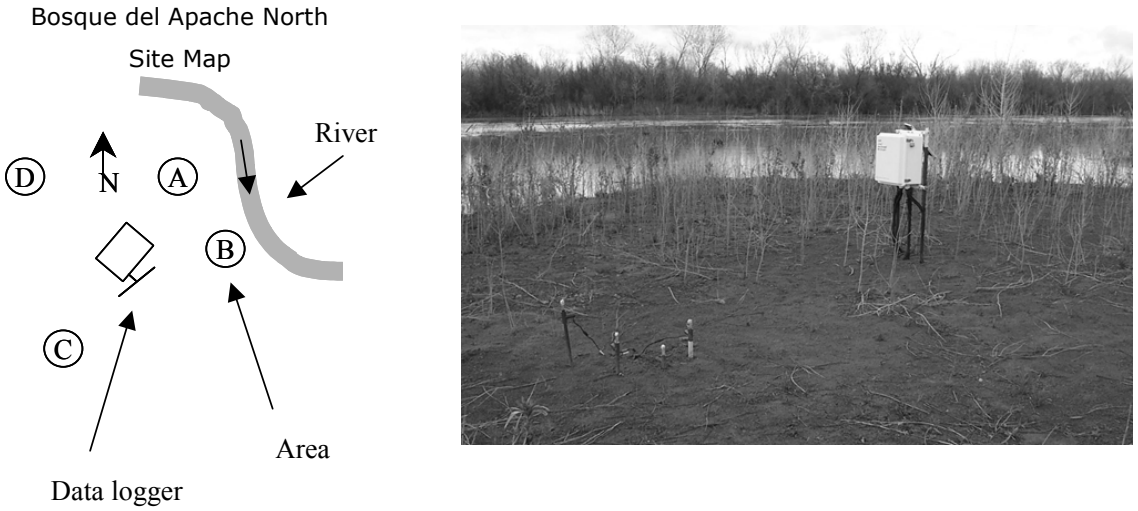

Figure 6 Site map and photograph of Bosque del Apache North

The four areas were installed in this site.

- bare soil shade Area A
- mulch soil shade Area B
- mulch soil sun Area C
- bare soil sun Area D

Each area has the following instrumentation:

- 4 TDR
- 4 tensiometers
- 4 thermocouples

Gage Labeling:

Label	Instrument	Location from the surf. cm [in]	Label	Instrument	Location from the surf. [in]
I.A.1	TDR 1	7.6 [3]	I.C.1	TDR 9	7.6 [3]
I.A.2	TDR 2	22.9 [9]	I.C.2	TDR 10	22.9 [9]
I.A.3	TDR 3	38.1 [15]	I.C.3	TDR 11	38.1 [15]
I.A.4	TDR 4	53.3 [21]	I.C.4	TDR 12	53.3 [21]
I.A.1	thermocouple 1	7.6 [3]	I.C.1	thermocouple 9	7.6 [3]
I.A.2	thermocouple 2	22.9 [9]	I.C.2	thermocouple 10	22.9 [9]
I.A.3	thermocouple 3	38.1 [15]	I.C.3	thermocouple 11	38.1 [15]
I.A.4	thermocouple 4	53.3 [21]	I.C.4	thermocouple 12	53.3 [21]
I.A.1	tensiometer 1	7.6 [3]	I.C.1	tensiometer 9	7.6 [3]
I.A.2	tensiometer 2	22.9 [9]	I.C.2	tensiometer 10	22.9 [9]
I.A.3	tensiometer 3	38.1 [15]	I.C.3	tensiometer 11	38.1 [15]
I.A.4	tensiometer 4	53.3 [21]	I.C.4	tensiometer 12	53.3 [21]
I.B.1	TDR 5	7.6 [3]	I.D.1	TDR 13	7.6 [3]
I.B.2	TDR 6	22.9 [9]	I.D.2	TDR 14	22.9 [9]
I.B.3	TDR 7	38.1 [15]	I.D.3	TDR 15	38.1 [15]
I.B.4	TDR 8	53.3 [21]	I.D.4	TDR 16	53.3 [21]
I.B.1	thermocouple 5	7.6 [3]	I.D.1	thermocouple 13	7.6 [3]
I.B.2	thermocouple 6	22.9 [9]	I.D.2	thermocouple 14	22.9 [9]
I.B.3	thermocouple 7	38.1 [15]	I.D.3	thermocouple 15	38.1 [15]
I.B.4	thermocouple 8	53.3 [21]	I.D.4	thermocouple 16	53.3 [21]
I.B.1	tensiometer 5	7.6 [3]	I.D.1	tensiometer 13	7.6 [3]
I.B.2	tensiometer 6	22.9 [9]	I.D.2	tensiometer 14	22.9 [9]
I.B.3	tensiometer 7	38.1 [15]	I.D.3	tensiometer 15	38.1 [15]
I.B.4	tensiometer 8	53.3 [21]	I.D.4	tensiometer 16	53.3 [21]

Significant field occurrences/observations:

There were no changes from the original plan due to field conditions. Near the end of April and beginning of May, snowmelt increased the level of the river. During a visit to the site on May 5, over banking of the site was observed. The instruments

were safe on an isolated location (an “island) as surface water surrounded the field site. Area C was underwater for some period of time. No re-installation of the equipment was required.

- Subsequent field density water content measurements

Measurements of water content were obtained at 4 zones adjacent to the TDR’s areas. The water content information was used for the TDRs calibration for these samples of the moisture content were taken at the level of the TDRs (figure 7). Also, a sand cone test was conducted every time that a change of soil texture was evident (figure 7). A 5th zone, close to area A was selected; samples for the moisture content and density were obtained every 5 cm (2 in) for this location using the core method (figure 8).

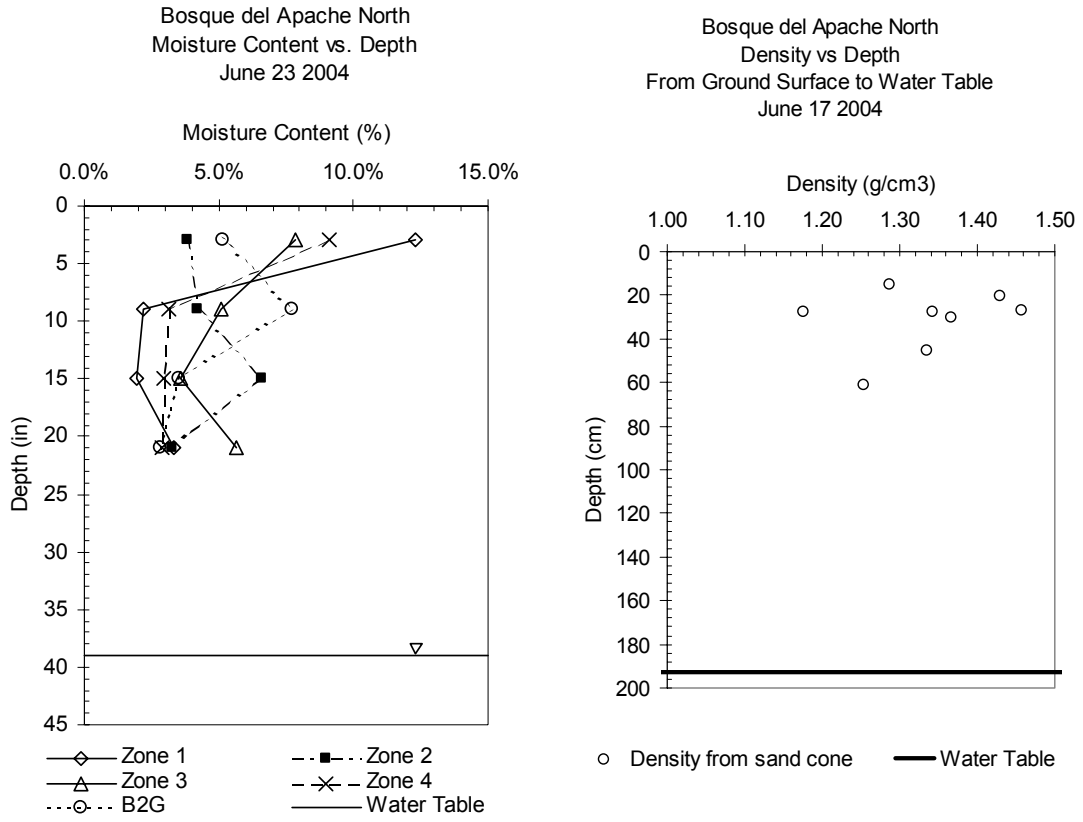

Figure 7 Gravimetric soil moisture content profile Site I and soil dry densities all zones

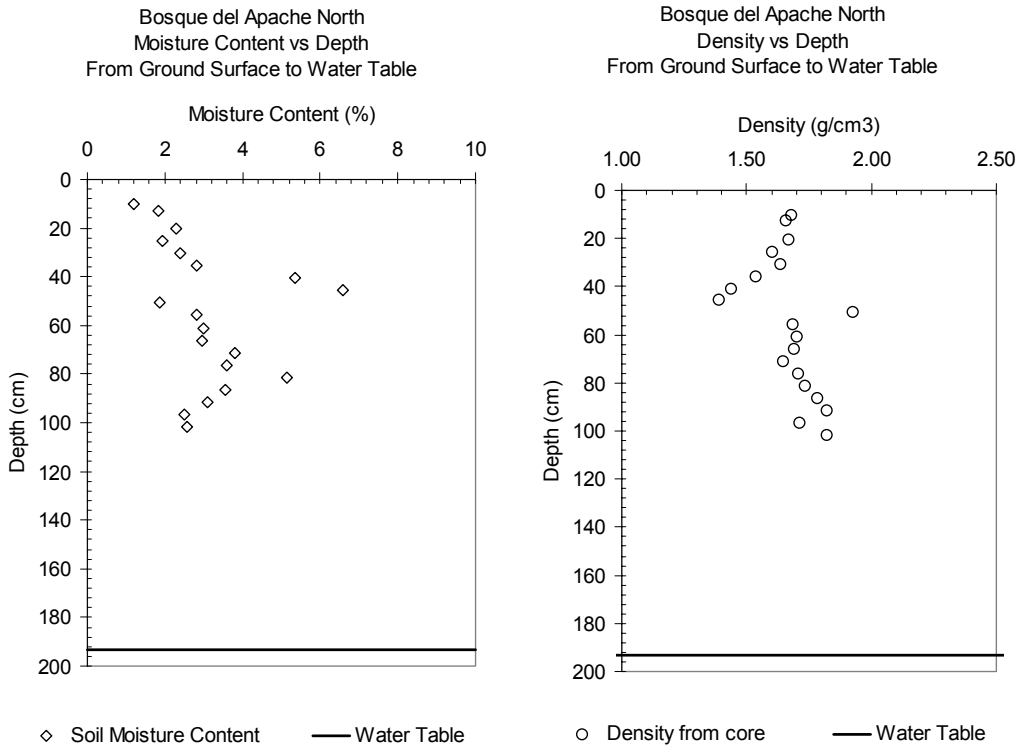

Figure 8 Core method results for zone 3

- Minimum density test

A representative sample of soil from the Bosque del Apache North site was mixed in a graduated cylinder with water, agitated, and allowed to settle under only the weight of the water. The volume, mass, and gravimetric moisture-content of the sample were taken after approximately 36 days.

This experiment was conducted to establish the minimum soil density that should be expected in areas where soils are deposited by overland water flow. Any soil density reported below this minimum should be subject to great scrutiny. The final dry density of the soil used in this experiment was determined to be 1.45 g/cm^3.

- Changes in water table

The change of the water table was evident. At the time of installation the water table was at 96.5 cm (38 in) (3/17/04), by June 14 the water table level was 121.9 cm (4 ft), and on July 2 the water table could not be found (no water table grater than 193cm (76 in.))

- Site-specific calibrations

With the information obtained from the soil density and the moisture content, the TDRs were calibrated. A relationship between volumetric soil water content and TDR response was established (figure 9) with $R^2 = 0.91$.

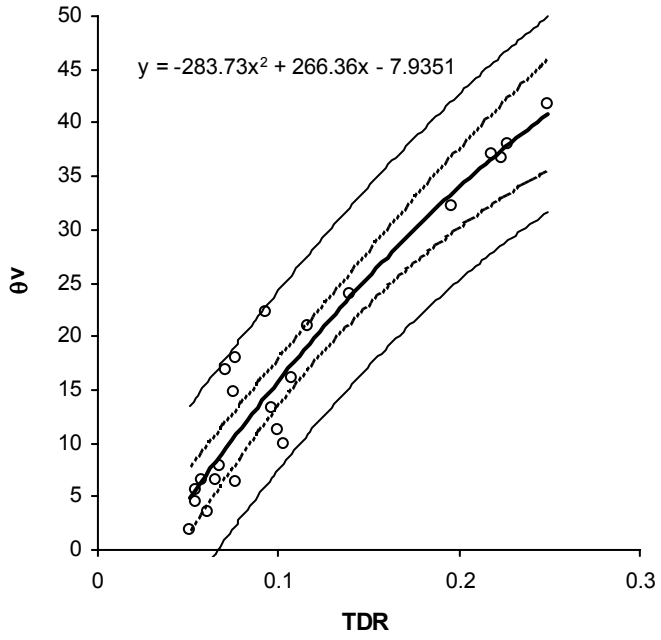

Figure 9 Calibration curve for TDR's Site I

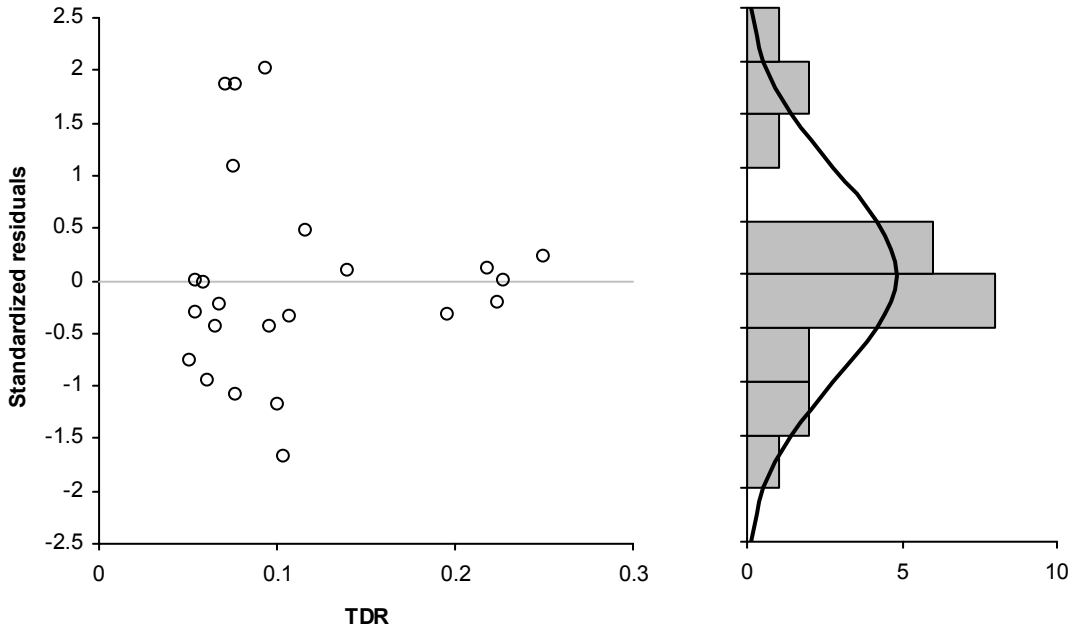

Figure 10 Standardized residuals for the calibration curve

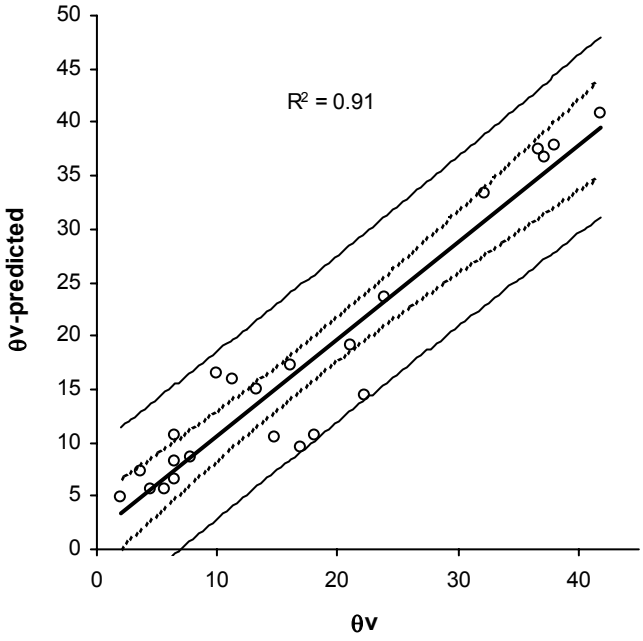

Figure 11 Volumetric water content measured (θv) vs. volumetric water content predicted (θv-predicted)

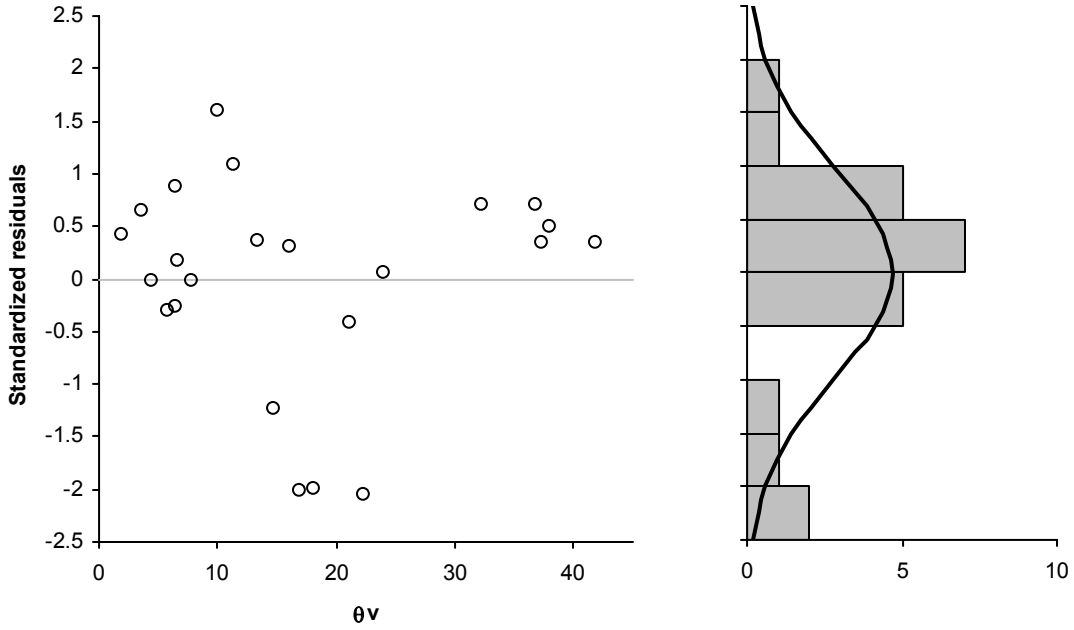

Figure 12 Standardized residuals for θv vs. θv-prediction

An assessment of the calibration curve can be made using standardized residuals. The standardized residual is a residual divided by its estimated standard error. The residuals should be randomly distributed about zero according to the normal distribution, so all but a few standardized residuals should be between –2 and +2. Figure 10 shows the standardized residuals for the established calibration curve. We can observe that the values are between the [–2, +2] range. The correlation between measured volumetric water content and predicted volumetric water content is shown in figure 11, and standardized residuals are shown in figure 12 which shows that all values are in the range [-2,+2].

- Soil Samples

    - Location (see figure 13)

      The soil samples were obtained from 5 areas.
      Zone 1 located near area B south
      Zone 2 located at the proximities of area D between D and A
      Zone 3 near area D, between D and the data logger
      Zone B2G near area D between area D and area 2
      Zone 4 between area C and area D closer to area C

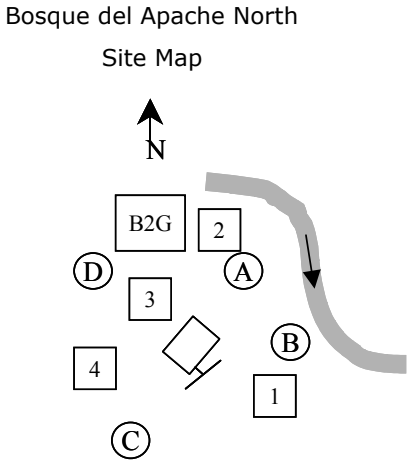

Figure 13 Site map of the sample zones

- Tests performed (see Appendix C,D and E)

    1. Water content
    2. Particle size analysis sieve analysis
    3. Particle size analysis hydrometer
    4. Field density test sand cone
    5. Field density test and moisture content sore method
    6. Specific Gravity

- Summary

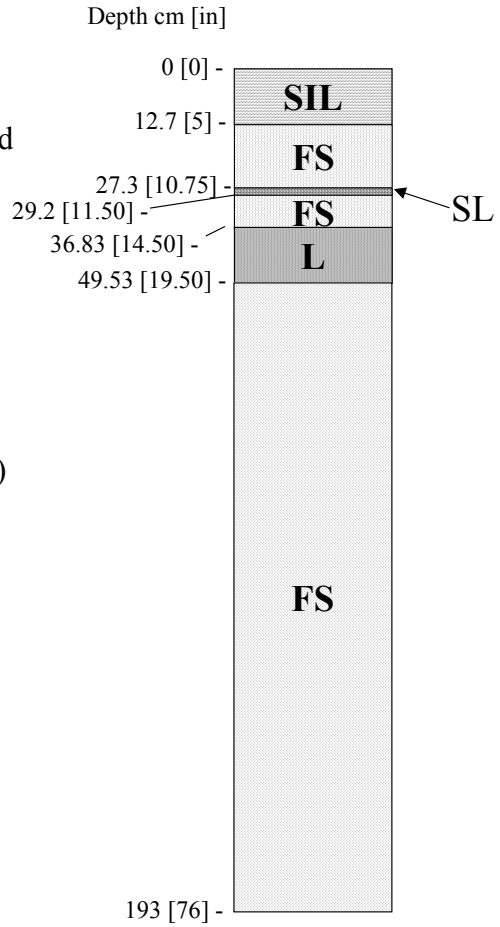

Bosque del Apache North

	cm	in	
SIL	0 - 12.7	0-5	(Silty loam)
FS	12.7 - 27.3	5-10.75	(Fine sand)
SL	27.3 - 29.3	10.75-11.50	(Sandy loam)
FS	29.3 - 36.83	11.50-14.50	(Fine sand)
L	36.83 - 49.53	14.50-19.50	(Loam)
FS	49.53 - 193	19.50-76	(Fine sand)

Average density	1.61	g/cm3
Specific Gravity	2.65	

Figure 14 Soil profile Site I

Field Installation Bosque del Apache South

Summary of the installation

Date: March 18, 2004
Coordinates: 33º 47’ 41.79” N 106º 52’ 00.04”W
Water table: 71.12 cm (28 in)

As-Built Configuration:

The site is located at 6.1 m (20 ft) from the river on the west side. In the initial configuration sites A and B were 3 m (10 ft) apart of the box toward the river. The distance between them was 2.4 m (8 ft). Sites C and D were located south 3 m (10 ft) from the box. They were 2.4 m(8 ft) apart.

The four installed in this site were:

- bare soil shade Area A
- mulch soil shade Area B
- mulch soil sun Area C
- bare soil sun Area D

Each area has the following instrumentation:

- 4 TDR
- 4 thermocouples

Gage Labeling:

Label	Instrument	Location from the surf. cm [in]	Label	Instrument	Location from the surf. [in]
II.A.1	TDR 1	7.2 [3]	II.C.1	TDR 9	7.2 [3]
II.A.2	TDR 2	22.9 [9]	II.C.2	TDR 10	22.9 [9]
II.A.3	TDR 3	38.1 [15]	II.C.3	TDR 11	38.1 [15]
II.A.4	TDR 4	53.3 [21]	II.C.4	TDR 12	53.3 [21]
II.A.1	thermocouple 1	2.5 [1]	II.C.1	thermocouple 9	2.5 [1]
II.A.2	thermocouple 2	7.2 [3]	II.C.2	thermocouple 10	7.2 [3]
II.A.3	thermocouple 3	15.2 [6]	II.C.3	thermocouple 11	15.2 [6]
II.A.4	thermocouple 4	30.5 [12]	II.C.4	thermocouple 12	30.5 [12]
II.B.1	TDR 5	7.2 [3]	II.D.1	TDR 13	7.2 [3]
II.B.2	TDR 6	22.9 [9]	II.D.2	TDR 14	22.9 [9]
II.B.3	TDR 7	38.1 [15]	II.D.3	TDR 15	38.1 [15]
II.B.4	TDR 8	53.3 [21]	II.D.4	TDR 16	53.3 [21]
II.B.1	thermocouple 5	2.5 [1]	II.D.1	thermocouple 13	2.5 [1]
II.B.2	thermocouple 6	7.2 [3]	II.D.2	thermocouple 14	7.2 [3]
II.B.3	thermocouple 7	15.2 [6]	II.D.3	thermocouple 15	15.2 [6]
II.B.4	thermocouple 8	30.5 [12]	II.D.4	thermocouple 16	30.5 [12]

Significant field occurrences/observations

- Over-Banking

Beginning near the end of March, snowmelt increased the water level of the river. During a visit to the site in May 5, over-banking in the site was observed. The river, which was located in the opposite site of the box's location, changed its course and began to undermine the site. The border of the river was very close to the box's foundation. The river under the areas A and B and C displaced the instruments out of their location.

Figure 15 Photograph of Site II. Increase of the river water level threatened the site and necessitated instrument re-installation.

- Re-installation

  On June 17, the equipment was recovered, cleaned and relocated.

- New configuration

Because of a lack of vegetation at this site that could provide shade during the day, the selected areas are all designed as bare soil sun.

- bare soil sun Area A
- bare soil sun Area B
- bare soil sun Area C
- bare soil sun Area D

As-Built Configuration:

The site is located at the west site of the river near the edge of the stream. Areas A and B are 2.4 m (8 ft) west of the box with 3 m (10 ft between areas. Areas C and D are 3 m (10 ft) away from the box toward north direction, with a 2.4 m (8 ft) separation between them (see figure 16.)

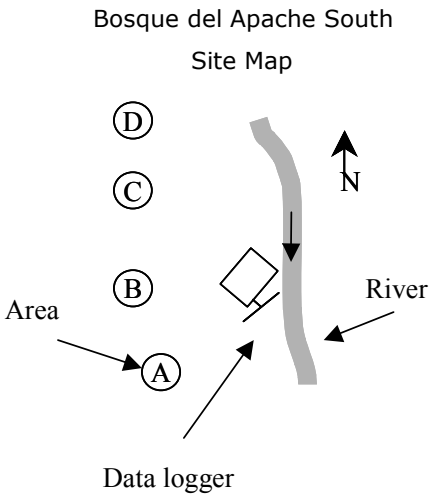

Figure 16 Site map of Bosque del Apache North

Areas B, C and D have the following instrumentation:

- 4 TDR
- 4 thermocouples

Areas A has the following instrumentation:

- 4 TDR

  Area A lost all the thermocouples in the flooding

- Subsequent field density water content measurements

In order to calibrate the TDRs, soil samples for water content were obtained at different zones adjacent to the TDR locations and TDR levels. The sand cone tests were conducted to determine the density of the soil in the different layers. The core method was used in one of the zones to obtain detailed information about the variations of moisture content throughout the soil profile. One sample was obtained every 2.5 cm (2 in.) The core method provides information about soil density and water content of the soil.

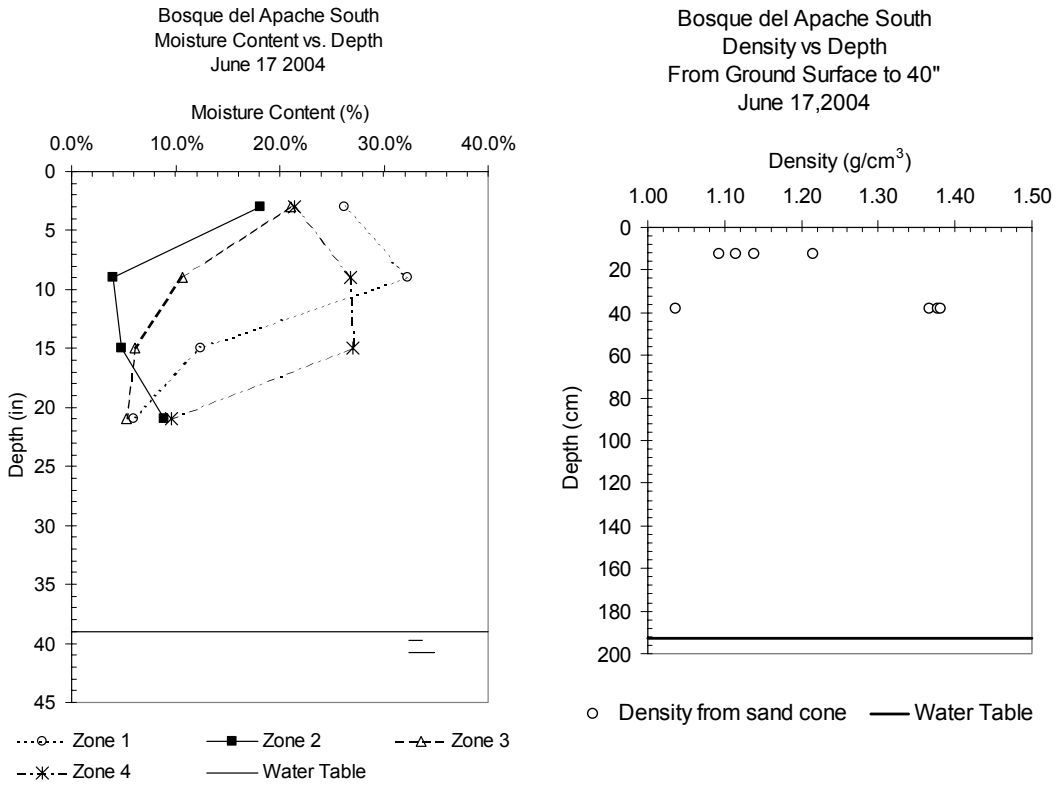

Figure 17 Gravimetric soil moisture content profile Site II and soil dry densities all zones

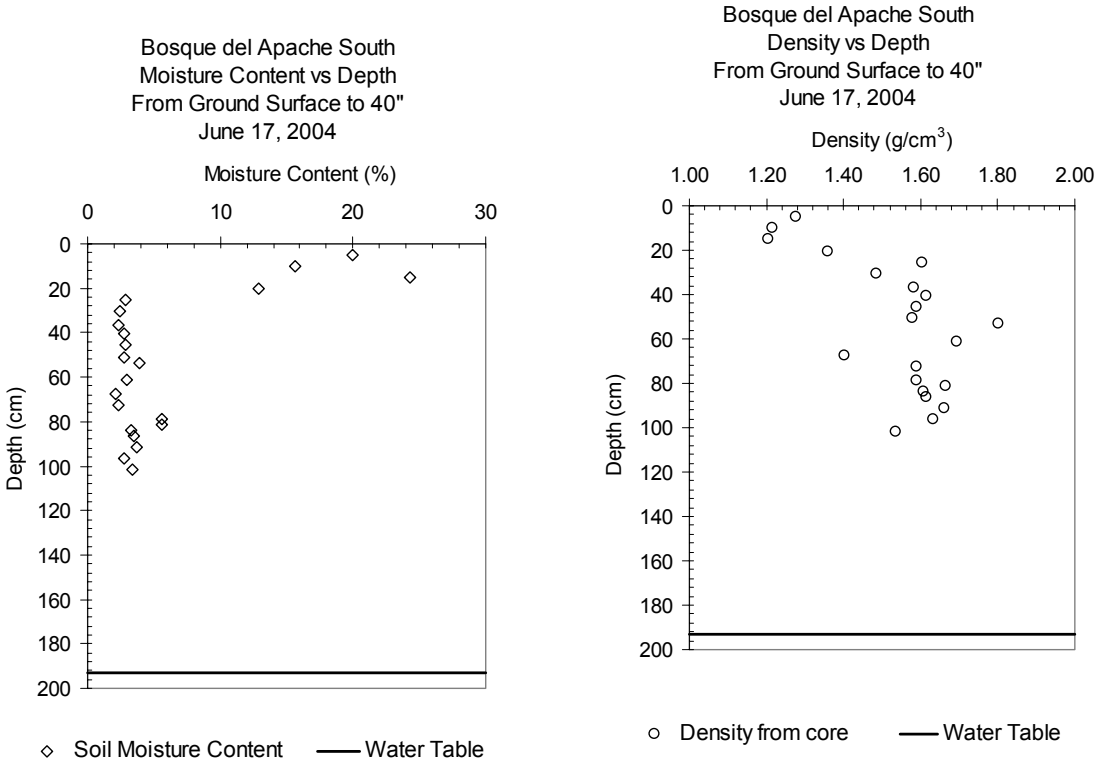

Figure 18 Core method results zone 1

- Changes in water table

The change of the water table was evident. At the time of installation the water table was at 71.1 cm (28 in) (3/18/04), at the day of re-installation of the instruments (June 17) the water table level was 121.92 cm (48 in.) in July 2 the water table could be found at 157.5 cm (62 in.)

Site-specific calibrations

With the information obtained from the soil density and the moisture content, the TDRs were calibrated. Figure 19 shows the calibration curve for Site II with a $R^2 = 0.7$.

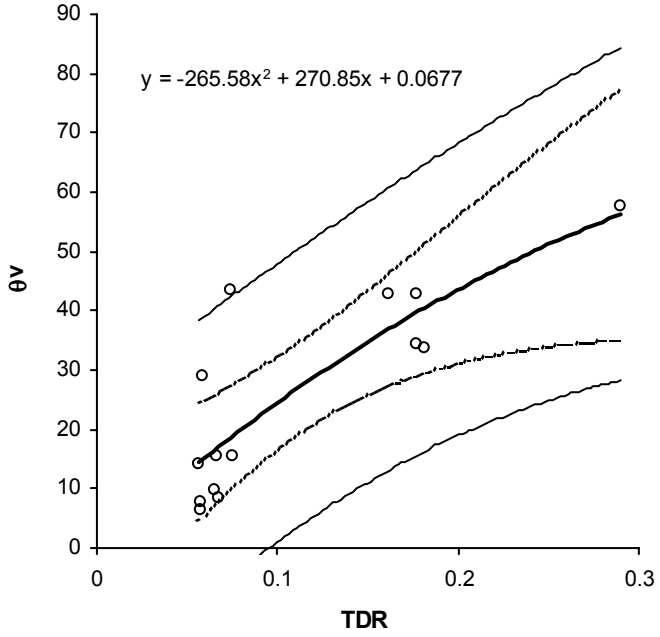

Figure 19 Calibration curve for TDR's Site II

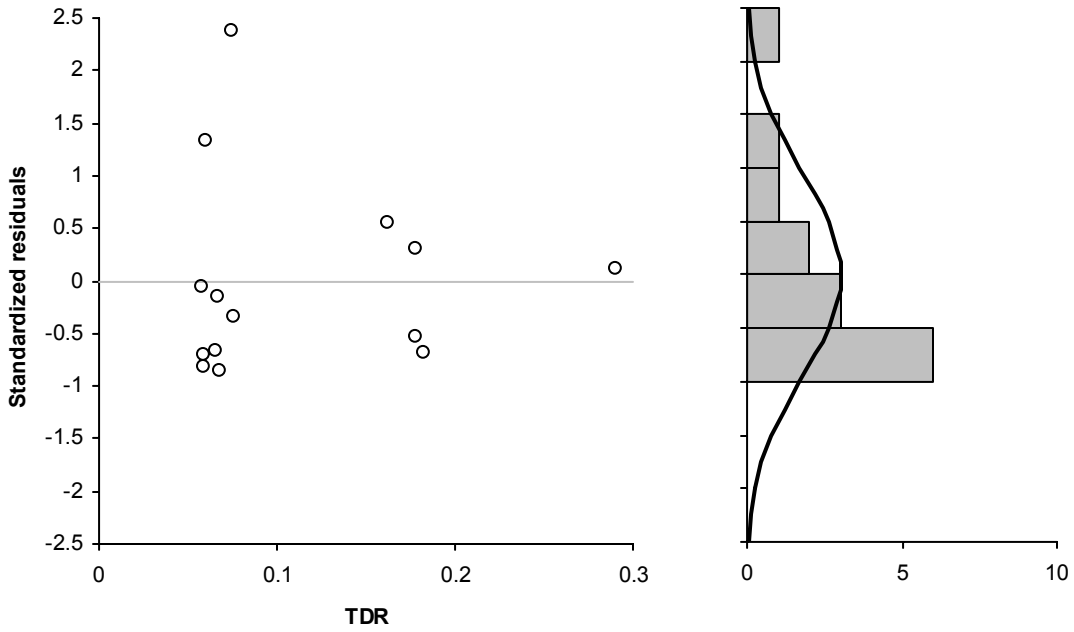

Figure 20 Standardized residuals for the calibration curve

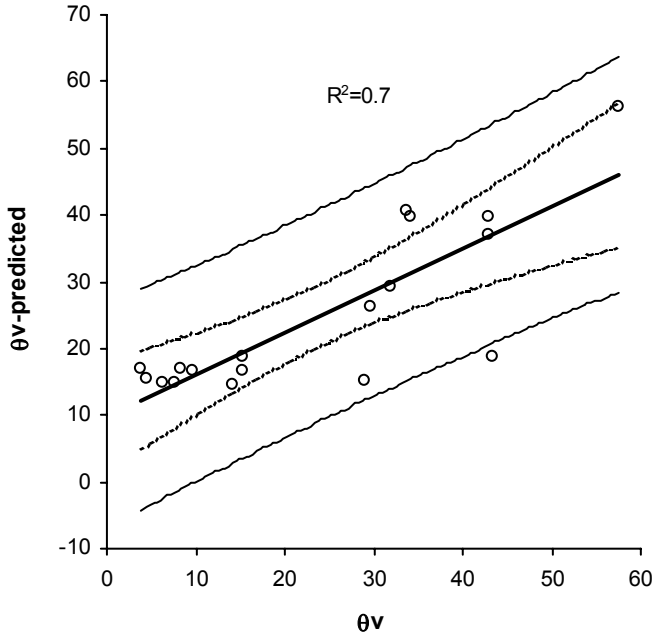

Figure 21 Volumetric water content measured (θv) vs. volumetric water content predicted (θv-predicted)

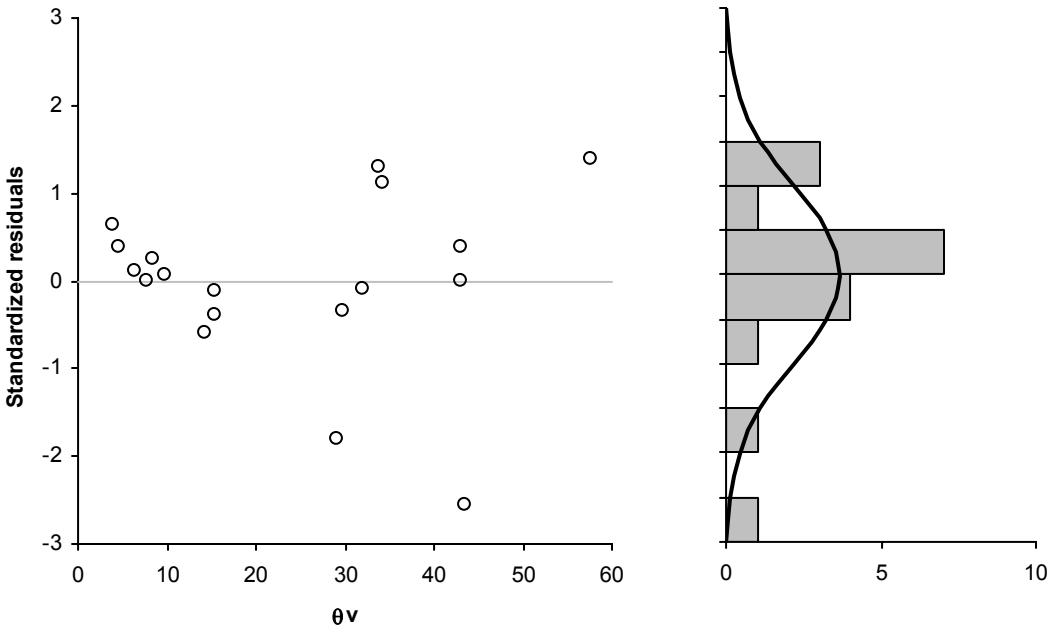

Figure 22 Standardized residuals for θv vs. θv-prediction

In figure 20 the standardized residuals are between the values –2 and +2 confirming the reasonableness of the proposed calibration curve. The quality of this curve is not as good as for the Site I, but it is considered to be reasonable considering all the uncertainties involved in the field calibration.

Soil Samples

- Location

  Zone 1 located near area B north
  Zone 2 located at the proximities of area C between area 1and C
  Zone 3 near area D between D and C
  Zone 4 near area A between area A and B

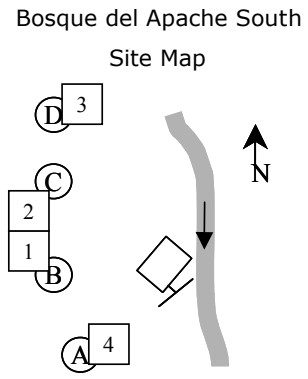

Figure 23 Site map of the sample zones

- Tests

1. Water content
2. Particle size analysis sieve analysis
3. Particle size analysis hydrometer
4. Field density test sand cone
5. Field density test and moisture content sore method
6. Specific Gravity

- Summary (see Appendix C,D and E)

Bosque del Apache South

	in		
SL	0- 17.8	0-7.0	(Sandy loam)
FS	17.8-101.6	7.0-40.0	(Fine sand)

Average density	1.50	g/cm3
Specific Gravity	2.64	

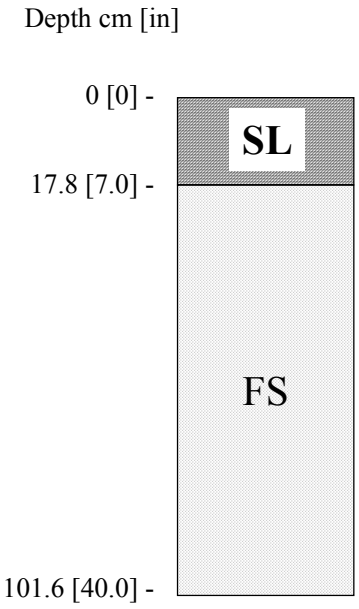

Figure 24 Soil profile Site II

Sevilleta

Summary of the installation

Date: May 18, 2004
Coordinates: 34º 15' 41.54" N 106º 52' 09.94"W
Water table: 21" (53.34 cm)

As-Built Configuration:

On the west side of the river about 15.2 m [50 ft] away from the river, the third data logger was installed. The site has four areas, which are 3 m (10 ft) apart between each other and about 6.1 m (20 ft) from the box.

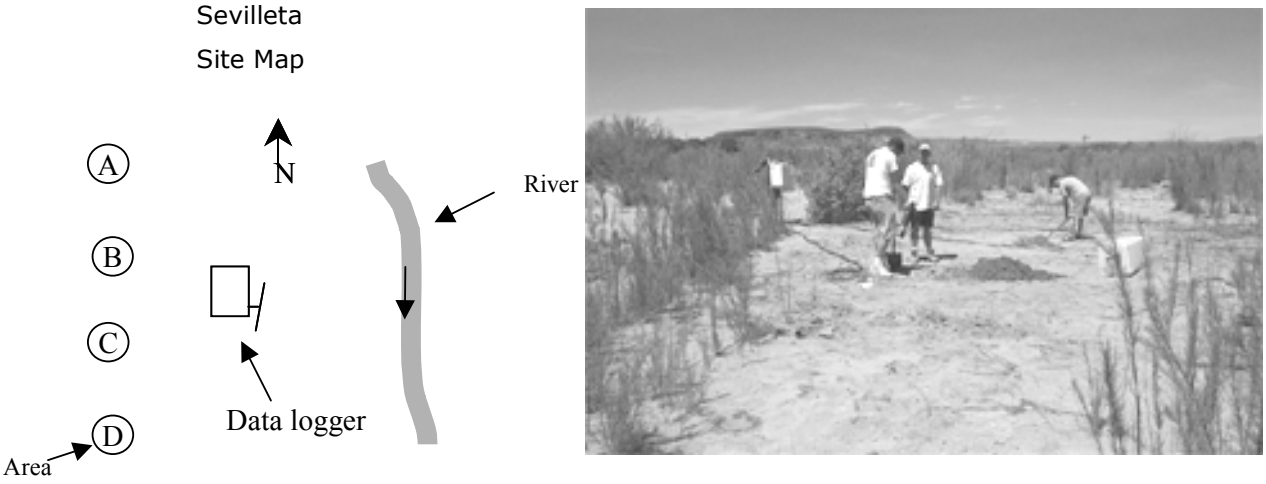

Figure 24 Site map and photograph of Sevilleta site

The four areas were installed in this site.

- bare soil sun Area A
- bare soil sun Area B
- bare soil sun Area C
- bare soil sun Area D

Each area has the following instrumentation:

- 4 TDR
- 4 tensimeters cable connection
- 5 thermocouples

Gage Labeling:

Label	Instrument	Location from the surf. cm [in]	Label	Instrument	Location from the surf. cm [in]
III.A.1	TDR 1	7.2 [3]	III.C.1	TDR 9	7.2 [3]
III.A.2	TDR 2	22.9 [9]	III.C.2	TDR 10	22.9 [9]
III.A.3	TDR 3	38.1 [15]	III.C.3	TDR 11	38.1 [15]
III.A.4	TDR 4	53.3 [21]	III.C.4	TDR 12	53.3 [21]
III.A.1	thermocouple 1	1.27 [0.5]	III.C.1	thermocouple 11	1.27 [0.5]
III.A.2	thermocouple 2	7.2 [3]	III.C.2	thermocouple 12	7.2 [3]
III.A.3	thermocouple 3	15.2 [6]	III.C.3	thermocouple 13	15.2 [6]
III.A.4	thermocouple 4	30.5 [12]	III.C.4	thermocouple 14	30.5 [12]
III.A.5	thermocouple 5	61 [24]	III.C.5	thermocouple 15	61 [24]
III.A.1	tensiometer 1	15.2 [6]	III.C.1	tensiometer 9	15.2 [6]
III.A.2	tensiometer 2	30.5 [12]	III.C.2	tensiometer 10	30.5 [12]
III.A.3	tensiometer 3	45.7 [18]	III.C.3	tensiometer 11	45.7 [18]
III.A.4	tensiometer 4	61 [24]	III.C.4	tensiometer 12	61 [24]
III.B.1	TDR 5	7.2 [3]	III.D.1	TDR 13	7.2 [3]
III.B.2	TDR 6	22.9 [9]	III.D.2	TDR 14	22.9 [9]
III.B.3	TDR 7	38.1 [15]	III.D.3	TDR 15	38.1 [15]
III.B.4	TDR 8	53.3 [21]	III.D.4	TDR 16	53.3 [21]
III.B.1	thermocouple 6	1.27 [0.5]	III.D.1	thermocouple 16	1.27 [0.5]
III.B.2	thermocouple 7	7.2 [3]	III.D.2	thermocouple 17	7.2 [3]
III.B.3	thermocouple 8	15.2 [6]	III.D.3	thermocouple 18	15.2 [6]
III.B.4	thermocouple 9	30.5 [12]	III.D.4	thermocouple 19	30.5 [12]
III.B.5	thermocouple 10	61 [24]	III.D.5	thermocouple 20	61 [24]
III.B.1	tensiometer 5	15.2 [6]	III.D.1	tensiometer 13	15.2 [6]
III.B.2	tensiometer 6	30.5 [12]	III.D.2	tensiometer 14	30.5 [12]
III.B.3	tensiometer 7	45.7 [18]	III.D.3	tensiometer 15	45.7 [18]
III.B.4	tensiometer 8	61 [24]	III.D.4	tensiometer 16	61 [24]

- Subsequent field density water content measurements

  Water contents were measured at 4 zones adjacent to the TDR locations. Water content information was used to calibrate the TDRs. Also sand cone test were conducted every time that a change of soil texture was evident. The core method was used to obtain more information about soil density and water content of the soil profile.

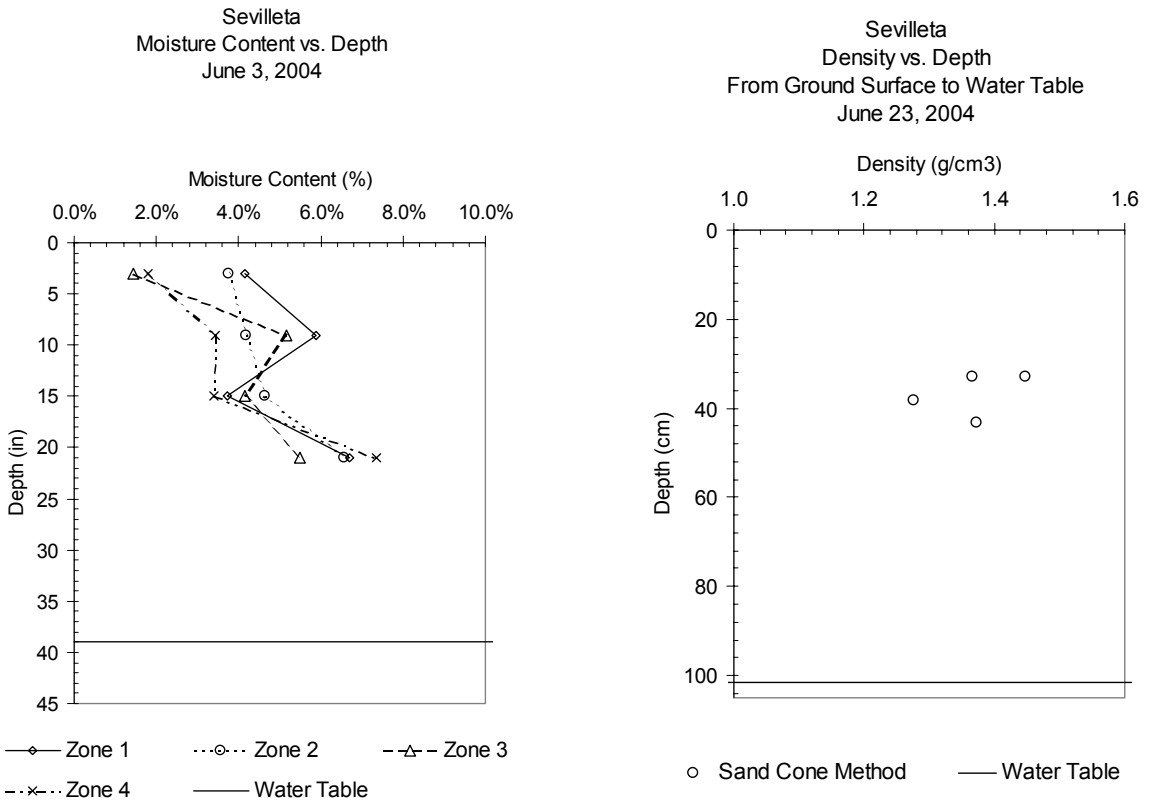

Figure 25 Gravimetric soil moisture content profile Site II and soil dry densities all zones

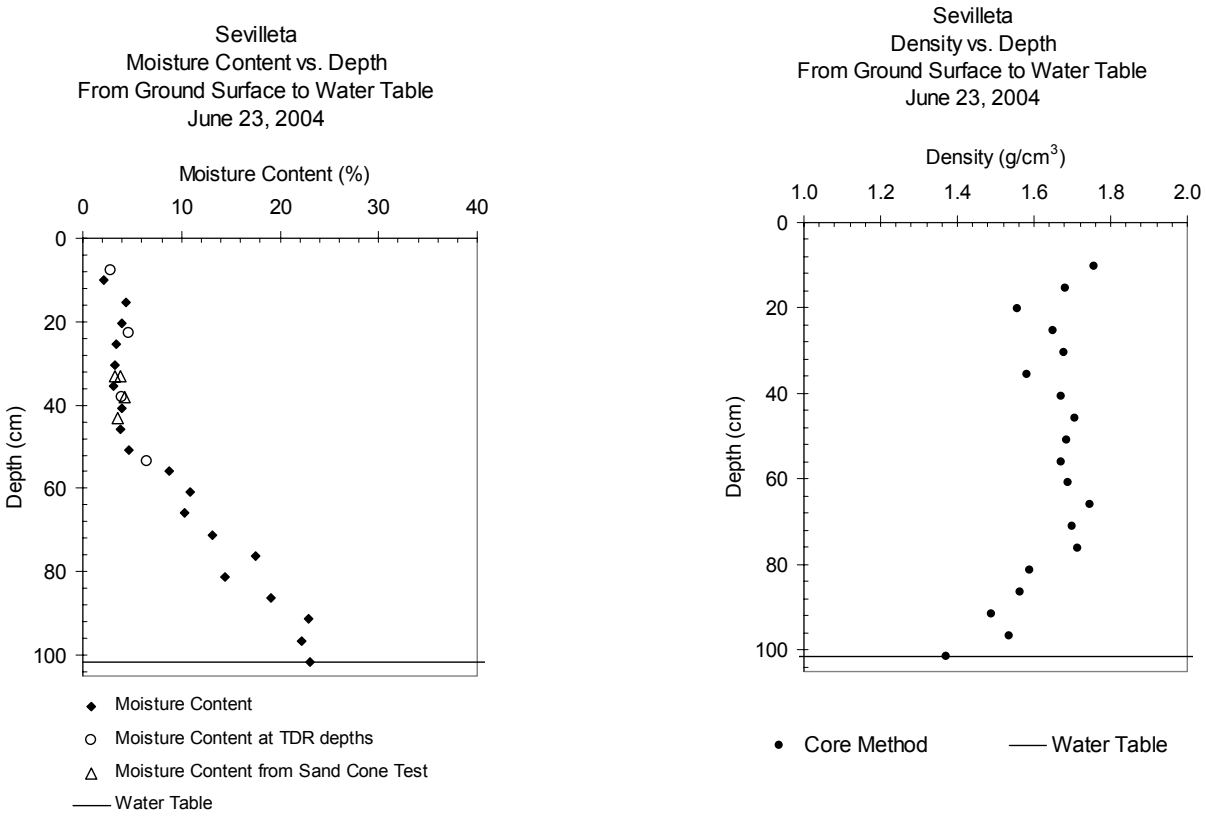

Figure 26 Core method results zone 1

Site-specific calibrations

Figure 27 shows the calibration curve for Site III with $R^2 = 0.99$. We can note that the calibration curve differs from the previous calibration curves. This difference is produced by the narrow information of the correlation between TDRs responses and water content. Most of the data is concentrated in the range of 5% moisture content.

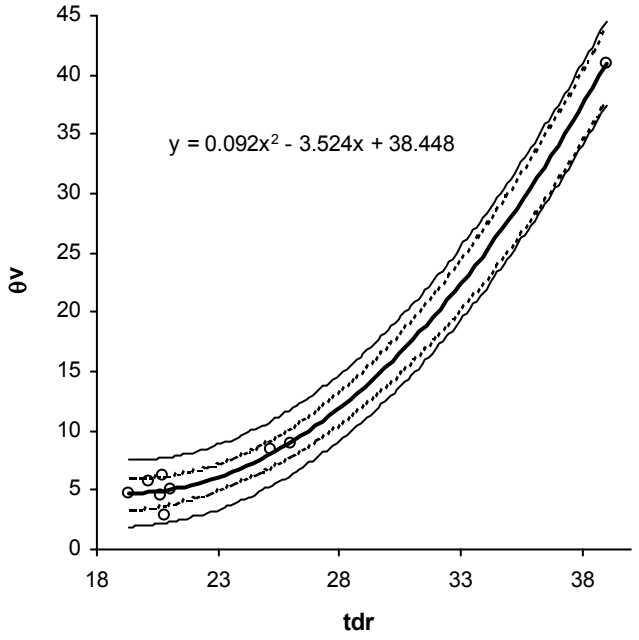

Figure 27 Calibration curve for TDR's Site III

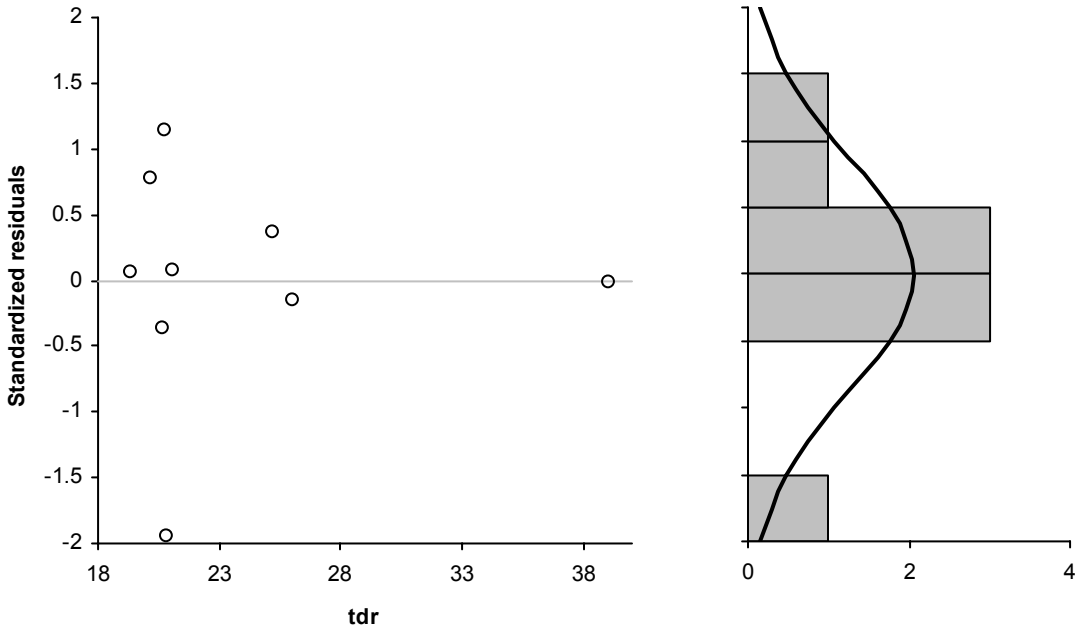

Figure 28 Standardized residuals for the calibration curve

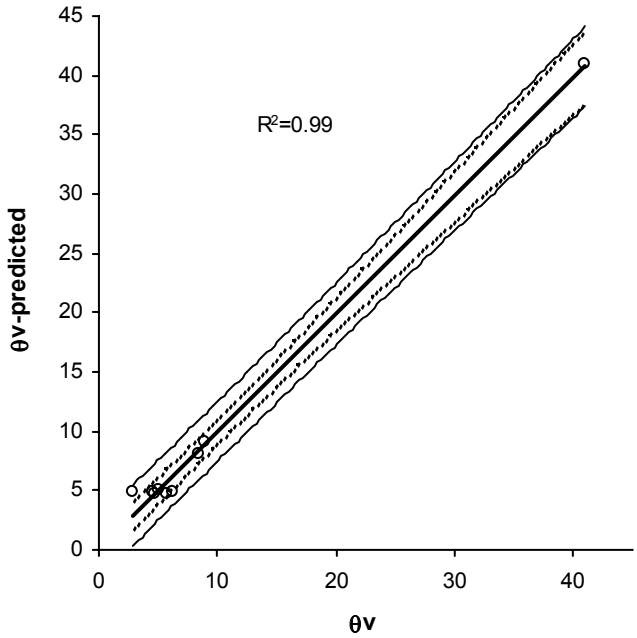

Figure 29 Volumetric water content measured (θv) vs. volumetric water content predicted (θv-predicted)

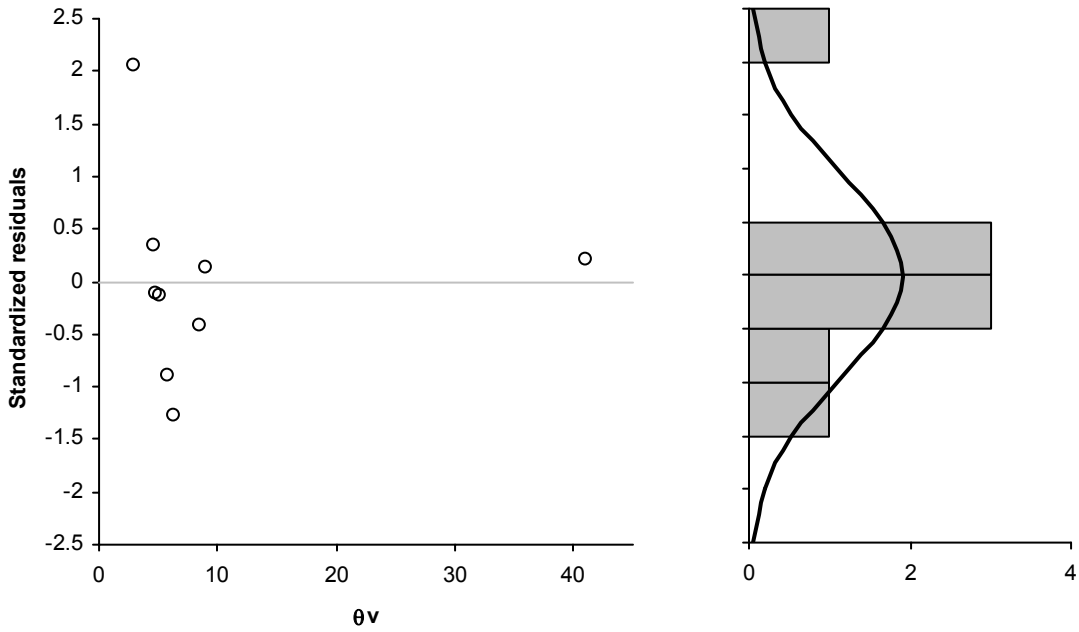

Figure 30 Standardized residuals for θv vs. θv-prediction

The values of the standardized residuals are between –2 and +2 (figure 26) for Site III. This indicates that the proposed calibration curve provides a reasonable correlation between the sensors readings and the soil water content.

- Changes in water table

At the time of installation the water table was at 53 cm (21 in) (5/18/04). June 14 the water table level was 97.8 cm (38.5 in,) and on July 2 the water table was located at 94 cm (37 in.)

Soil Samples

- Location

The soil samples were obtained from 5 areas.
Zone 1 between A and B
Zone 2 near B, between B and C
Zone 3 near C between area 1 and area C

Zone 4 between C and D

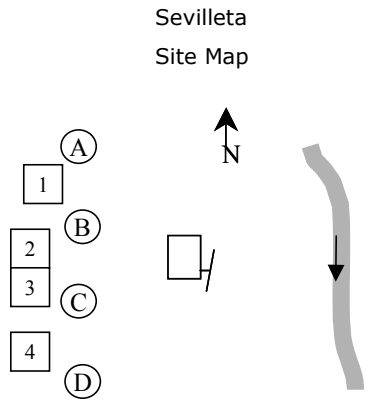

Figure 31 Site map of the sample zones

- Tests (see Appendix C,D and E)

1. Water content
2. Particle size analysis sieve analysis
3. Particle size analysis hydrometer
4. Field density test sand cone
5. Field density test and moisture content sore method
6. Specific Gravity

- Summary

Sevilleta

	cm	in	
SL	0-10.2	0-4.00	(Sandy loam)
S	10.2-102	4.00-40.00	(Sand)

Average density	1.60	g/cm3
Specific Gravity	2.64	

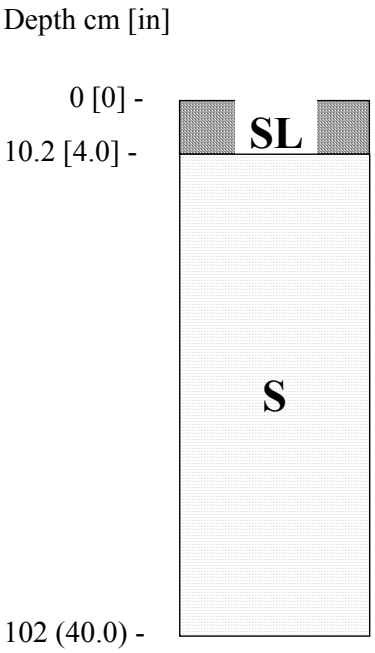

Figure 32 Soil profile Site III

Civil Engineering Bosque Laboratory (CEBL)

Summary of the installation

Date: June 29, 2004
Coordinates:
Water table: 38.1 cm (15 in)

As-Built Configuration:

The CEBL site is located along the Rio Grande about a mile north of Central Ave. in Albuquerque. This area is adopted by the Civil Engineering Department from the City of Albuquerque – Open Space Division for the purpose of service, education, and research. The equipment was installed along the bank of an artificial wetland approximately 183 m (200 yd) west of the river. The instrumentation was installed on a slope that provides different water table levels. Areas A and B are 1.3 m (4.3 ft) apart and between B and C, are 1.1 m (3.5 ft) apart (see Appendix F).

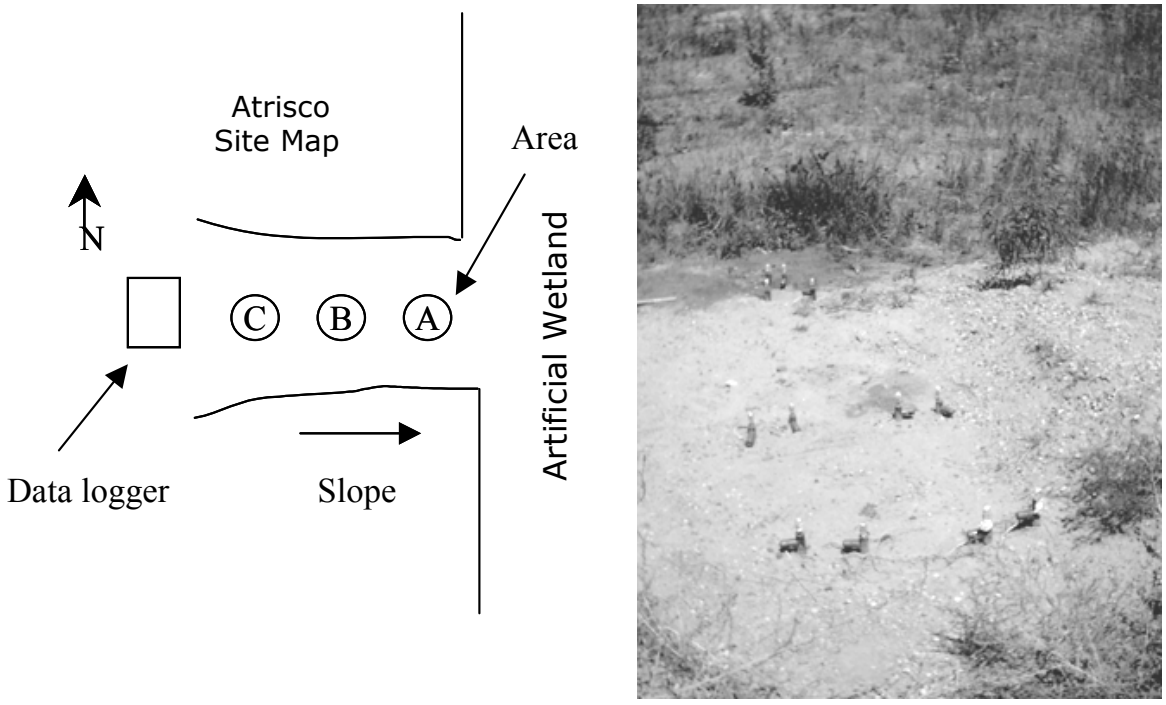

Figure 33 Site map and photograph (top view) of Atrisco

The Three areas were installed in this site.

- Bare soil sun Area A

- Bare soil sun Area B
- Bare soil sun Area C

Each area has the following instrumentation:

- 4 TDR
- 4 tensimeters cable connection
- 5 thermocouples

Gage Labeling:

Label	Instrument	Location from the surf. [in]	Label	Instrument	Location from the surf. [in]
IV.A.1	TDR 1	7.2 [3]	IV.C.1	TDR 9	7.2 [3]
IV.A.2	TDR 2	22.9 [9]	IV.C.2	TDR 10	22.9 [9]
IV.A.3	TDR 3	38.1 [15]	IV.C.3	TDR 11	38.1 [15]
IV.A.4	TDR 4	53.3 [21]	IV.C.4	TDR 12	53.3 [21]
IV.A.1	thermocouple 1	1.27 [0.5]	IV.C.1	thermocouple 11	1.27 [0.5]
IV.A.2	thermocouple 2	7.2 [3]	IV.C.2	thermocouple 12	7.2 [3]
IV.A.3	thermocouple 3	15.2 [6]	IV.C.3	thermocouple 13	15.2 [6]
IV.A.4	thermocouple 4	30.5 [12]	IV.C.4	thermocouple 14	30.5 [12]
IV.A.5	thermocouple 5	61 [24]	IV.C.5	thermocouple 15	61 [24]
IV.A.1	tensiometer 1	15.2 [6]	IV.C.1	tensiometer 9	15.2 [6]
IV.A.2	tensiometer 2	30.5 [12]	IV.C.2	tensiometer 10	30.5 [12]
IV.A.3	tensiometer 3	45.7 [18]	IV.C.3	tensiometer 11	45.7 [18]
IV.A.4	tensiometer 4	61 [24]	IV.C.4	tensiometer 12	61 [24]
IV.B.1	TDR 5	7.2 [3]			
IV.B.2	TDR 6	22.9 [9]			
IV.B.3	TDR 7	38.1 [15]			
IV.B.4	TDR 8	53.3 [21]			
IV.B.1	thermocouple 6	1.27 [0.5]			
IV.B.2	thermocouple 7	7.2 [3]			
IV.B.3	thermocouple 8	15.2 [6]			
IV.B.4	thermocouple 9	30.5 [12]			
IV.B.5	thermocouple 10	61 [24]			
IV.B.1	tensiometer 5	15.2 [6]			
IV.B.2	tensiometer 6	30.5 [12]			
IV.B.3	tensiometer 7	45.7 [18]			
IV.B.4	tensiometer 8	61 [24]			

- Subsequent field density water content measurements

Measurements of water content were obtained at 3 areas adjacent to the TDR locations. This water content information was used for the TDR calibration. A sample of the water content was taken at the level of the TDRs. Also sand cone tests were conducted every time that a

change of soil texture was evident. In order to confirm the results, the core test was also used to

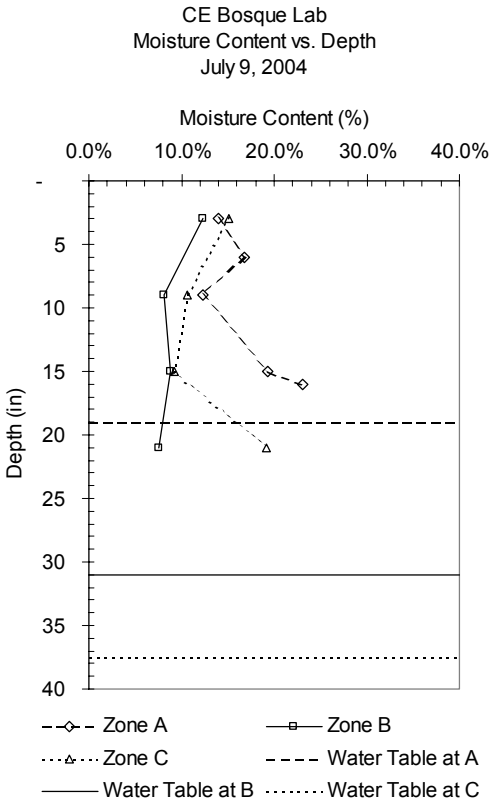

determine water content profiles.

Figure 34 Gravimetric soil moisture content profil zones

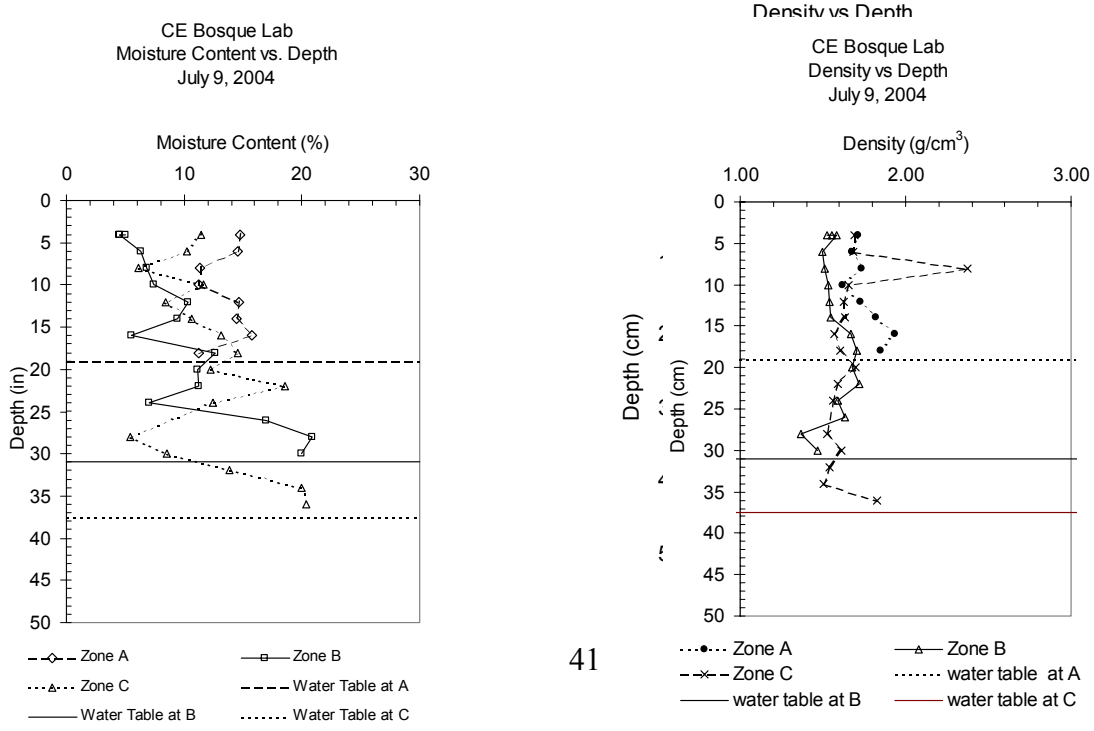

Figure 35 Core method results

Site-specific calibrations

With the information obtained from the soil density and the moisture content TDRs were calibrated. The pressure transducers from the tensiometers were calibrated in the laboratory. Figure 37 shows the TDR calibration curve for CEBL site with $R^2 = 0.77$.

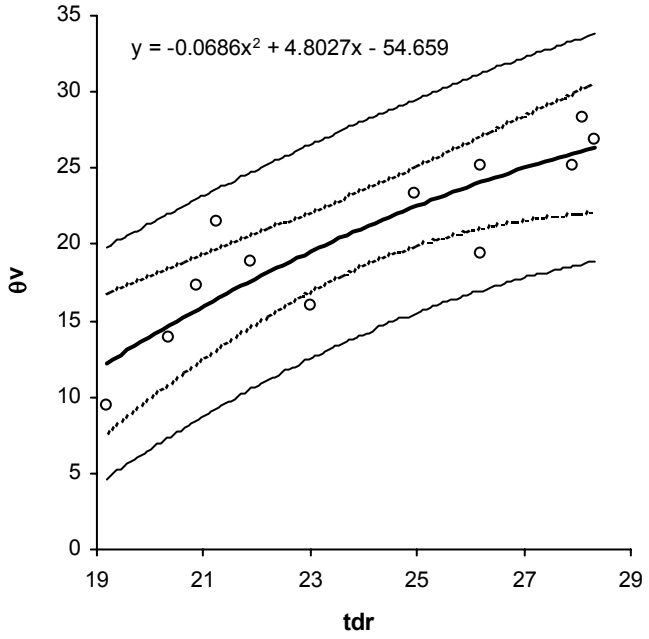

Figure 36 Calibration curve for TDR's Site IV

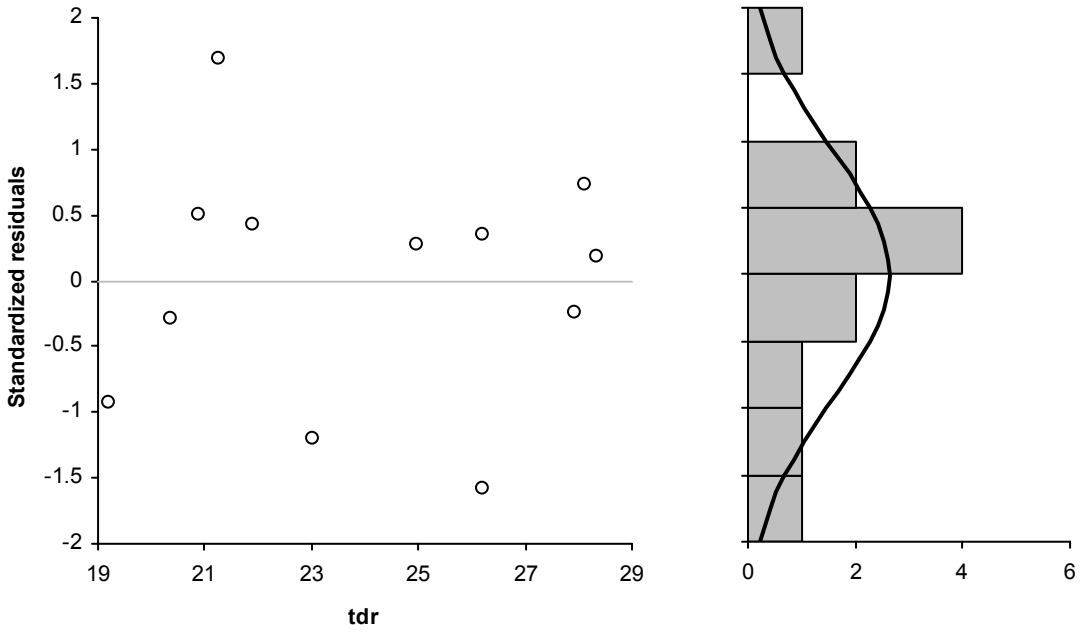

Figure 37 Standardized residuals for the calibration curve

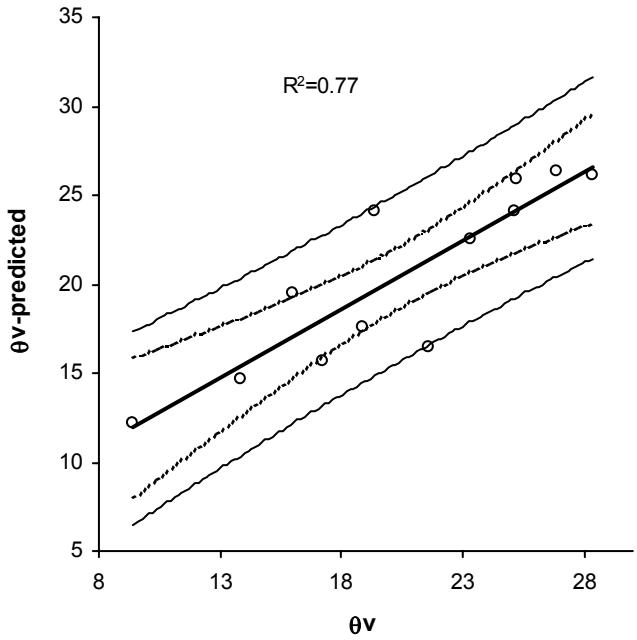

Figure 38 Volumetric water content measured (θv) vs. volumetric water content predicted (θv-predicted)

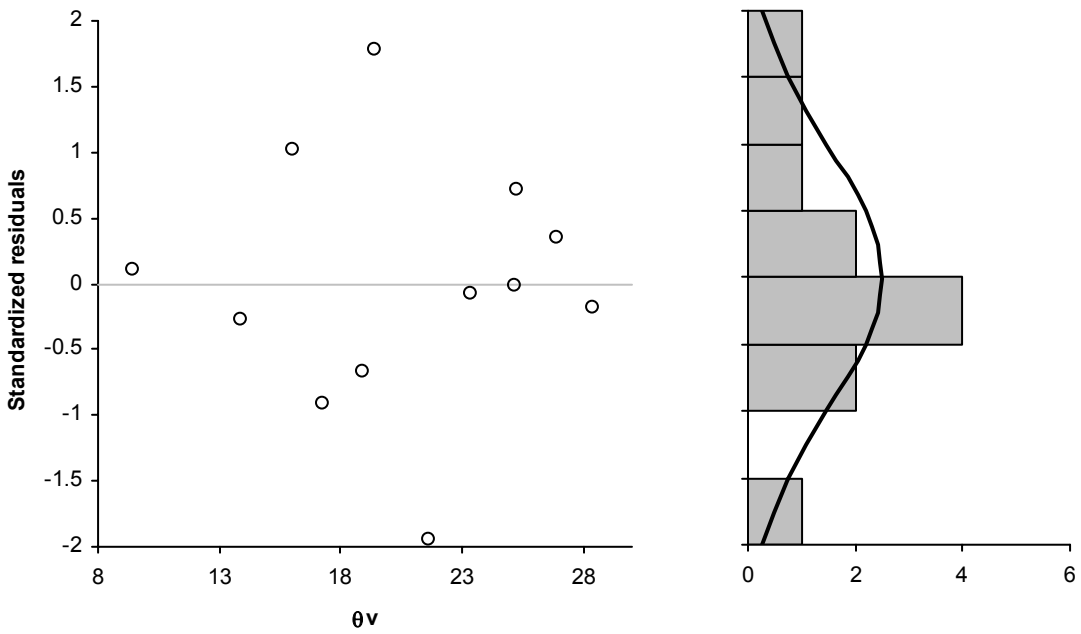

Figure 39 Standardized residuals for θv vs. θv-prediction

Figure 37 shows the standardized residuals for the calibration curve. The residuals are randomly distributed about zero according to the normal distribution and all standardized residuals lie between –2 and +2. Figure 38 shows the correlation between measured water content and predicted water content. The standardized residuals for θv vs. θv-prediction are shown in figure 39.

Soil Samples

- Location (see figure 40)

  The soil samples were obtained from 3 areas.
  Zone 1 near area A
  Zone 2 near area B
  Zone 3 near area C

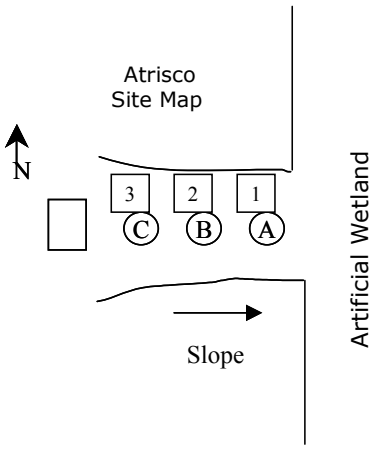

Figure 40 Site map of the sample zones

- Tests (see Appendix C,D and E)

1. Water content
2. Particle size analysis sieve analysis
3. Particle size analysis hydrometer
4. Field density test sand cone
5. Field density test and moisture content sore method
6. Specific Gravity

- Summary

CEBL

	cm	in	
SL	0-15.2	0-6.0	(Sandy loam)
CS	15.2-102	6.00-40.00	(Course Sand)

Average density	1.60	g/cm3
Specific Gravity	2.64	

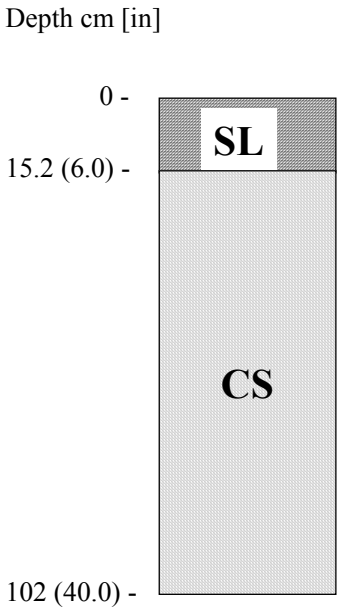

Figure 41 Soil profile Site IV

Belen

Summary of the installation

Date: May 20, 2004
Coordinates:
Water table: could not be measured

As-Built Configuration:

Because the lack of security in the site, the data logger was installed inside of the fence near the ET tower. Two areas were selected inside of the fenced area. Areas A and B are 1.5 m (5 ft) apart and 1.2 (4 ft) from the box.

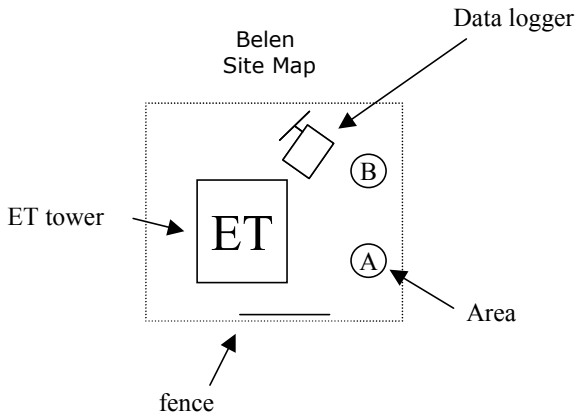

Figure 42 Site map of Belen

Only 2 areas were installed at this site.

- bare soil shade Area A
- bare soil shade Area B

Each area has the following instrumentation:

- 4 TDR
- 4 tensimeters cable connection
- 5 thermocouples

Gage Labeling:

Label	Instrument	Location from the surf. cm [in]	Label	Instrument	Location from the surf. cm [in]
V.A.1	TDR 1	7.2 [3]	V.B.1	TDR 5	7.2 [3]
V.A.2	TDR 2	22.9 [9]	V.B.2	TDR 6	22.9 [9]
V.A.3	TDR 3	38.1 [15]	V.B.3	TDR 7	38.1 [15]
V.A.4	TDR 4	53.3 [21]	V.B.4	TDR 8	53.3 [21]
V.A.1	thermocouple 1	1.27 [0.5]	V.B.1	thermocouple 6	1.27 [0.5]
V.A.2	thermocouple 2	7.2 [3]	V.B.2	thermocouple 7	7.2 [3]
V.A.3	thermocouple 3	15.2 [6]	V.B.3	thermocouple 8	15.2 [6]
V.A.4	thermocouple 4	30.5 [12]	V.B.4	thermocouple 9	30.5 [12]
V.A.5	thermocouple 5	61 [24]	V.B.5	thermocouple 10	61 [24]
V.A.1	tensiometer 1	15.2 [6]	V.B.1	tensiometer 5	15.2 [6]
V.A.2	tensiometer 2	30.5 [12]	V.B.2	tensiometer 6	30.5 [12]
V.A.3	tensiometer 3	45.7 [18]	V.B.3	tensiometer 7	45.7 [18]
V.A.4	tensiometer 4	61 [24]	V.B.4	tensiometer 8	61 [24]

Significant field occurrences/observations

This site was vandalized shortly after field installation. Consequently, no further work has been conducted at this site.

Unified Calibration curve

Although there is a variability of soil textures at different sites, a combination of water content and TDR responses from all sites can be considered for a unified calibration curve. The soil profiles show us that the variations in soil texture at different sites are in the sandy soil range. These types of soils have very stable particles with very low electrical activity compared with clay minerals. Topp (1980) concluded that a single equation could be used to describe the relationship between the soil water content and the dielectric constant for different soils.

Figure 43 shows the unified calibration curve proposed for all sites. A good correlation can be observed with R^2=0.81 and a confidence of 95%. Figure 44 sustains this correlation; the standardized residuals are randomly distributed around zero and most of the values for the standardized residuals are between the range –2 and +2.

The unified calibration curve can be expressed as:

$$\theta_v = -0.0807 * \tau^2 + 6.746 * \tau + 94.802 \qquad \text{eq. 2}$$

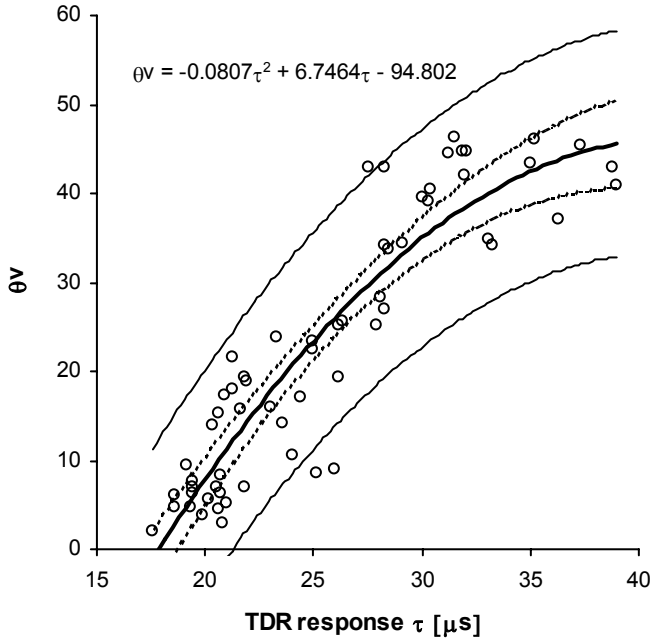

Figure 42 CS616 quadratic calibration

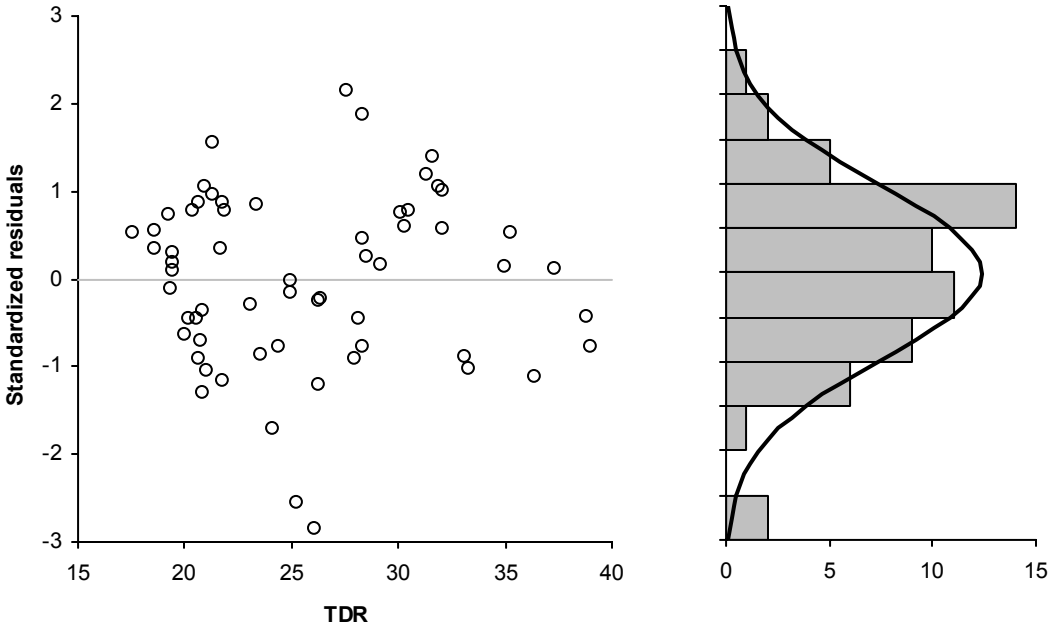

Figure 44 Standardized residuals for the unified calibration curve

APPENDIX A

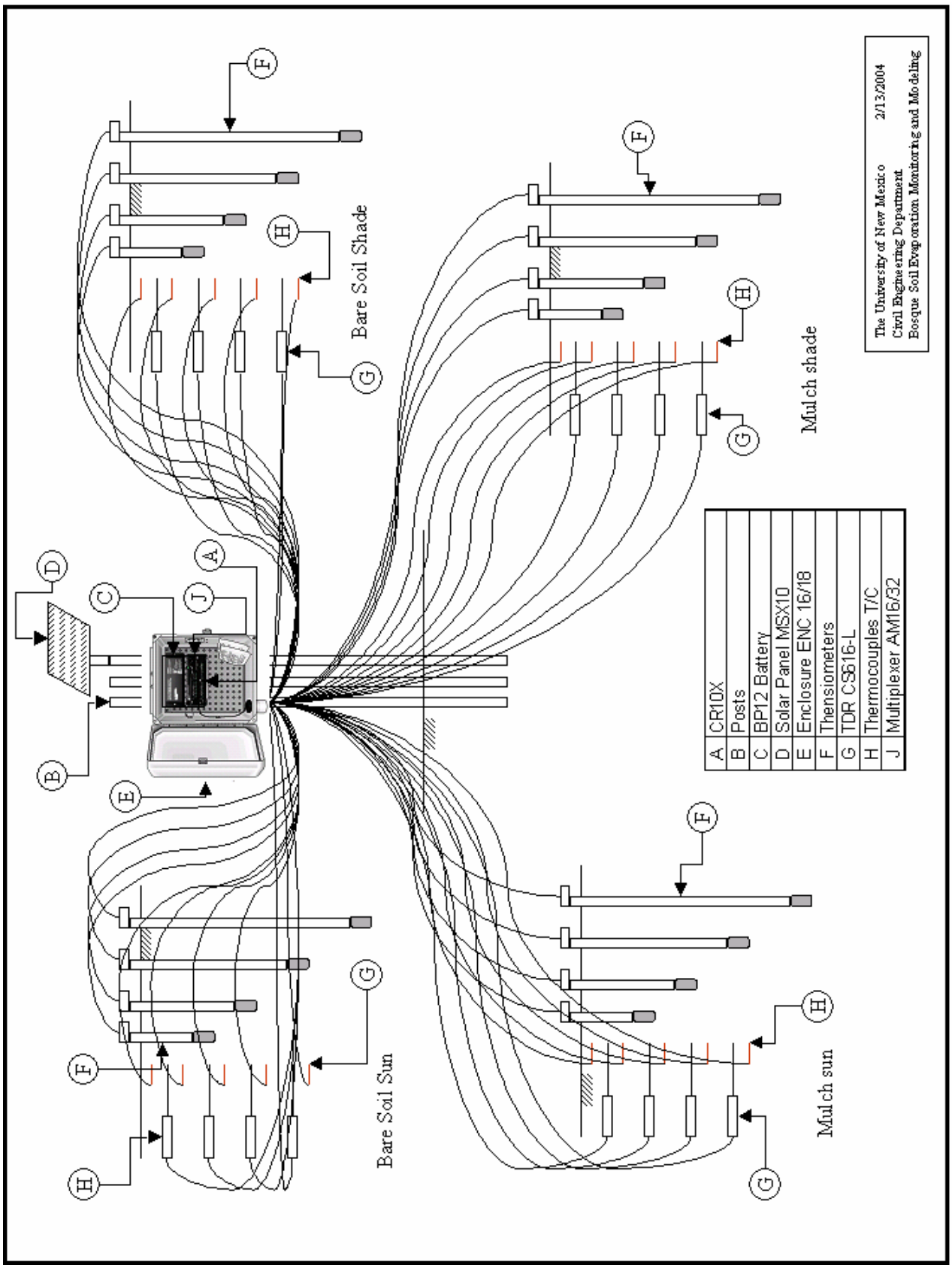
Bare Soil Shade
Mulch shade
Bare Soil Sun
Mulch sun
A CR10X
B Posts
C BP12 Battery
D Solar Panel MSX10
E Enclosure ENC 16/18
F Thensiometers
G TDR CS616-L
H Thermocouples T/C
J Multiplexer AM16/32
The University of New Mexico 2/13/2004
Civil Engineering Department
Bosque Soil Evaporation Monitoring and Modeling

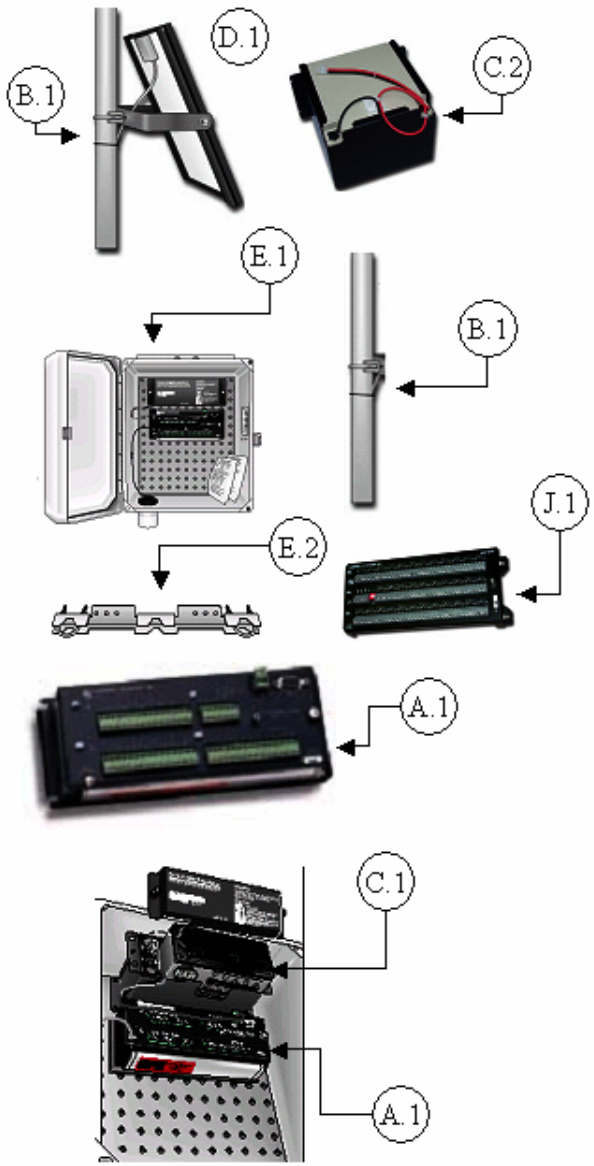

		Qty	Description
A.1	CR10X	1	
A.1.2	cable	1	From the data loger to the battery
A.1.3	screws	4	
B.1	Post	3	1.00" to 1.25" IPS pipe
B.2	Post Driver	1	
C.1	BP12 Baterry	1	
C.2	Regulator CH100	1	
C.3	screws	8	
D.1	Solar Panel	1	
D.2	U bolt	1	1.00" to 1.25" IPS pipe
E.1	Enclosure ENC 16/18	1	
E.2	Bracket	2	Triple notch for use with a UT30
E.3	Screws	4	
E.4	U bolt	6	
J.1	Multiplexer AM16/32	1	
J.2	Screws	4	
J.3	cable	1	Fom the CR10X to the Mult.

The University of New Mexico 2/13/2004
Civil Engineering Department
Bosque Soil Evaporation Monitoring and Modeling

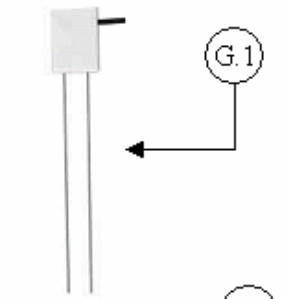

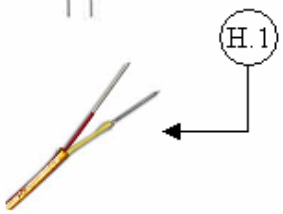

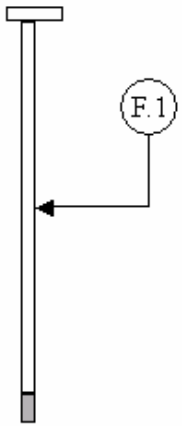

		Qty	Description
F.1	Tensiometers	20	(2x12" 1x18 1x32")*4
F.2	post hole diger	1	
F.3	plug	20	
F.4	insolation	20	cups
F.4	cable	20	
G.1	TDR CS616-L	16	
H.1	Thermocouples	20	end welded

The University of New Mexico 2/13/2004
Civil Engineering Department
Bosque Soil Evaporation Monitoring and Modeling

APPENDIX B
Tensiometer Calibration

Tensiometer calibrations Site I (Bosque del Apache South)

Instrument	Calibration curve
I.A.1	y = 129.87x + 84.044
I.A.2	y = 126.11x + 96.381
I.A.3	y = 126.11x + 94.943
I.A.4	y = 122.78x + 82.262
I.B.1	y = 127.26x + 119.44
I.B.2	y = 127.82x + 111.57
I.B.3	y = 123.38x + 110.86
I.B.4	y = 130.93x + 135.23
I.C.1	y = 126.69x + 118.36
I.C.2	y = 130.81x + 121.65
I.C.3	y = 126.69x + 98.275
I.C.4	y = 128.71x + 109.03
I.D.1	y = 128.14x + 108.73
I.D.2	y = 128.42x + 116.87
I.D.3	y = 130.21x + 119.98
I.D.4	y = 123.44x + 108.98

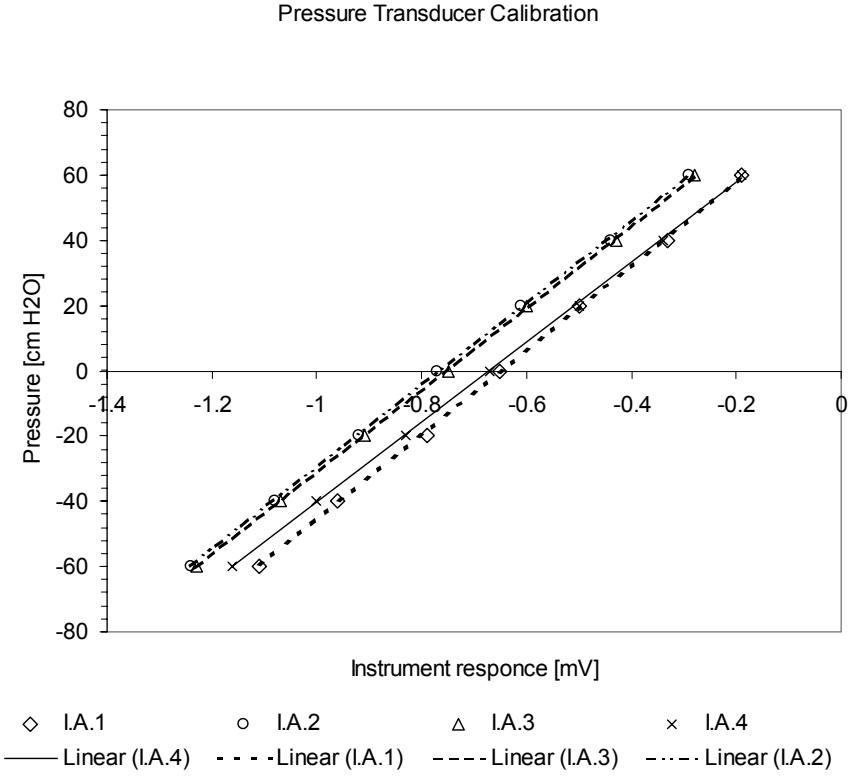

Pressure Transducer Calibration

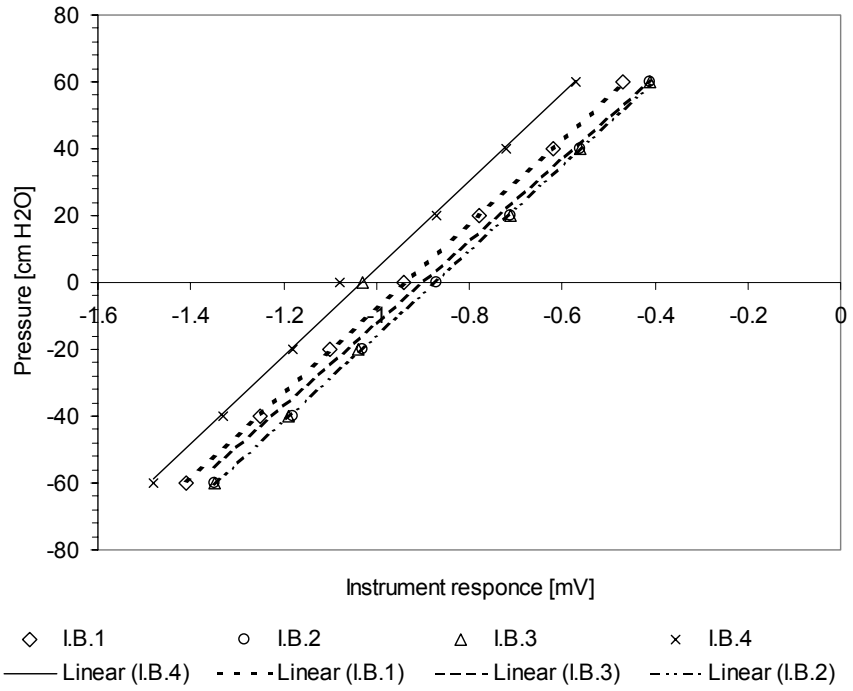

Pressure Transducer Calibration

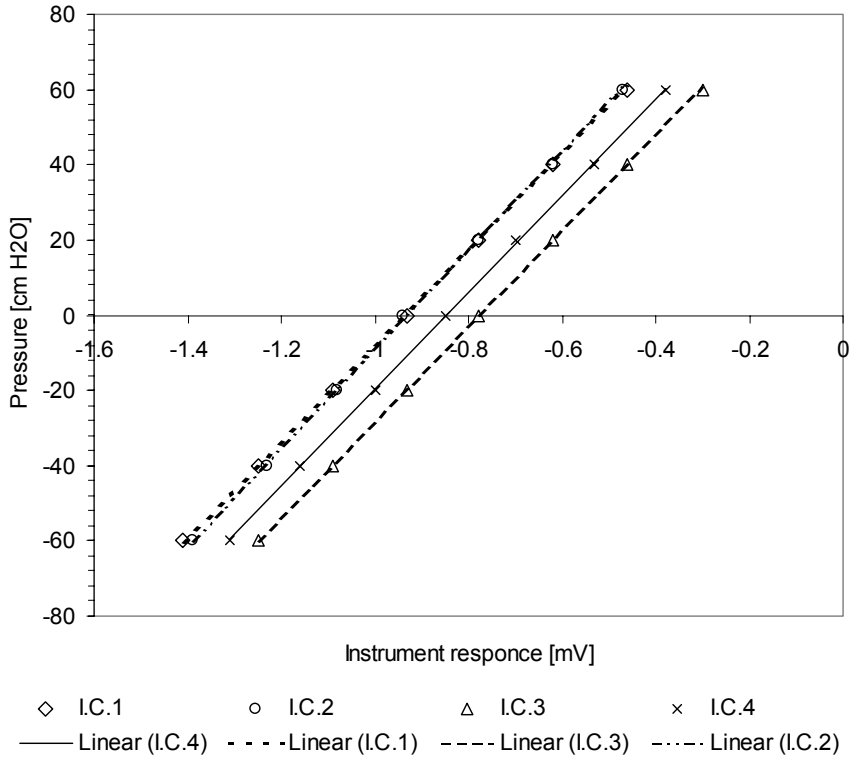

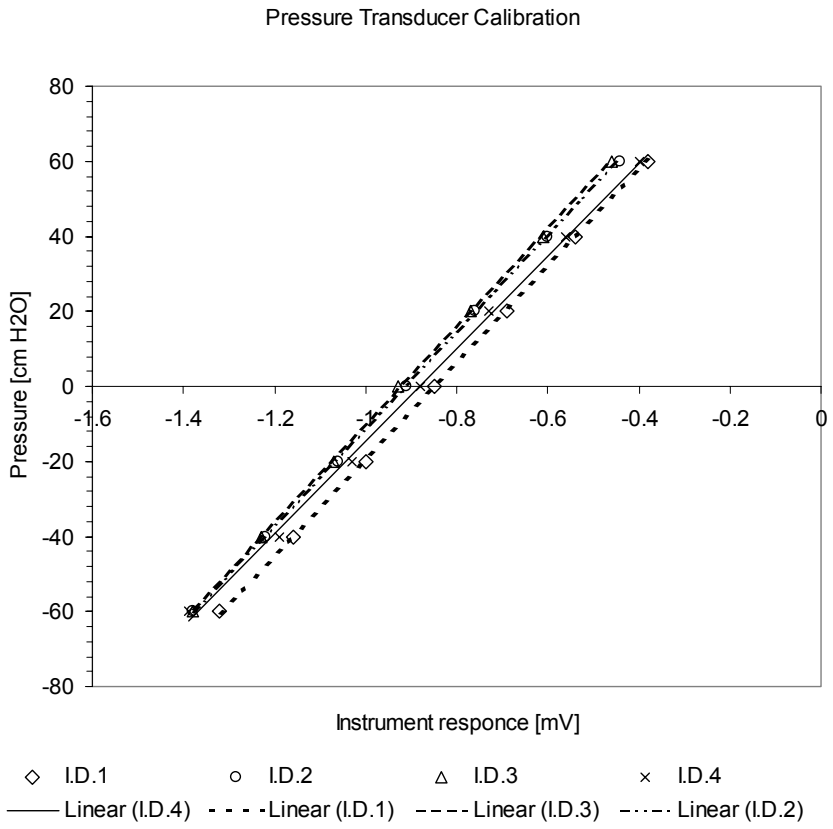

Tensiometer calibrations Site IV (Civil Engineering Bosque Laboratory)

Instrument	Calibration curve
IV.A.1	y = 154.95x + 57.776
IV.A.2	y = 145.35x + 45.68
IV.A.3	y = 150.05x + 66.879
IV.A.4	y = 149.26x + 47.976
IV.B.1	y = 148.09x + 55.006
IV.B.2	y = 145.02x + 20.717
IV.B.3	y = 150.44x + 46.207
IV.B.4	y = 153.8x + 85.688
IV.C.1	y = 145.69x + 33.925
IV.C.2	y = 146.2x + 44.277
IV.C.3	y = 149.32x + 52.474
IV.C.4	y = 146.2x + 54.511

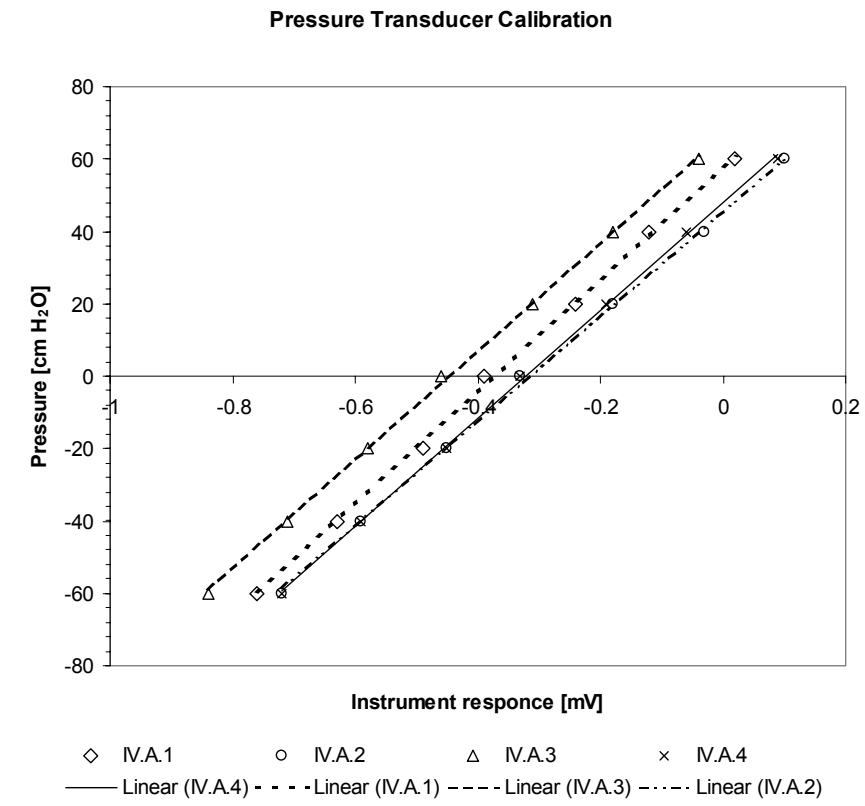
Pressure Transducer Calibration
Pressure [cm H2O]
Instrument responce [mV]
IV.A.1
IV.A.2
IV.A.3
IV.A.4
Linear (IV.A.4)
Linear (IV.A.1)
Linear (IV.A.3)
Linear (IV.A.2)

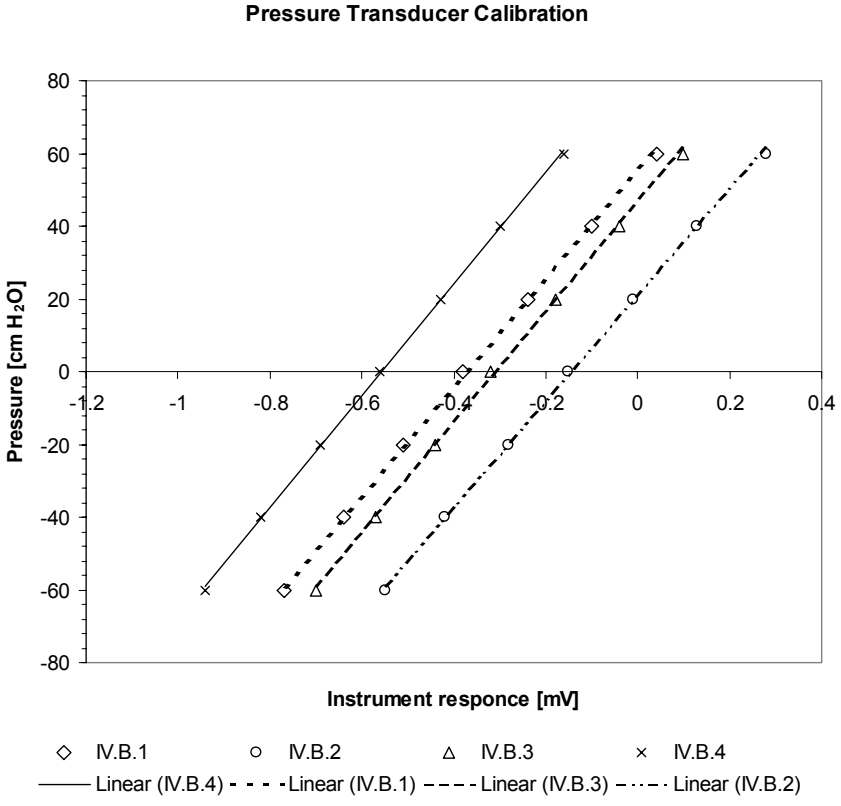
Pressure Transducer Calibration
Pressure [cm H2O]
Instrument responce [mV]
IV.B.1
IV.B.2
IV.B.3
IV.B.4
Linear (IV.B.4)
Linear (IV.B.1)
Linear (IV.B.3)
Linear (IV.B.2)

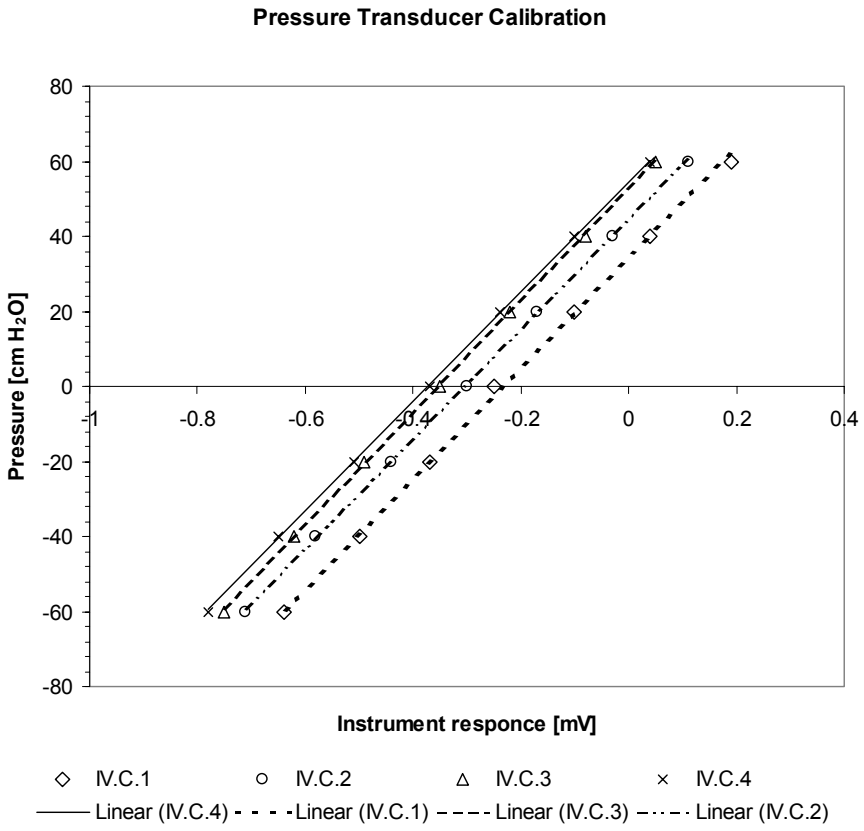
Pressure Transducer Calibration
80
60
40
20
0
-20
-40
-60
-80
-1
-0.8
-0.6
-0.4
-0.2
0
0.2
0.4
Pressure [cm H2O]
Instrument responce [mV]
IV.C.1
IV.C.2
IV.C.3
IV.C.4
Linear (IV.C.4)
Linear (IV.C.1)
Linear (IV.C.3)
Linear (IV.C.2)

APPENDIX C
Soil Classification

C.1 Sieve Analysis
C.2 Hydrometer Analysis
C.3 Particle Size Distribution
C.4 Soil Classification Results

C.1 Sieve Analysis

Sieve Analysis for Fine Grained Soil

Site **Sevilleta**

Zone S3 Depth 0-4"
Tested by Sarah and Craig
Date Time

Initial dry mass	827.3 g	Mass after washing through #200	513.2 g	Percent finer than No 200 sieve	38.0%

Sieve No.	Sieve Opening (mm)	Mass of Sieve	Mass of Sieve + retained soil	Mass of soil retained on each sieve, W_n (g)	Percent of mass retained on each sieve, R_n	Percent mass retained adjusted, R_n	Cumulative percent retained, ΣR_n	Percent Finer, 100-ΣR_n
3/8"	9.525	0	0	0.0	0.0%	0.0%	0.0%	100.0%
4	4.75	530.6	531	0.4	0.1%	0.0%	0.0%	100.0%
10	2	464.5	464.9	0.4	0.1%	0.0%	0.1%	99.9%
20	0.85	413.2	415.0	1.8	0.4%	0.2%	0.3%	99.7%
40	0.425	369.9	434.7	64.8	12.6%	7.8%	8.1%	91.9%
60	0.25	353.4	586.8	233.4	45.5%	28.2%	36.4%	63.6%
140	0.106	342.1	526.1	184.0	35.9%	22.2%	58.6%	41.4%
200	0.075	339	364	25.0	4.9%	3.0%	61.6%	38.4%
Pan	0	495.8	499.7	3.9	0.8%	38.4%	100.1%	-0.1%
			Total Mass	**513.7**	**100%**	**100.1%**		

Zone S3 Depth 4-20"
Tested by Sarah and Craig
Date 8-Jul-04 Time 10:15 AM

Initial dry mass	680.8 g	Mass after washing through #200	660.4 g	Percent finer than No 200 sieve	3.0%

Sieve No.	Sieve Opening (mm)	Mass of Sieve	Mass of Sieve + retained soil	Mass of soil retained on each sieve, W_n (g)	Percent of mass retained on each sieve, R_n	Percent mass retained adjusted, R_n	Cumulative percent retained, ΣR_n	Percent Finer, 100-ΣR_n
3/8"	9.525	482.7	482.7	0.0	0.0%	0.0%	0.0%	100.0%
4	4.75	530.6	531.4	0.8	0.1%	0.1%	0.1%	99.9%
10	2	464.6	474.0	9.4	1.4%	1.4%	1.5%	98.5%
20	0.85	413.3	430.8	17.5	2.6%	2.6%	4.1%	95.9%
40	0.425	369.9	468.3	98.4	14.9%	14.5%	18.5%	81.5%
60	0.25	353.5	673.5	320.0	48.5%	47.0%	65.5%	34.5%
140	0.106	342.1	542.2	200.1	30.3%	29.4%	94.9%	5.1%
200	0.075	338.9	352.6	13.7	2.1%	2.0%	96.9%	3.1%
Pan	0	495.9	496.5	0.6	0.1%	3.1%	100.0%	0.0%
			Total Mass	**660.5**	**100%**	**100.0%**		

C.1 Sieve Analysis (continued)

Sieve Analysis for Fine Grained Soil

Site **Bosque del Apache Site 1**

Zone B1 Depth Top-5"
Tested by Sarah and Craig
Date 19-Jul-04 Time

Initial dry mass	547.0 g	Mass after washing through #200	122.1 g	Percent finer than No 200 sieve	77.7%

Sieve No.	Sieve Opening (mm)	Mass of Sieve	Mass of Sieve + retained soil	Mass of soil retained on each sieve, W_n (g)	Percent of mass retained on each sieve, R_n	Percent mass retained adjusted, R_n	Cumulative percent retained, ΣR_n	Percent Finer, 100-ΣR_n
3/8"	9.525	0	0	0	0%	0.0%	0.0%	100.0%
4	4.75	530.6	530.6	0	0%	0.0%	0.0%	100.0%
10	2	464.4	464.8	0.4	0%	0.1%	0.1%	99.9%
20	0.85	413.1	414.0	0.9	1%	0.2%	0.2%	99.8%
40	0.425	370	372.1	2.1	2%	0.4%	0.6%	99.4%
60	0.25	353.5	373.4	19.9	16%	3.6%	4.3%	95.7%
140	0.106	342.2	417.3	75.1	62%	13.7%	18.0%	82.0%
200	0.075	338.9	352.5	13.6	11%	2.5%	20.5%	79.5%
Pan	0	495.8	506.3	10.5	9%	79.6%	100.1%	-0.1%
			Total Mass	**122.5**	**100.3%**	**100.1%**		

Zone B1 Depth 5-10.75"
Tested by Sarah and Craig
Date 15-Jul-04 Time

Initial dry mass	846.5 g	Mass after washing through #200	794.9 g	Percent finer than No 200 sieve	6.1%

Sieve No.	Sieve Opening (mm)	Mass of Sieve	Mass of Sieve + retained soil	Mass of soil retained on each sieve, W_n (g)	Percent of mass retained on each sieve, R_n	Percent mass retained adjusted, R_n	Cumulative percent retained, ΣR_n	Percent Finer, 100-ΣR_n
3/8"	9.525			0	0%	0.0%	0.0%	100.0%
4	4.75	530.6	531	0.4	0%	0.0%	0.0%	100.0%
10	2	464.5	464.7	0.2	0%	0.0%	0.1%	99.9%
20	0.85	413.2	413.6	0.4	0%	0.0%	0.1%	99.9%
40	0.425	370	389.6	19.6	2%	2.3%	2.4%	97.6%
60	0.25	353.5	682.6	329.1	41%	38.9%	41.3%	58.7%
140	0.106	342.1	751.2	409.1	51%	48.3%	89.6%	10.4%
200	0.075	338.9	371.3	32.4	4%	3.8%	93.5%	6.5%
Pan	0	495.8	499.0	3.2	0%	6.5%	99.9%	0.1%
			Total Mass	**794.4**	**99.9%**	**99.9%**		

C.1 Sieve Analysis (continued)

Zone	B1	Depth	10.75-11.5"
Tested by	Sarah and Craig		
Date	15-Jul-04	Time	

Initial dry mass	611 g	Mass after washing through #200	188.9 g	Percent finer than No 200 sieve	69.1%

Sieve No.	Sieve Opening (mm)	Mass of Sieve	Mass of Sieve + retained soil	Mass of soil retained on each sieve, W_n (g)	Percent of mass retained on each sieve, R_n	Percent mass retained adjusted, R_n	Cumulative percent retained, ΣR_n	Percent Finer, 100-ΣR_n
3/8"	9.525			0	0%	0.0%	0.0%	100.0%
4	4.75	530.6	530.6	0	0%	0.0%	0.0%	100.0%
10	2	464.6	464.7	0.1	0%	0.0%	0.0%	100.0%
20	0.85	413.2	414.0	0.8	0%	0.1%	0.1%	99.9%
40	0.425	370.0	374.7	4.7	2%	0.8%	0.9%	99.1%
60	0.25	353.5	364.1	10.6	6%	1.7%	2.7%	97.3%
140	0.106	342.1	411.3	69.2	37%	11.3%	14.0%	86.0%
200	0.075	339.0	407.2	68.2	36%	11.2%	25.1%	74.9%
Pan	0	495.9	531.7	35.8	19%	74.9%	100.1%	-0.1%
			Total Mass	**189.4**	**100.3%**	**100.1%**		

Zone	B1	Depth	11.5-14.5"
Tested by	Sarah and Craig		
Date	15-Jul-04	Time	

Initial dry mass	600.1 g	Mass after washing through #200	568.4 g	Percent finer than No 200 sieve	5.3%

Sieve No.	Sieve Opening (mm)	Mass of Sieve	Mass of Sieve + retained soil	Mass of soil retained on each sieve, W_n (g)	Percent of mass retained on each sieve, R_n	Percent mass retained adjusted, R_n	Cumulative percent retained, ΣR_n	Percent Finer, 100-ΣR_n
3/8"	9.525	0	0	0	0%	0.0%	0.0%	100.0%
4	4.75	530.6	530.7	0.1	0%	0.0%	0.0%	100.0%
10	2	464.5	464.7	0.2	0%	0.0%	0.0%	100.0%
20	0.85	413.1	413.6	0.5	0%	0.1%	0.1%	99.9%
40	0.425	370	381.2	11.2	2%	1.9%	2.0%	98.0%
60	0.25	353.5	506.6	153.1	27%	25.5%	27.5%	72.5%
140	0.106	342.1	694.5	352.4	62%	58.7%	86.2%	13.8%
200	0.075	338.9	382.4	43.5	8%	7.2%	93.5%	6.5%
Pan	0	495.8	503.3	7.5	1%	6.5%	100.0%	0.0%
			Total Mass	**568.5**	**100.0%**	**100.0%**		

C.1 Sieve Analysis (continued)

Zone	B1	Depth	14.5-19.5" Clay layer
Tested by	Sarah and Craig		
Date	15-Jul-04	Time	

Initial dry mass	596.1 g	Mass after washing through #200	232.5 g	Percent finer than No 200 sieve	61.0%

Sieve No.	Sieve Opening (mm)	Mass of Sieve	Mass of Sieve + retained soil	Mass of soil retained on each sieve, W_n (g)	Percent of mass retained on each sieve, R_n	Percent mass retained adjusted, R_n	Cumulative percent retained, ΣR_n	Percent Finer, 100-ΣR_n
3/8"	9.525	0.0	0.0	0.0	0.0	0.0%	0.0%	100.0%
4	4.75	530.5	530.6	0.1	0.0	0.0%	0.0%	100.0%
10	2	464.4	464.6	0.2	0.0	0.0%	0.1%	99.9%
20	0.85	413.1	414.3	1.2	0.0	0.2%	0.3%	99.7%
40	0.425	370.0	372.7	2.7	0.0	0.5%	0.7%	99.3%
60	0.25	353.5	360.0	6.5	0.0	1.1%	1.8%	98.2%
140	0.106	342.1	431.8	89.7	0.4	15.0%	16.8%	83.2%
200	0.075	338.9	439.5	100.6	0.4	16.9%	33.7%	66.3%
Pan	0	495.9	528.2	32.3	14%	66.4%	100.1%	-0.1%
			Total Mass	**233.3**	**100.3%**	**100.1%**		

Zone	B1	Depth	19.5-76"
Tested by	Sarah and Craig		
Date	19-Jul-04	Time	2:13 PM

Initial dry mass	566.5 g	Mass after washing through #200	551.1 g	Percent finer than No 200 sieve	2.7%

Sieve No.	Sieve Opening (mm)	Mass of Sieve	Mass of Sieve + retained soil	Mass of soil retained on each sieve, W_n (g)	Percent of mass retained on each sieve, R_n	Percent mass retained adjusted, R_n	Cumulative percent retained, ΣR_n	Percent Finer, 100-ΣR_n
3/8"	9.525	0	0	0	0%	0.0%	0.0%	100.0%
4	4.75	530.5	530.5	0	0%	0.0%	0.0%	100.0%
10	2	464.5	464.5	0	0%	0.0%	0.0%	100.0%
20	0.85	413.1	413.3	0.2	0%	0.0%	0.0%	100.0%
40	0.425	369.9	375.5	5.6	1%	1.0%	1.0%	99.0%
60	0.25	353.4	592.4	239	43%	42.2%	43.2%	56.8%
140	0.106	342	625.5	283.5	51%	50.0%	93.3%	6.7%
200	0.075	338.9	359	20.1	4%	3.5%	96.8%	3.2%
Pan	0	495.8	498.5	2.7	0%	3.2%	100.0%	0.0%
			Total Mass	**551.1**	**100.0%**	**100.0%**		

C.1 Sieve Analysis (continued)

Sieve Analysis for Fine Grained Soil

Site **Bosque del Apache Site 2**

Zone II B2 Depth 5" Silty Layer
Tested by Sarah and Craig
Date 25-Jun-04 Time 9:20 AM

Initial dry mass	833.1 g	Mass after washing through #200	121.0 g	Percent finer than No 200 sieve	85.5%

Sieve No.	Sieve Opening (mm)	Mass of Sieve	Mass of Sieve + retained soil	Mass of soil retained on each sieve, W_n (g)	Percent of mass retained on each sieve, R_n	Percent mass retained adjusted, R_n	Cumulative percent retained, ΣR_n	Percent Finer, 100-ΣR_n
3/8"	9.525	482.7	482.7	0.0	0.0%	0.0%	0.0%	100.0%
4	4.75	530.5	530.7	0.2	0.2%	0.0%	0.0%	100.0%
10	2	464.4	464.7	0.3	0.2%	0.0%	0.1%	99.9%
20	0.85	413.0	414.2	1.2	1.0%	0.1%	0.2%	99.8%
40	0.425	370.0	372.7	2.7	2.2%	0.3%	0.5%	99.5%
60	0.25	353.6	362.5	8.9	7.4%	1.1%	1.6%	98.4%
140	0.106	336.1	409.1	73.0	60.4%	8.8%	10.4%	89.6%
200	0.075	339.5	370.6	31.1	25.7%	3.7%	14.1%	85.9%
Pan	0	378.1	382.1	4.0	3.3%	86.0%	100.1%	-0.1%
			Total Mass	**121.4**	**100%**	**100.1%**		

Zone II B2 Depth 15"
Tested by Sarah and Craig
Date 25-Jun-04 Time 9:20 AM

Initial dry mass	589.4 g	Mass after washing through #200	557.7 g	Percent finer than No 200 sieve	5.4%

Sieve No.	Sieve Opening (mm)	Mass of Sieve	Mass of Sieve + retained soil	Mass of soil retained on each sieve, W_n (g)	Percent of mass retained on each sieve, R_n	Percent mass retained adjusted, R_n	Cumulative percent retained, ΣR_n	Percent Finer, 100-ΣR_n
3/8"	9.525	482.7	482.7	0.0	0.0%	0.0%	0.0%	100.0%
4	4.75	530.6	530.6	0.0	0.0%	0.0%	0.0%	100.0%
10	2	464.5	464.5	0.0	0.0%	0.0%	0.0%	100.0%
20	0.85	413.1	413.3	0.2	0.0%	0.0%	0.0%	100.0%
40	0.425	370.0	373.9	3.9	0.7%	0.7%	0.7%	99.3%
60	0.25	353.5	465.3	111.8	20.0%	19.0%	19.7%	80.3%
140	0.106	336.1	749.9	413.8	74.2%	70.2%	89.9%	10.1%
200	0.075	339.6	366.1	26.5	4.8%	4.5%	94.4%	5.6%
Pan	0	378.2	380.0	1.8	0.3%	5.7%	100.1%	-0.1%
			Total Mass	**558.0**	**100%**	**100.1%**		

C.1 Sieve Analysis (continued)

Sieve Analysis for Fine Grained Soil

Site **CE Bosque Lab**

Zone C Depth 1-6" Clay layer
Tested by Craig & Sarah
Date 12-Jul-04 Time 10:30 AM

Initial dry mass	636.6 g	Mass after washing through #200	263.4 g	Percent finer than No 200 sieve	58.6%

Sieve No.	Sieve Opening (mm)	Mass of Sieve	Mass of Sieve + retained soil	Mass of soil retained on each sieve, W_n (g)	Percent of mass retained on each sieve, R_n	Percent mass retained adjusted, R_n	Cumulative percent retained, ΣR_n	Percent Finer, 100-ΣR_n
3/8"	9.525	0.0	0.0	0.0	0.0%	0.0%	0.0%	100.0%
4	4.75	530.4	530.4	0.0	0.0%	0.0%	0.0%	100.0%
10	2	464.3	465.2	0.9	0.3%	0.1%	0.1%	99.9%
20	0.85	413.1	416.1	3.0	1.1%	0.5%	0.6%	99.4%
40	0.425	370.0	384.3	14.3	5.4%	2.2%	2.9%	97.1%
60	0.25	353.3	402.3	49.0	18.6%	7.7%	10.6%	89.4%
140	0.106	336.2	488.4	152.2	57.8%	23.9%	34.5%	65.5%
200	0.075	339.4	376.0	36.6	13.9%	5.7%	40.2%	59.8%
Pan	0	364.2	371.9	7.7	2.9%	59.8%	100.0%	0.0%
			Total Mass	**263.7**		**100.0%**		

Zone A Depth 6-15"
Tested by Sarah
Date 8-Jul-04 Time 10:30 AM

Initial dry mass	907.6 g	Mass after washing through #200	869.3 g	Percent finer than No 200 sieve	4.2%

Sieve No.	Sieve Opening (mm)	Mass of Sieve	Mass of Sieve + retained soil	Mass of soil retained on each sieve, W_n (g)	Percent of mass retained on each sieve, R_n	Percent mass retained adjusted, R_n	Cumulative percent retained, ΣR_n	Percent Finer, 100-ΣR_n
3/8"	9.525	482.6	517.1	34.5	4.0%	3.8%	3.8%	96.2%
4	4.75	530.6	539.8	9.2	1.1%	1.0%	4.8%	95.2%
10	2	464.5	484.8	20.3	2.3%	2.2%	7.1%	92.9%
20	0.85	413.2	482.2	69.0	7.9%	7.6%	14.7%	85.3%
40	0.425	369.9	628.4	258.5	29.7%	28.5%	43.1%	56.9%
60	0.25	353.4	603.8	250.4	28.8%	27.6%	70.7%	29.3%
140	0.106	342.1	553.4	211.3	24.3%	23.3%	94.0%	6.0%
200	0.075	338.9	354.2	15.3	1.8%	1.7%	95.7%	4.3%
Pan	0	495.9	497.1	1.2	0.1%	4.4%	100.0%	0.0%
			Total Mass	**869.7**		**100.0%**		

C.2 Hydrometer Analysis

Hydrometer Analysis

Site **Sevilleta**

Zone S3 — Depth 0-4"
Tested by Sarah and Craig
Date 12-Jul-04 — Time 2:56 PM
G_s 2.63 — Hydrometer Type
Dry mass of soil, W_s 50.01 g — Temperature of test, T 26 °C 27 °C
Meniscus correction, F_m 1.0 — Zero Correction, F_s 2.5 2
G_s correction, a 1.00

Time (actual)	Time (min)	Hydrometer Reading, R	Temperature, °C	Temp. Correction Factor, F_T	R_{cp}	Percent Finer $(a*R_{cp})*100/50$	R_{cL}	L (cm)	A	D (mm)
	2	31.0	26							
	4	17.0	26							
2:56 PM	2	30.0	26	1.65	29.15	59	31	11.2	0.0128	0.0303
2:58 PM	4	18.0	26	1.65	17.15	34	19	13.2	0.0128	0.0233
3:02 PM	8	14.0	26	1.65	13.15	26	15	13.8	0.0128	0.0168
3:10 PM	16	11.0	26	1.65	10.15	20	12	14.3	0.0128	0.0121
3:26 PM	30	9.0	26	1.65	8.15	16	10	14.7	0.0128	0.0090
3:56 PM	60	7.0	26	1.65	6.15	12	8	15.0	0.0128	0.0064
4:56 PM	120	6.5	26	1.65	5.65	11	8	15.0	0.0128	0.0045
6:56 PM	240	6.0	26	1.65	5.15	10	7	15.2	0.0128	0.0032
10:56 PM	480	6.0	26	1.65	5.15	10	7	15.2	0.0128	0.0023
6:56 AM	960	6.0	26	1.65	5.15	10	7	15.2	0.0128	0.0016
10:56 PM	1,920	5.5	26	1.65	4.65	9	7	15.2	0.0128	0.0011
6:56 AM	3,840	6.0	22	0.65	4.15	8	7	15.2	0.0134	0.0008
11:00 AM	4,076	6.0	25	1.40	4.90	10	7	15.2	0.0130	0.0008
2:56 PM	5,760	5.0	27	1.90	4.90	10	6	15.3	0.0127	0.0007

Zone S3 — Depth 4-40"
Tested by Sarah and Craig
Date 12-Jul-04 — Time 3:33 PM
G_s 2.66 — Hydrometer Type
Dry mass of soil, W_s 50.00 g — Temperature of test, T 26 °C 27 °C
Meniscus correction, F_m 0.5 — Zero Correction, F_s 4 4
G_s correction, a 1.00

Time (actual)	Time (min)	Hydrometer Reading, R	Temperature, °C	Temp. Correction Factor, F_T	R_{cp}	Percent Finer $(a*R_{cp})*100/50$	R_{cL}	L (cm)	A	D (mm)
3:27 PM	2	19.0	26							
	4	13.0	26							
3:33 PM	2	19.0	26	1.65	16.65	33	20	13.0	0.0127	0.0324
	4	13.0	26	1.65	10.65	21	14	14.0	0.0127	0.0238
3:41 PM	8	11.0	26	1.65	8.65	17	12	14.3	0.0127	0.0170
3:49 PM	16	9.5	26	1.65	7.15	14	11	14.5	0.0127	0.0121
4:03 PM	30	9.0	26	1.65	6.65	13	10	14.7	0.0127	0.0089
4:33 PM	60	8.0	26	1.65	5.65	11	9	14.8	0.0127	0.0063
5:33 PM	120	8.0	26	1.65	5.65	11	9	14.8	0.0127	0.0045
7:33 PM	240	7.0	26	1.65	4.65	9	8	14.8	0.0127	0.0032
11:33 PM	480	7.0	26	1.65	4.65	9	8	14.8	0.0127	0.0022
7:33 AM	960	7.0	26	1.65	4.65	9	8	14.8	0.0127	0.0016
11:33 PM	1,920	7.0	26	1.65	4.65	9	8	14.8	0.0127	0.0011
7:33 AM	3,840	7.0	22	0.65	3.65	7	8	14.8	0.0133	0.0008
11:00 AM	4,047	7.0	25	1.40	4.40	9	8	14.8	0.0129	0.0008
3:33 PM	5,760	6.5	27	1.90	4.40	9	8	14.8	0.0126	0.0006

C.2 Hydrometer Analysis (continued)

Hydrometer Analysis

Site **Bosque del Apache-North**

Zone B1
Tested by Sarah and Craig
Date
G_s 2.63
Dry mass of soil, W_s 50.07 g
Meniscus correction, F_m 1.0
G_s correction, a 1.00

Depth 0-5"
Time 2:56 PM
Hydrometer Type
Temperature of test, T 26 °C
Zero Correction, F_s 3.3

Time (actual)	Time (min)	Hydrometer Reading, R	Temperature, °C	Temp. Correction Factor, F_T	R_{cp}	Percent Finer $(a*R_{cp})*100/50$	R_{cL}	L (cm)	A	D (mm)
9:39 AM	2	34.0	26							
	4	28.0	26							
9:46 AM	2	34.0	26	1.65	32.35	65	35	10.6	0.0128	0.0295
	4	27.0	26	1.65	25.35	51	28	11.7	0.0128	0.0219
9:54 AM	8	22.0	26	1.65	20.35	41	23	12.5	0.0128	0.0160
10:02 AM	16	17.5	26	1.65	15.85	32	19	13.2	0.0128	0.0116
10:16 AM	30	14.5	26	1.65	12.85	26	16	13.7	0.0128	0.0086
10:46 AM	60	12.0	26	1.65	10.35	21	13	14.2	0.0128	0.0062
11:46 AM	120	10.0	26	1.65	8.35	17	11	14.5	0.0128	0.0044
1:46 PM	240	9.0	26	1.65	7.35	15	10	14.7	0.0128	0.0032
5:07 PM	441	9.0	27	1.90	7.60	15	10	14.7	0.0127	0.0023
1:37 AM	951	8.5	27	1.78	6.98	14	10	14.7	0.0127	0.0016
5:41 PM	1,915	7.5	27	1.90	6.10	12	9	14.8	0.0127	0.0011
1:18 AM	3,822	7.5	27	1.90	6.10	12	9	14.8	0.0127	0.0008
9:35 AM	5,749	7.5	26	1.65	5.85	12	9	14.8	0.0128	0.0006

Zone B1
Tested by Sarah and Craig
Date
G_s 2.67
Dry mass of soil, W_s 50.00 g
Meniscus correction, F_m 1.0
G_s correction, a 1.00

Depth 5-10.75"
Time 2:56 PM
Hydrometer Type
Temperature of test, T 26 °C
Zero Correction, F_s 3.3

Time (actual)	Time (min)	Hydrometer Reading, R	Temperature, °C	Temp. Correction Factor, F_T	R_{cp}	Percent Finer $(a*R_{cp})*100/50$	R_{cL}	L (cm)	A	D (mm)
9:30 AM	2	18.0	26							
	4	13.0	26							
9:36 AM	2	17.0	26	1.65	15.35	31	18	13.3	0.0126	0.0325
	4	13.5	26	1.65	11.85	24	15	13.8	0.0126	0.0234
9:44 AM	8	11.5	26	1.65	9.85	20	13	14.0	0.0126	0.0167
9:52 AM	16	10.0	26	1.65	8.35	17	11	14.5	0.0126	0.0120
10:06 AM	30	9.0	26	1.65	7.35	15	10	14.7	0.0126	0.0088
10:36 AM	60	8.0	26	1.65	6.35	13	9	14.8	0.0126	0.0063
11:36 AM	120	7.0	26	1.65	5.35	11	8	15.0	0.0126	0.0045
1:36 PM	240	6.7	26	1.65	5.05	10	8	15.0	0.0126	0.0032
5:05 AM	449	6.5	27	1.90	5.10	10	8	15.0	0.0125	0.0023
1:36 AM	960	6.1	27	1.78	4.58	9	7	15.2	0.0125	0.0016
5:40 PM	1,924	5.7	27	1.90	4.30	9	7	15.2	0.0125	0.0011
1:15 AM	3,819	5.5	27	1.90	4.10	8	7	15.2	0.0125	0.0008
9:34 AM	5,758	6.0	26	1.65	4.35	9	7	15.2	0.0126	0.0006

C.2 Hydrometer Analysis (continued)

Zone	B1	Depth	10.75-11.5"
Tested by	Sarah and Craig		
Date		Time	2:56 PM
G_s	2.65	Hydrometer Type	
Dry mass of soil, W_s	50.02 g	Temperature of test, T	26 °C
Meniscus correction, F_m	1.0	Zero Correction, F_s	3.3
G_s correction, a	1.00		

Time (actual)	Time (min)	Hydrometer Reading, R	Temperature, °C	Temp. Correction Factor, F_T	R_{cp}	Percent Finer $(a*R_{cp})*100/50$	R_{cL}	L (cm)	A	D (mm)
9:22 AM	2	16.5	26							
9:24 AM	4	13.0	26							
9:26 AM	2	17.0	26	1.65	15.35	31	18	13.3	0.0127	0.0328
9:28 AM	4	13.0	26	1.65	11.35	23	14	14.0	0.0127	0.0238
9:34 AM	8	11.0	26	1.65	9.35	19	12	14.3	0.0127	0.0170
9:42 AM	16	10.0	26	1.65	8.35	17	11	14.5	0.0127	0.0121
9:56 AM	30	9.0	26	1.65	7.35	15	10	14.7	0.0127	0.0089
10:26 AM	60	8.5	26	1.65	6.85	14	10	14.7	0.0127	0.0063
11:26 AM	120	7.5	26	1.65	5.85	12	9	14.8	0.0127	0.0045
1:26 PM	217	6.5	26	1.65	4.85	10	8	15.0	0.0127	0.0033
5:03 PM	480	6.0	27	1.90	4.60	9	7	15.2	0.0126	0.0022
1:34 AM	968	6.0	27	1.78	4.48	9	7	15.2	0.0126	0.0016
5:38 PM	1,932	5.5	27	1.90	4.10	8	7	15.2	0.0126	0.0011
1:10 AM	3,824	5.0	27	1.90	3.60	7	6	15.3	0.0126	0.0008
9:33 AM	5,767	5.5	26	1.65	3.85	8	7	15.2	0.0127	0.0007

Zone	B1	Depth	11.5-14.5"
Tested by	Sarah and Craig		
Date	20-Jul-04	Time	2:56 PM
G_s	2.67	Hydrometer Type	
Dry mass of soil, W_s	50.04 g	Temperature of test, T	26 °C
Meniscus correction, F_m	1.0	Zero Correction, F_s	3.3
G_s correction, a	1.00		

Time (actual)	Time (min)	Hydrometer Reading, R	Temperature, °C	Temp. Correction Factor, F_T	R_{cp}	Percent Finer $(a*R_{cp})*100/50$	R_{cL}	L (cm)	A	D (mm)
9:01 AM	2	7.0	26							
	4	5.5	26							
9:02 AM	2	6.8	26	1.65	5.15	10	8	15.2	0.0126	0.0347
	4	6.0	26	1.65	4.35	9	7	15.3	0.0126	0.0246
9:10 AM	8	5.0	26	1.65	3.35	7	6	15.5	0.0126	0.0175
9:18 AM	16	5.0	26	1.65	3.35	7	6	15.5	0.0126	0.0124
9:32 AM	30	5.0	26	1.65	3.35	7	6	15.5	0.0126	0.0091
10:02 AM	60	5.0	26	1.65	3.35	7	6	15.5	0.0126	0.0064
11:02 AM	120	5.0	26	1.65	3.35	7	6	15.5	0.0126	0.0045
1:02 PM	240	4.2	26	1.65	2.55	5	5	15.6	0.0126	0.0032
5:00 PM	478	4.0	27	1.90	2.60	5	5	15.6	0.0125	0.0023
1:32 AM	990	4.0	27	1.78	2.48	5	5	15.6	0.0125	0.0016
5:37 PM	1,955	4.0	27	1.90	2.60	5	5	15.6	0.0125	0.0011
1:07 AM	3,845	4.0	27	1.90	2.60	5	5	15.6	0.0125	0.0008
9:32 AM	5,790	4.0	26	1.65	2.35	5	5	15.6	0.0126	0.0007

C.2 Hydrometer Analysis (continued)

Zone	B1	Depth	14.5-19.5
Tested by	Sarah and Craig		
Date		Time	2:56 PM
G_s	2.64	Hydrometer Type	
Dry mass of soil, W_s	50.00 g	Temperature of test, T	25 °C
Meniscus correction, F_m	1.0	Zero Correction, F_s	4
G_s correction, a	1.00		

Time (actual)	Time (min)	Hydrometer Reading, R	Temperature, °C	Temp. Correction Factor, F_T	R_{cp}	Percent Finer $(a*R_{cp})*100/50$	R_{cL}	L (cm)	A	D (mm)
	2	26.5	25							
	4	21.5	25							
	2	26.0	25	1.40	23.40	46.91	27	11.9	0.0129	0.0315
	4	21.0	25	1.40	18.40	36.88	22	12.7	0.0129	0.0230
	8	17.5	25	1.40	14.90	29.87	19	13.2	0.0129	0.0166
	16	14.5	25	1.40	11.90	23.85	16	13.7	0.0129	0.0119
	30	12.0	25	1.40	9.40	18.84	13	14.2	0.0129	0.0089
	60	10.5	25	1.40	7.90	15.84	12	14.3	0.0129	0.0063
	120	9.5	25	1.40	6.90	13.83	11	14.5	0.0129	0.0045
	240	9.0	25	1.40	6.40	12.83	10	14.7	0.0129	0.0032
	577	8.2	25	1.40	5.60	11.23	9	14.8	0.0129	0.0021
	1,242	9.0	24	1.15	6.15	12.33	10	14.7	0.0130	0.0014
	4,312	8.0	25.5	1.53	5.53	11.08	9	14.8	0.0130	0.0008
	5,790	7.6	25	1.40	5.00	10.02	9	14.8	0.0129	0.0007

Zone	B1	Depth	19.5-76"
Tested by	Sarah and Craig		
Date		Time	10:11 AM
G_s	2.66	Hydrometer Type	
Dry mass of soil, W_s	50.04 g	Temperature of test, T	26 °C
Meniscus correction, F_m	1.0	Zero Correction, F_s	3.3
G_s correction, a	1.00		

Time (actual)	Time (min)	Hydrometer Reading, R	Temperature, °C	Temp. Correction Factor, F_T	R_{cp}	Percent Finer $(a*R_{cp})*100/50$	R_{cL}	L (cm)	A	D (mm)
10:04 AM	2	24	26							
	4	19	26							
10:11 AM	2	24	26	1.65	22.4	44.6	25	12.2	0.0127	0.0314
	4	19	26	1.65	17.4	34.6	20	13.0	0.0127	0.0229
10:19 AM	8	16	26	1.65	13.9	27.6	17	13.5	0.0127	0.0165
10:27 AM	16	12	26	1.65	10.4	20.6	13	14.2	0.0127	0.0120
10:41 AM	30	10	26	1.65	8.4	16.6	11	14.5	0.0127	0.0088
11:11 AM	60	9	26	1.65	6.9	13.7	10	14.7	0.0127	0.0063
12:11 PM	120	7	26	1.65	5.4	10.7	8	15.0	0.0127	0.0045
2:11 PM	240	7	26	1.65	4.9	9.7	8	15.0	0.0127	0.0032
5:11 PM	420	6	27	1.90	4.8	9.6	7	15.2	0.0126	0.0024
1:41 AM	930	6	27	1.78	4.7	9.3	7	15.2	0.0126	0.0016
5:44 PM	1,893	6	27	1.90	4.1	8.2	7	15.2	0.0126	0.0011
1:21 AM	3,790	6	27	1.90	4.1	8.2	7	15.2	0.0126	0.0008
9:37 AM	5,726	6	26	1.65	4.4	8.7	7	15.2	0.0127	0.0007

C.2 Hydrometer Analysis (continued)

Hydrometer Analysis

Site **Bosque del Apache South**

Zone	IIB2	Depth	5"
Tested by	Sarah and Craig		
Date	12-Jul-04	Time	3:09 PM
G_s	2.65	Hydrometer Type	
Dry mass of soil, W_s	50.01 g	Temperature of test, T	26 °C 27 °C
Meniscus correction, F_m	0.5	Zero Correction, F_s	3 3
G_s correction, a	1.00		

Time (actual)	Time (min)	Hydrometer Reading, R	Temperature, °C	Temp. Correction Factor, F_T	R_{cp}	Percent Finer $(a*R_{cp})*100/50$	R_{cL}	L (cm)	A	D (mm)
3:15 PM	2	26.0	26							
	4	19.0	26							
3:21 PM	2	27.0	26	1.65	25.65	51	28	11.7	0.0129	0.0312
	4	20.0	26	1.65	18.65	37	21	12.9	0.0129	0.0232
3:29 PM	8	14.0	26	1.65	12.65	25	15	13.8	0.0129	0.0169
3:37 PM	16	11.0	26	1.65	9.65	19	12	14.3	0.0129	0.0122
3:51 PM	30	9.0	26	1.65	7.65	15	10	14.7	0.0129	0.0090
4:21 PM	60	8.0	26	1.65	6.65	13	9	14.8	0.0129	0.0064
5:21 PM	120	7.5	26	1.65	6.15	12	8	15.0	0.0129	0.0046
7:21 PM	240	6.5	26	1.65	5.15	10	7	15.2	0.0129	0.0032
11:21 PM	480	6.5	26	1.65	5.15	10	7	15.2	0.0129	0.0023
7:09 AM	960	6.5	26	1.65	5.15	10	7	15.2	0.0129	0.0016
11:09 PM	1,920	6.0	26	1.65	4.65	9	7	15.2	0.0129	0.0011
7:09 AM	3,840	6.5	22	0.65	4.15	8	7	15.2	0.0129	0.0008
11:00 AM	4,076	6.0	25	1.40	4.40	9	7	15.2	0.0129	0.0008
3:09 PM	5,760	5.3	27	1.90	4.15	8	6	15.3	0.0129	0.0007

Zone	IIB2	Depth	15"
Tested by	Sarah and Craig		
Date	12-Jul-04	Time	3:09 PM
G_s	2.63	Hydrometer Type	
Dry mass of soil, W_s	50.02 g	Temperature of test, T	26 °C
Meniscus correction, F_m	1.0	Zero Correction, F_s	3.3
G_s correction, a	1.00		

Time (actual)	Time (min)	Hydrometer Reading, R	Temperature, °C	Temp. Correction Factor, F_T	R_{cp}	Percent Finer $(a*R_{cp})*100/50$	R_{cL}	L (cm)	A	D (mm)
9:50 AM	2	8.0	26							
	4	6.0	26							
9:56 AM	2	8.0	26	1.65	6.35	13	9	14.8	0.0128	0.0348
	4	6.0	26	1.65	4.35	9	7	15.2	0.0128	0.0250
10:04 AM	8	5.5	26	1.65	3.85	8	7	15.2	0.0128	0.0176
10:12 AM	16	5.0	26	1.65	3.35	7	6	15.3	0.0128	0.0125
10:26 AM	30	5.0	26	1.65	3.35	7	6	15.3	0.0128	0.0091
10:56 AM	60	5.0	26	1.65	3.35	7	6	15.3	0.0128	0.0065
11:56 AM	120	5.0	26	1.65	3.35	7	6	15.3	0.0128	0.0046
1:56 PM	240	4.5	26	1.65	2.85	6	6	15.3	0.0128	0.0032
5:08 PM	432	4.5	27	1.90	3.10	6	6	15.3	0.0127	0.0024
1:38 AM	942	4.5	27	1.78	2.98	6	6	15.3	0.0127	0.0016
5:43 PM	1,907	4.5	27	1.90	3.10	6	6	15.3	0.0127	0.0011
1:20 AM	3,804	4.5	27	1.90	3.10	6	6	15.3	0.0127	0.0008
9:36 AM	5,740	5.0	26	1.65	3.35	7	6	15.3	0.0128	0.0007

C.2 Hydrometer Analysis (continued)

Hydrometer Analysis

Site **CE Bosque Lab**

Zone	C	Depth	1-6"
Tested by	Sarah and Craig		
Date	12-Jul-04	Time	3:09 PM
G_s	2.67	Hydrometer Type	
Dry mass of soil, W_s	50.00 g	Temperature of test, T	26 °C 27 °C
Meniscus correction, F_m	1.0	Zero Correction, F_s	3.3 3
G_s correction, a	1.00		

Time (actual)	Time (min)	Hydrometer Reading, R	Temperature, °C	Temp. Correction Factor, F_T	R_{cp}	Percent Finer ($a*R_{cp}$)*100 /50	R_{cL}	L (cm)	A	D (mm)
10:16 AM	2	22.0	26							
	4	16.5	26							
10:23 AM	2	22.5	26	1.65	20.85	42	24	12.4	0.0126	0.0314
	4	17.0	26	1.65	15.35	31	18	13.3	0.0126	0.0230
10:31 AM	8	13.5	26	1.65	11.85	24	15	13.8	0.0126	0.0165
10:39 AM	16	11.5	26	1.65	9.85	20	13	14.2	0.0126	0.0119
10:53 AM	30	10.5	26	1.65	8.85	18	12	14.3	0.0126	0.0087
11:23 AM	60	9.5	26	1.65	7.85	16	11	14.5	0.0126	0.0062
12:23 PM	120	9.0	26	1.65	7.35	15	10	14.7	0.0126	0.0044
2:23 PM	240	8.0	26	1.65	6.35	13	9	14.8	0.0126	0.0031
5:12 AM	409	8.0	27	1.90	6.60	13	9	14.8	0.0125	0.0024
1:43 AM	920	7.5	27	1.78	5.98	12	9	14.8	0.0125	0.0016
5:46 PM	1,883	7.0	27	1.90	5.60	11	8	15.0	0.0125	0.0011
1:22 AM	3,779	7.0	27	1.90	5.60	11	8	15.0	0.0125	0.0008
9:37 AM	5,714	7.0	26	1.65	5.35	11	8	15.0	0.0126	0.0006

Zone	IIB2	Depth	6-40"
Tested by	Sarah and Craig		
Date	12-Jul-04	Time	10:23 AM
G_s	2.63	Hydrometer Type	
Dry mass of soil, W_s	50.01 g	Temperature of test, T	26 °C
Meniscus correction, F_m	1.0	Zero Correction, F_s	3.3
G_s correction, a	1.00		

Time (actual)	Time (min)	Hydrometer Reading, R	Temperature, °C	Temp. Correction Factor, F_T	R_{cp}	Percent Finer ($a*R_{cp}$)*100 /50	R_{cL}	L (cm)	A	D (mm)
10:31 AM	2	11.0	26							
	4	8.5	26							
10:36 AM	2	11.0	26	1.65	9.35	18.8	12	14.3	0.0128	0.0342
	4	9.0	26	1.65	7.35	14.8	10	14.7	0.0128	0.0245
10:44 AM	8	7.5	26	1.65	5.85	11.8	9	14.8	0.0128	0.0174
10:52 AM	16	7.0	26	1.65	5.35	10.7	8	15.0	0.0128	0.0124
11:06 AM	30	6.5	26	1.65	4.85	9.7	8	15.0	0.0128	0.0091
11:36 AM	60	6.0	26	1.65	4.35	8.7	7	15.2	0.0128	0.0064
12:36 PM	120	5.5	26	1.65	3.85	7.7	7	15.2	0.0128	0.0046
2:36 PM	240	5.0	26	1.65	3.35	6.7	6	15.3	0.0128	0.0032
5:15 PM	405	5.0	27	1.90	3.60	7.2	6	15.3	0.0127	0.0025
1:45 AM	909	5.0	27	1.78	3.48	7.0	6	15.3	0.0127	0.0016
5:47 PM	1,883	4.9	27	1.90	3.50	7.0	6	15.3	0.0127	0.0011
1:23 AM	3,767	5.0	27	1.90	3.60	7.2	6	15.3	0.0127	0.0008
9:38 AM	5,702	5.0	26	1.65	3.35	6.7	6	15.3	0.0128	0.0007

C.3 Particle Size Distribution

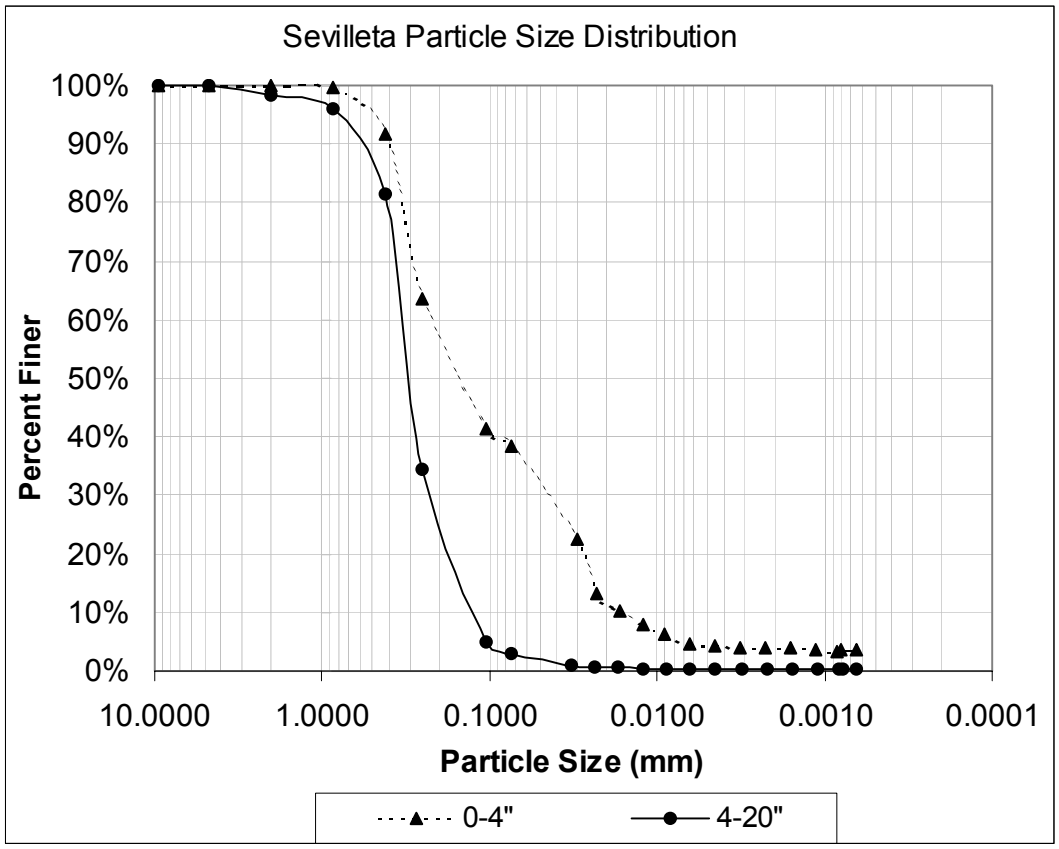

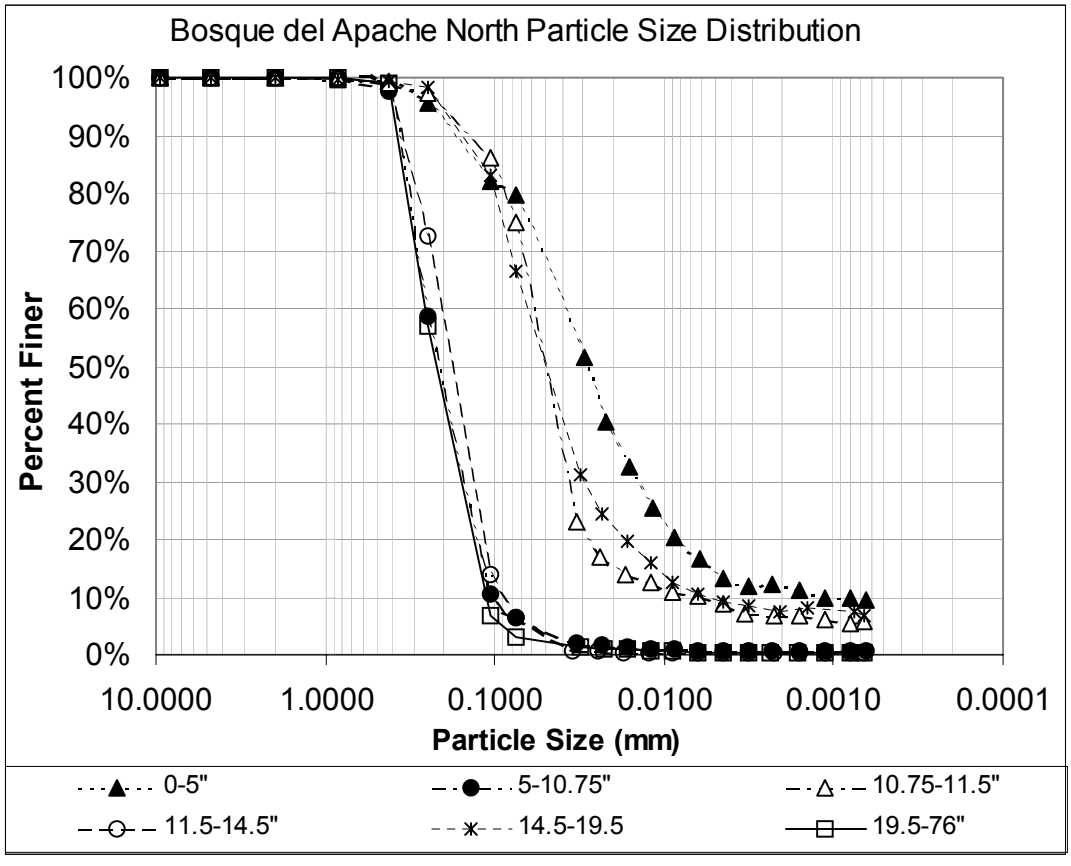

C.3 Particle Size Distribution (continued)

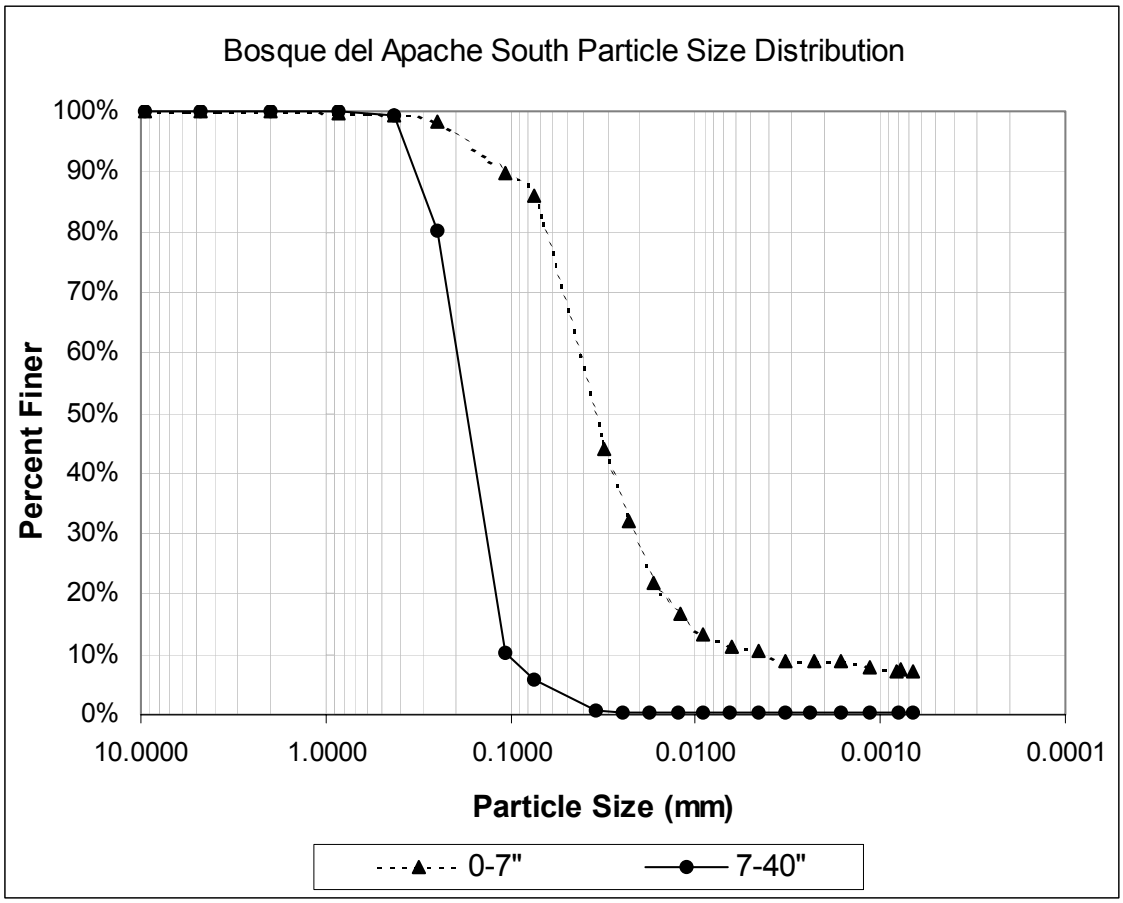

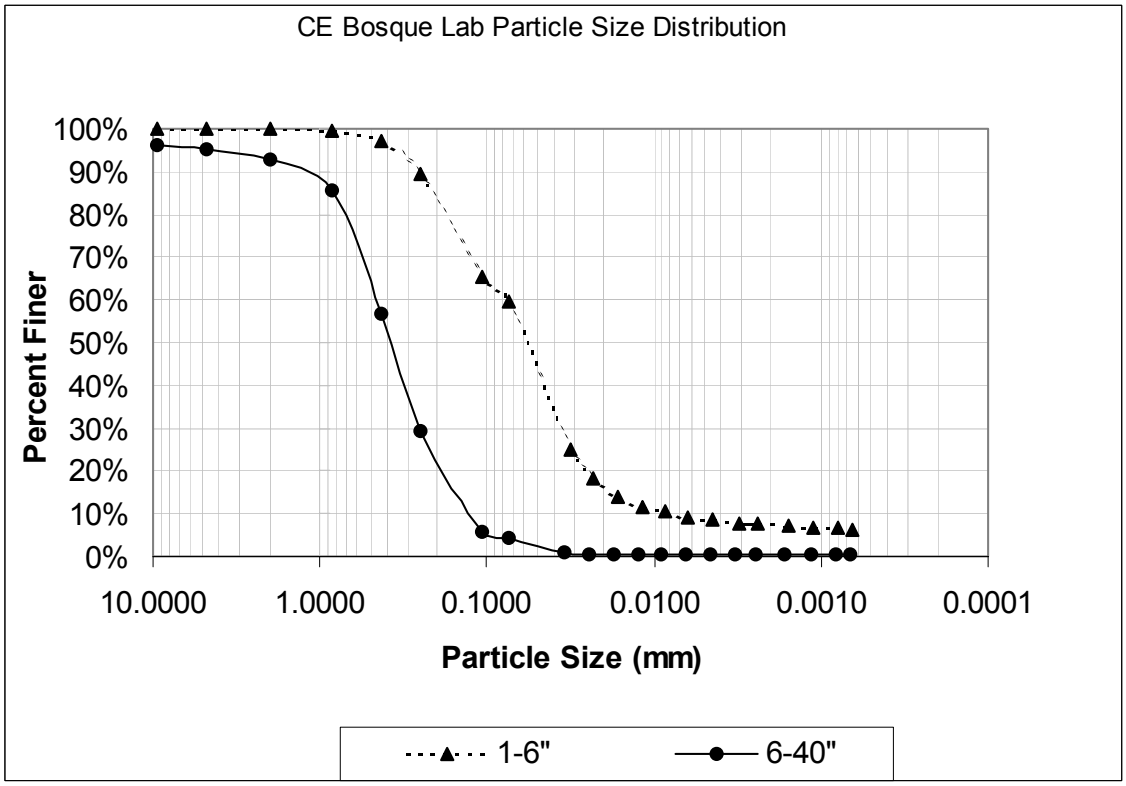

C.4 Soil Classification Results

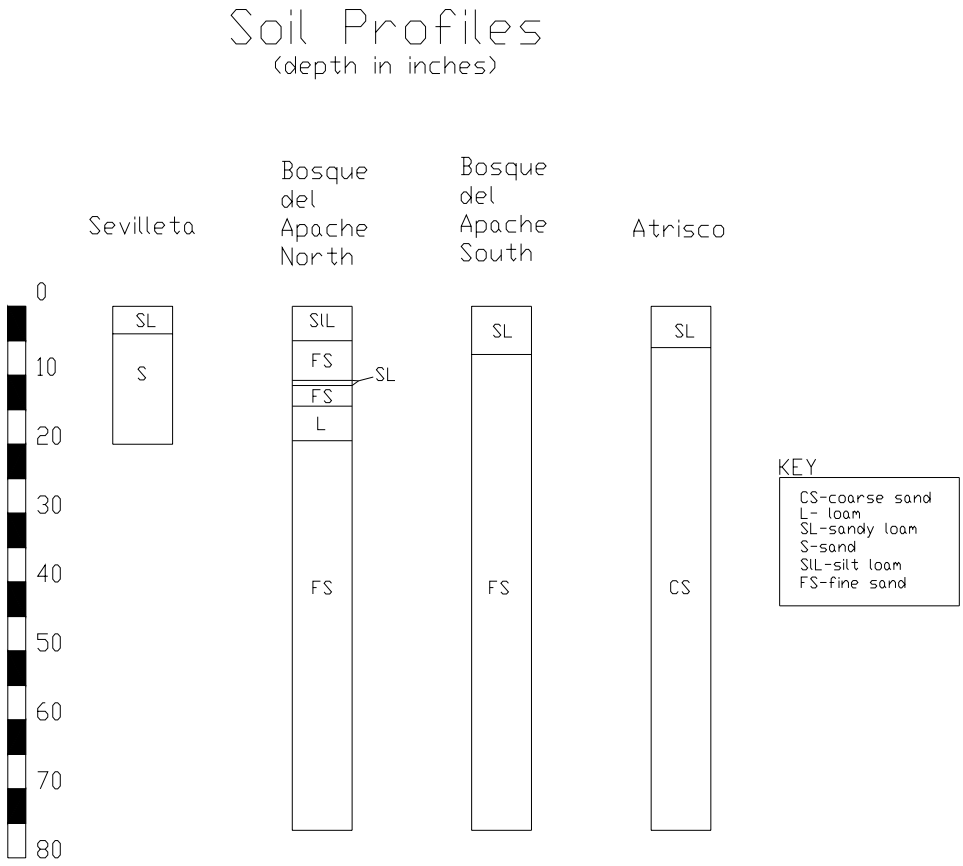

APPENDIX D
Specific Gravity

APPENDIX D. Specific Gravity Results

Pycnometer Calibration		
Descr.	Clean,Dry Mass	Filled to Calibration
#1	107.07	356.22
#2	95.85	344.85
#3	116.94	366.06
#4	117.63	366.65
#5	118.24	367.33
LL3B	114.32	363.43

13-Jul							26.5 [C]
Descr.	*Soil*	*Mass of Dry Soil [g]*	*Mass of Pycnometer with Water and Soil [g]*	*Mass of Pycnometer Filled with Water [g]*	*Specific Gravity*	*Value based on Water at 20C*	
#1	B1 11.5-14.5	85.82	410.0	356.22	2.68	2.67	
#2	B1 11.5-14.5	100.21	407.5	344.85	2.66	2.66	
#3	B1 10.75-11.5	71.13	424.0	366.06	5.39	5.38	
#4	B1 10.75-11.5	128.52	446.9	366.65	2.66	2.66	
#5	B1 5-10.75	145.44	458.2	367.33	2.67	2.66	
LL3B	B1 5-10.75	147.94	456.1	363.43	2.68	2.67	

*need largest particle size. extra step 20 min after adding water under vacuum.

14-Jul							26
Descr.	*Soil*	*Mass of Dry Soil [g]*	*Mass of Pycnometer with Water and Soil [g]*	*Mass of Pycnometer Filled with Water [g]*	*Specific Gravity*	*Value based on Water at 20C*	
#1	B1 14.5-19.5	51.66	388.34	356.22	2.64	2.64	
#2	B1 14.5-19.5	61.96	383.36	344.85	2.64	2.64	
#3	B1 0-5	51.74	398.09	366.06	2.63	2.62	
LL3B	B1 0-5	50.47	394.78	363.43	2.64	2.64	
#4	B1 19.5-76	70.09	410.46	366.65	2.67	2.66	
#5	B1 19.5-76	61.4	405.72	367.33	2.67	2.66	

16-Jul							26
Descr.	*Soil*	*Mass of Dry Soil [g]*	Mass of Pycnometer with Water and Soil [g]	*Mass of Pycnometer Filled with Water [g]*	Specific Gravity	Value based on Water at 20C	
#1	Atrisco 6-water table	107.42	422.9	356.22	2.64	2.63	
#2	Atrisco 6-water table	102.31	408.37	344.85	2.64	2.63	
#3	Atrisco 1-6	52.97	399.3	366.06	2.68	2.68	
LL3B	B1 10.75-11.5	50.27	394.9	363.43	2.67	2.67	
#4	Atrisco 1-6	53.92	400.3	366.65	2.66	2.66	
#5	B1 10.75-11.5	56.11	402.2	367.33	2.64	2.64	

18-Jul							26
Descr.	*Soil*	*Mass of Dry Soil [g]*	*Mass of Pycnometer with Water and Soil [g]*	*Mass of Pycnometer Filled with Water [g]*	*Specific Gravity*	*Value based on Water at 20C*	
#1	S3 0-4	55.13	390.50	356.22	2.64	2.64	
#2	S3 0-4	58.77	381.30	344.85	2.63	2.63	
#3	IIB1 5"	51.45	398.20	366.06	2.66	2.66	
LL3B	S3 4-20	108.49	431.30	363.43	2.67	2.67	
#4	2B1 5"	52.71	399.40	366.65	2.64	2.64	
#5	S3 4-20	107.32	434.40	367.33	2.67	2.66	

APPENDIX D. Specific Gravity Results (continued)

Soil Layer	Average Specific Gravity (nearest 0.01)
Sevilleta	
0.00-4.00[in.]	2.63
*4.00-40.00[in.]	2.66
Bosque Del Apache North	
0.00-5.00[in.]	2.63
5.00-10.75[in.]	2.67
10.75-11.50[in.]	2.65
11.50-14.50[in.]	2.67
14.50-19.50[in.]	2.64
19.5-76.00[in.]	2.66
Bosque Del Apache South	
0.00-7.00[in.]	2.65
7.00-40.00[in.]	2.63
CE Bosque Lab	
0.00-6.00[in.]	2.67
*6.00-40.00[in.]	2.63

** Even though these samples were comprised of material greater than 4.75[mm] diameter, ASTM D 854 was followed since a large enough sample was not available to perform ASTM C 127. Refer to sieve analysis results for percent-mass retained on No.4 sieve.*

APPENDIX E
Sand Cone Test

E.1 Calibration of Ottowa Sand (Trial 1) and Cones

Site **Soils Lab**

Tested by Craig and Enrique

Date 11-Jun-04 Time

Calibration of Unit Weight of Ottowa Sand	**Trial 1**	**Trial 2**	**Trial 3**	**Average**
Weight of Proctor mold, W_1	5272.0	5272.0	5272.0	5272.0
Weight of Proctor mold+sand, W_2	7387.0	7405.0	7405.0	7399.0
Volume of mold, V_1	1372.8	1372.8	1372.8	1372.8
Dry unit weight, $\gamma_{d(sand)}=(W_2-W_1)/V_1$	1.54	1.55	1.55	1.55

Calibration of Cone #1 (Small Glass)	**Trial 1**	**Trial 2**	**Trial 3**	**Average**
Weight of bottle+cone+sand (before use), W_3	3130.0	3205.0	2793.8	3042.9
Weight of bottle+cone+sand (after use), W_4	2717.7	2793.8	2381.9	2631.133
Weight of sand to fill the cone, W_c	412.3	411.2	411.9	411.8

Calibration of Cone #6 (New Plastic)	**Trial 1**	**Trial 2**	**Trial 3**	**Average**
Weight of bottle+cone+sand (before use), W_3	3859.0	3442.0	3025.6	3442.2
Weight of bottle+cone+sand (after use), W_4	3442	3025.6	2609	3025.533
Weight of sand to fill the cone, W_c	417	416.4	416.6	416.7

E.2 Calibration of Ottowa Sand (Trial 2)

Calibration of Sand (July 11, 2004)			
TRIAL	MASS[g]		AVERAGE[g]
1	2107.2		
2	2125.8		2121.1
3	2130.2		
	Diameter of Cylinder[cm]		AVERAGE[cm]
1	10.15		
2	10.14		10.14
3	10.13		
	Height of Cylinder [cm]		AVERAGE[cm]
1	16.90		
2	16.97		16.93
3	16.92		
	Volume of Cylinder[cm^3]		**1367.17**
	Density of Ottawa Sand		**1.55**

E.3 Sand Cone Density Test Results

Site **Sevilleta**

Cone #1

Dry unit weight, $\gamma_{d(sand)}=(W_2-W_1)/V_1$	1.55
Weight of sand to fill the cone, W_c	411.8

Cone #6

Dry unit weight, $\gamma_{d(sand)}=(W_2-W_1)/V_1$	1.55
Weight of sand to fill the cone, W_c	416.7

Zone 1
Tested by Sarah and Craig
Date 23-Jun-04 Time 1:32 PM
Cone # 1

Item	Sand Cone Depth 13"
Mass of bottle+cone+sand (before use), W_6 (g)	3330.0
Mass of bottle+cone+sand (after use), W_8 (g)	2030.0
Volume of hole, $V_2=(W_6-W_8-W_c)/\gamma_{d(sand)}$	573.3
Weight of Moist Soil, W_7	861.1
Weight of Dry soil, W_8	829.6
Moist unit weight, $\gamma_{sat}=W_7/V_2$	1.50
Moisture Content, w (%)$=(W_7-W_8)/(W_8)*100$	3.8%
Dry unit weight in the field, $\gamma_{d(sample)}=\gamma_{sat}/(1+w(\%))$	1.45

Zone 2
Tested by Sarah and Craig
Date 23-Jun-04 Time
Cone # 1

Item	Sand Cone Depth 15"
Mass of bottle+cone+sand (before use), W_6 (g)	3551.2
Mass of bottle+cone+sand (after use), W_8 (g)	2372.4
Volume of hole, $V_2=(W_6-W_8-W_c)/\gamma_{d(sand)}$	495.0
Weight of Moist Soil, W_7	657.9
Weight of Dry soil, W_8	631.4
Moist unit weight, $\gamma_{sat}=W_7/V_2$	1.33
Moisture Content, w (%)$=(W_7-W_8)/(W_8)*100$	4.2%
Dry unit weight in the field, $\gamma_{d(sample)}=\gamma_{sat}/(1+w(\%))$	1.28

S2 had more organic material than usual.

Zone 3
Tested by Sarah and Craig
Date 23-Jun-04 Time 12:12 PM
Cone # 1

Item	Sand Cone Depth 17"
Mass of bottle+cone+sand (before use), W_6 (g)	3485.1
Mass of bottle+cone+sand (after use), W_8 (g)	2471.2
Volume of hole, $V_2=(W_6-W_8-W_c)/\gamma_{d(sand)}$	388.6
Weight of Moist Soil, W_7	552.1
Weight of Dry soil, W_8	533.6
Moist unit weight, $\gamma_{sat}=W_7/V_2$	1.42
Moisture Content, w (%)$=(W_7-W_8)/(W_8)*100$	3.5%
Dry unit weight in the field, $\gamma_{d(sample)}=\gamma_{sat}/(1+w(\%))$	1.37

Zone 4
Tested by Sarah and Craig
Date 23-Jun-04 Time
Cone # 1

Item	Sand Cone Depth 13"
Mass of bottle+cone+sand (before use), W_6 (g)	2963.3
Mass of bottle+cone+sand (after use), W_8 (g)	1924.5
Volume of hole, $V_2=(W_6-W_8-W_c)/\gamma_{d(sand)}$	404.7
Weight of Moist Soil, W_7	570.5
Weight of Dry soil, W_8	552.6
Moist unit weight, $\gamma_{sat}=W_7/V_2$	1.41
Moisture Content, w (%)$=(W_7-W_8)/(W_8)*100$	3.2%
Dry unit weight in the field, $\gamma_{d(sample)}=\gamma_{sat}/(1+w(\%))$	1.37

E.3 Sand Cone Density Test Results (continued)

Site **Bosque del Apache North**

Cone #1

Dry unit weight, $\gamma_{d(sand)}=(W_2-W_1)/V_1$	1.55
Weight of sand to fill the cone, W_c	411.8

Cone #6

Dry unit weight, $\gamma_{d(sand)}=(W_2-W_1)/V_2$	1.55
Weight of sand to fill the cone, W_c	416.7

Zone 1
Tested by Craig & Sarah
Date 2-Jul-04 Time
Cone # 1 12:24 PM 12:34 PM 12:44 PM

Item	Sand Cone Depth 8"	Sand Cone Depth 18"	Sand Cone Depth 24"
Mass of bottle+cone+sand (before use), W_6 (g)	3161.7	2883.2	2527.3
Mass of bottle+cone+sand (after use), W_8 (g)	2364.6	1917.8	1666.7
Volume of hole, $V_2=(W_6-W_8-W_c)/\gamma_{d(sand)}$	248.7	357.3	289.7
Weight of Moist Soil, W_7	361.5	495.6	373.3
Weight of Dry soil, W_8	355.3	476.8	363.4
Moist unit weight, $\gamma_{sat}=W_7/V_2$	1.45	1.39	1.29
Moisture Content, w (%)$=(W_7-W_8)/(W_8)*100$	2%	4%	3%
Dry unit weight in the field, $\gamma_{d(sample)}=\gamma_{sat}/(1+w(\%))$	1.43	1.33	1.25

Zone 2
Tested by
Date 17-Jun-04 Time
Cone # 1 12:40 PM

Item	Sand Cone Depth 10.5"
Mass of bottle+cone+sand (before use), W_6 (g)	3517.7
Mass of bottle+cone+sand (after use), W_8 (g)	2405.8
Volume of hole, $V_2=(W_6-W_8-W_c)/\gamma_{d(sand)}$	451.9
Weight of Moist Soil, W_7	706.7
Weight of Dry soil, W_8	658.8
Moist unit weight, $\gamma_{sat}=W_7/V_2$	1.56
Moisture Content, w (%)$=(W_7-W_8)/(W_8)*100$	7%
Dry unit weight in the field, $\gamma_{d(sample)}=\gamma_{sat}/(1+w(\%))$	1.46

Zone 3
Tested by
Date 17-Jun-04 Time
Cone # 1 1:05 PM" 1:15 PM

Item	Sand Cone Depth 12"	Sand Cone Depth 6"
Mass of bottle+cone+sand (before use), W_6 (g)	3634.2	3311.5
Mass of bottle+cone+sand (after use), W_8 (g)	2590.2	2435.4
Volume of hole, $V_2=(W_6-W_8-W_c)/\gamma_{d(sand)}$	408.0	299.7
Weight of Moist Soil, W_7	578.2	396.6
Weight of Dry soil, W_8	557.9	385.5
Moist unit weight, $\gamma_{sat}=W_7/V_2$	1.42	1.32
Moisture Content, w (%)$=(W_7-W_8)/(W_8)*100$	3.6%	2.9%
Dry unit weight in the field, $\gamma_{d(sample)}=\gamma_{sat}/(1+w(\%))$	1.37	1.29

Zone 4 Sun w/ mulch
Tested by
Date 17-Jun-04 Time
Cone # 1 1:30 PM

Item	Sand Cone Depth 11"
Mass of bottle+cone+sand (before use), W_6 (g)	3615.2
Mass of bottle+cone+sand (after use), W_8 (g)	2678.2
Volume of hole, $V_2=(W_6-W_8-W_c)/\gamma_{d(sand)}$	339.0
Weight of Moist Soil, W_7	410.5
Weight of Dry soil, W_8	398.8
Moist unit weight, $\gamma_{sat}=W_7/V_2$	1.21
Moisture Content, w (%)$=(W_7-W_8)/(W_8)*100$	2.9%
Dry unit weight in the field, $\gamma_{d(sample)}=\gamma_{sat}/(1+w(\%))$	1.18

E.3 Sand Cone Density Test Results (continued)

Site **Bosque del Apache South**

Cone #1

Dry unit weight, $\gamma_{d(sand)}=(W_2-W_1)/V_1$	1.55
Weight of sand to fill the cone, W_c	411.8

Cone #6

Dry unit weight, $\gamma_{d(sand)}=(W_2-W_1)/V_1$	1.55
Weight of sand to fill the cone, W_c	416.7

Zone 1
Tested by
Date 17-Jun-04 Time
Cone # 6 3:54 PM 4:11 PM

Item	Sand Cone Depth 5"	Sand Cone Depth 15"
Mass of bottle+cone+sand (before use), W_6 (g)	3865.2	3636.4
Mass of bottle+cone+sand (after use), W_8 (g)	2650.1	2316.9
Volume of hole, $V_2=(W_6-W_8-W_c)/\gamma_{d(sand)}$	515.3	582.7
Weight of Moist Soil, W_7	699.5	845.8
Weight of Dry soil, W_8	575.0	796.4
Moist unit weight, $\gamma_{sat}=W_7/V_2$	1.36	1.45
Moisture Content, w (%)$=(W_7-W_8)/(W_8)*100$	21.7%	6.2%
Dry unit weight in the field, $\gamma_{d(sample)}=\gamma_{sat}/(1+w(\%))$	1.12	1.37

Zone 2
Tested by
Date 17-Jun-04 Time
Cone # 6 4:30 PM

Item	Sand Cone Depth 5"
Mass of bottle+cone+sand (before use), W_6 (g)	3568.5
Mass of bottle+cone+sand (after use), W_8 (g)	2617.2
Volume of hole, $V_2=(W_6-W_8-W_c)/\gamma_{d(sand)}$	345.1
Weight of Moist Soil, W_7	520.0
Weight of Dry soil, W_8	393.0
Moist unit weight, $\gamma_{sat}=W_7/V_2$	1.51
Moisture Content, w (%)$=(W_7-W_8)/(W_8)*100$	32.3%
Dry unit weight in the field, $\gamma_{d(sample)}=\gamma_{sat}/(1+w(\%))$	1.14

Zone 3
Tested by
Date 17-Jun-04 Time
Cone # 6 5:15 PM 5:20 PM

Item	Sand Cone Depth 5"	Sand Cone Depth 15"
Mass of bottle+cone+sand (before use), W_6 (g)	3606.5	2765.2
Mass of bottle+cone+sand (after use), W_8 (g)	2475.9	1332.1
Volume of hole, $V_2=(W_6-W_8-W_c)/\gamma_{d(sand)}$	460.8	656.0
Weight of Moist Soil, W_7	686.1	950.6
Weight of Dry soil, W_8	559.8	906.1
Moist unit weight, $\gamma_{sat}=W_7/V_2$	1.49	1.45
Moisture Content, w (%)$=(W_7-W_8)/(W_8)*100$	22.6%	4.9%
Dry unit weight in the field, $\gamma_{d(sample)}=\gamma_{sat}/(1+w(\%))$	1.21	1.38

Zone 4
Tested by Dave, Sandra
Date 17-Jun-04 Time
Cone # 1 5:20 PM

Item	Sand Cone Depth 5"
Mass of bottle+cone+sand (before use), W_6 (g)	2690.3
Mass of bottle+cone+sand (after use), W_8 (g)	1718.6
Volume of hole, $V_2=(W_6-W_8-W_c)/\gamma_{d(sand)}$	361.4
Weight of Moist Soil, W_7	502.0
Weight of Dry soil, W_8	394.9
Moist unit weight, $\gamma_{sat}=W_7/V_2$	1.39
Moisture Content, w (%)$=(W_7-W_8)/(W_8)*100$	27.1%
Dry unit weight in the field, $\gamma_{d(sample)}=\gamma_{sat}/(1+w(\%))$	1.09

E.3 Sand Cone Density Test Results (continued)

Site **CE Bosque Lab**

Cone #1

Dry unit weight, $\gamma_{d(sand)}=(W_2-W_1)/V_1$	1.55
Weight of sand to fill the cone, W_c	411.8

Cone #6

Dry unit weight, $\gamma_{d(sand)}=(W_2-W_1)/V_1$	1.55
Weight of sand to fill the cone, W_c	416.7

Zone 1
Tested by Sarah & Craig
Date 9-Jul-04 Time 10:03 AM
Cone #

Item	Sand Cone Depth 6.5"
Mass of bottle+cone+sand (before use), W_6 (g)	3268.8
Mass of bottle+cone+sand (after use), W_8 (g)	2204.5
Volume of hole, $V_2=(W_6-W_8-W_c)/\gamma_{d(sand)}$	418.0
Weight of Moist Soil, W_7	691.3
Weight of Dry soil, W_8	614.9
Moist unit weight, $\gamma_{sat}=W_7/V_2$	1.6539
Moisture Content, w (%)$=(W_7-W_8)/(W_8)*100$	12.4%
Dry unit weight in the field, $\gamma_{d(sample)}=\gamma_{sat}/(1+w(\%))$	1.4711

Zone 2
Tested by Sarah & Craig
Date 9-Jul-04 Time
Cone #

Item	Sand Cone Depth 6"
Mass of bottle+cone+sand (before use), W_6 (g)	2615.6
Mass of bottle+cone+sand (after use), W_8 (g)	1705.9
Volume of hole, $V_2=(W_6-W_8-W_c)/\gamma_{d(sand)}$	318.2
Weight of Moist Soil, W_7	476.0
Weight of Dry soil, W_8	446.1
Moist unit weight, $\gamma_{sat}=W_7/V_2$	1.4959
Moisture Content, w (%)$=(W_7-W_8)/(W_8)*100$	6.7%
Dry unit weight in the field, $\gamma_{d(sample)}=\gamma_{sat}/(1+w(\%))$	1.4019

Zone 3
Tested by Sarah & Craig
Date 9-Jul-04 Time 12:25 PM
Cone #

Item	Sand Cone Depth 9"
Mass of bottle+cone+sand (before use), W_6 (g)	2603.8
Mass of bottle+cone+sand (after use), W_8 (g)	1629
Volume of hole, $V_2=(W_6-W_8-W_c)/\gamma_{d(sand)}$	360.2
Weight of Moist Soil, W_7	501.4
Weight of Dry soil, W_8	468.7
Moist unit weight, $\gamma_{sat}=W_7/V_2$	1.3919
Moisture Content, w (%)$=(W_7-W_8)/(W_8)*100$	7.0%
Dry unit weight in the field, $\gamma_{d(sample)}=\gamma_{sat}/(1+w(\%))$	1.3011

APPENDIX E
Survey of CE Bosque Lab Site

APPENDIX E. Survey of CE Bosque Lab Site

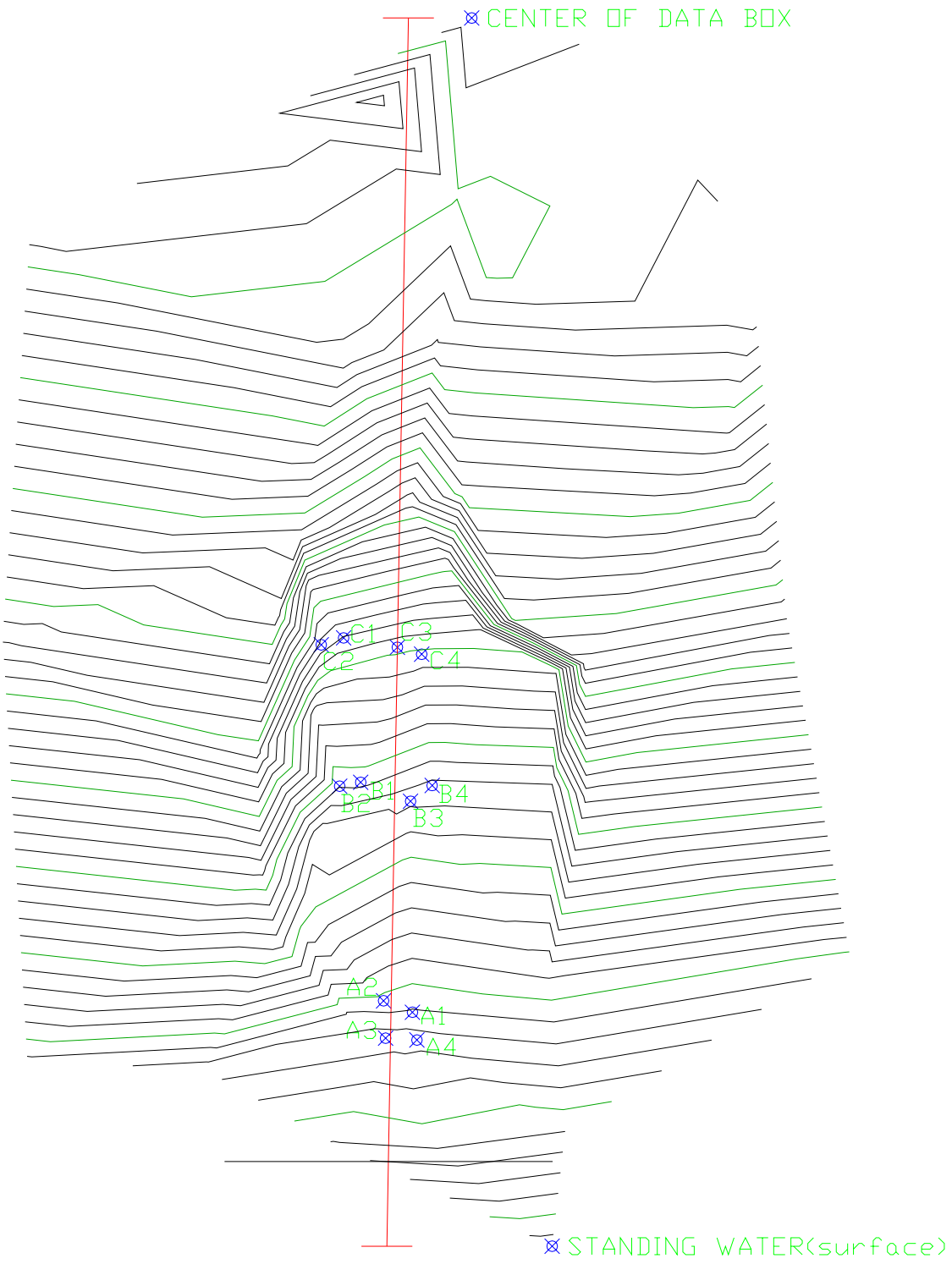

APPENDIX E. Survey of CE Bosque Lab Site (continued)

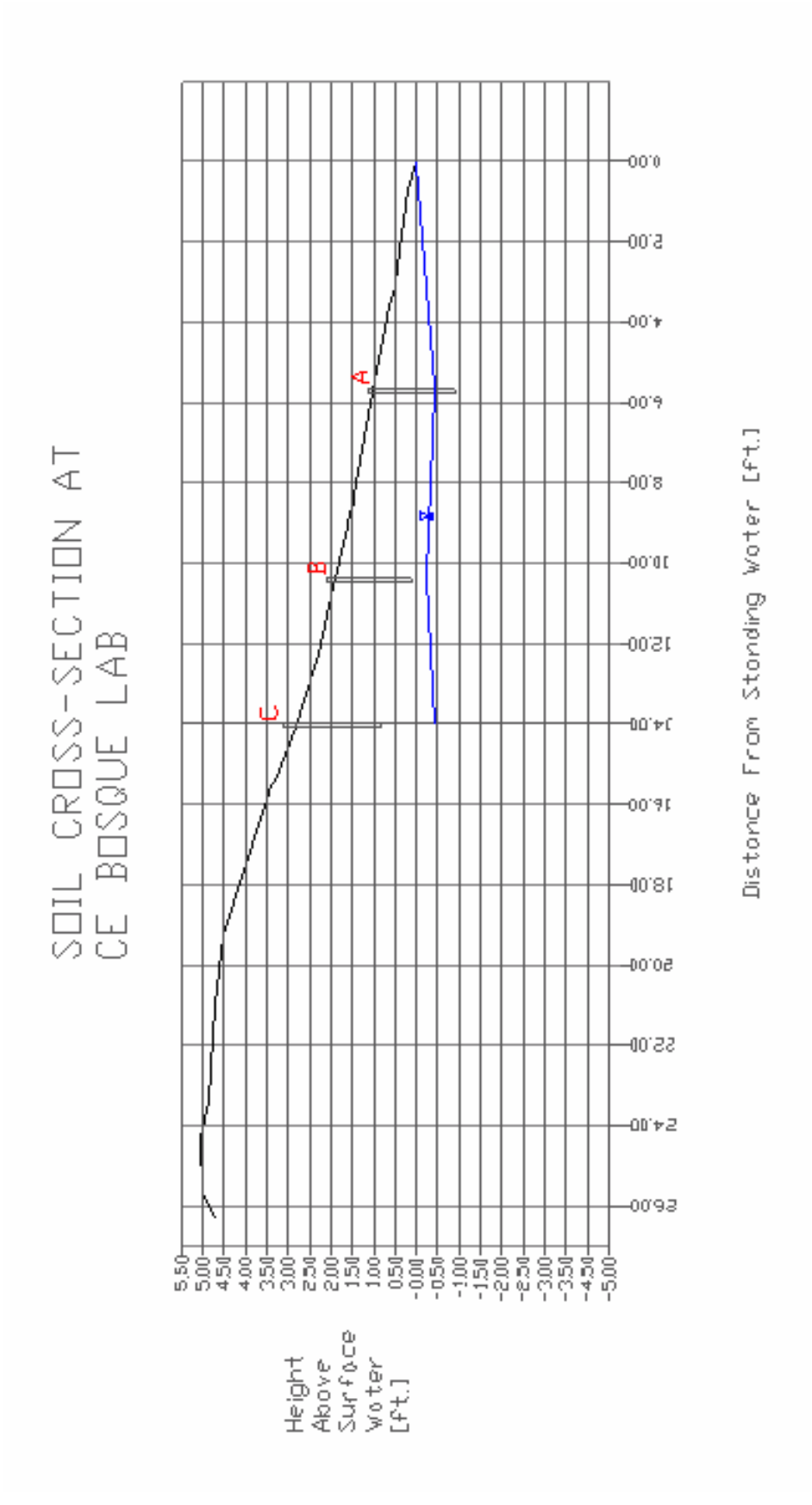

Appendix 2

Progress Report for Task 13 – Measure Evaporation with the Infrared Thermometry Method

1. Background

The simplified one-dimensional energy balance experiment (the experiment) was initiated in January 2004. The objective of the experiment is to develop a method to estimate evaporation from bare soil collected from the Shirk site located south of Albuquerque. The simplified one-dimensional energy balance is a tool that is being used to develop a relationship between bare soil evaporation and easily measured parameters in the field. The experiment consists of a 1.2 m by 1.2 m wooden box filled with Shirk soil to approximately 0.3 m depth, compacted to a typical Shirk site soil dry density of 1.5 g/cm^3 (see figures 1 and 2). The wooden box is surrounded by 1.2 m by 2.4 m sheets of black painted plywood, making the width of the experiment from plywood edge to plywood edge 3.64 m. Two pyranometers, one upright and one inverted, are located 0.5 m diagonally from the northeast corner of the box and are situated 0.17 m above the surface of the soil in correlation with research performed by Matthias et al. (1999). An ambient sample scale lysimeter, dry sample, wet sample, and water reservoir are located so that the centers of the samples are 0.7 m from the eastern edge of the wooden box in a line running north-south. A manual lysimeter is positioned so that the center of the sample is 0.17 m from the western edge of the wooden box, and 0.22 m from the southern edge of the wooden box. All soil

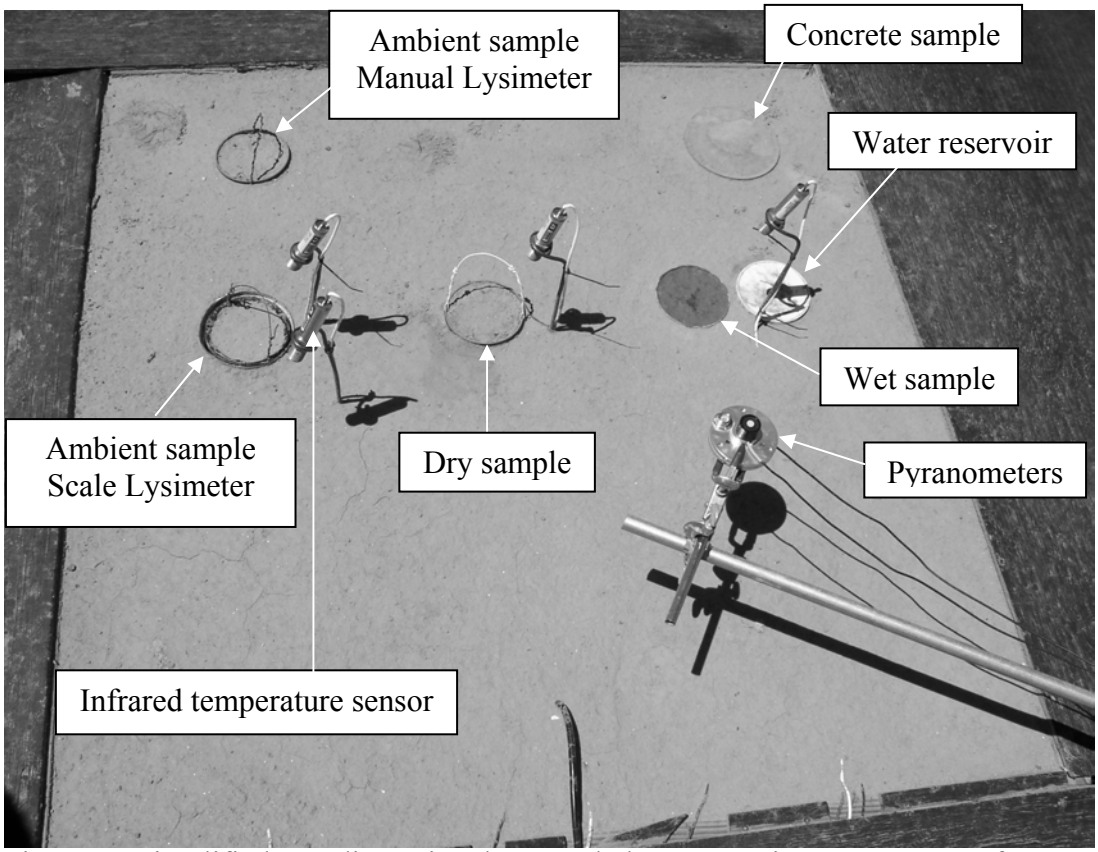

Figure 1. Simplified one-dimensional energy balance experiment – Tapy rooftop UNM – bottom of the picture is the east side of the experiment box.

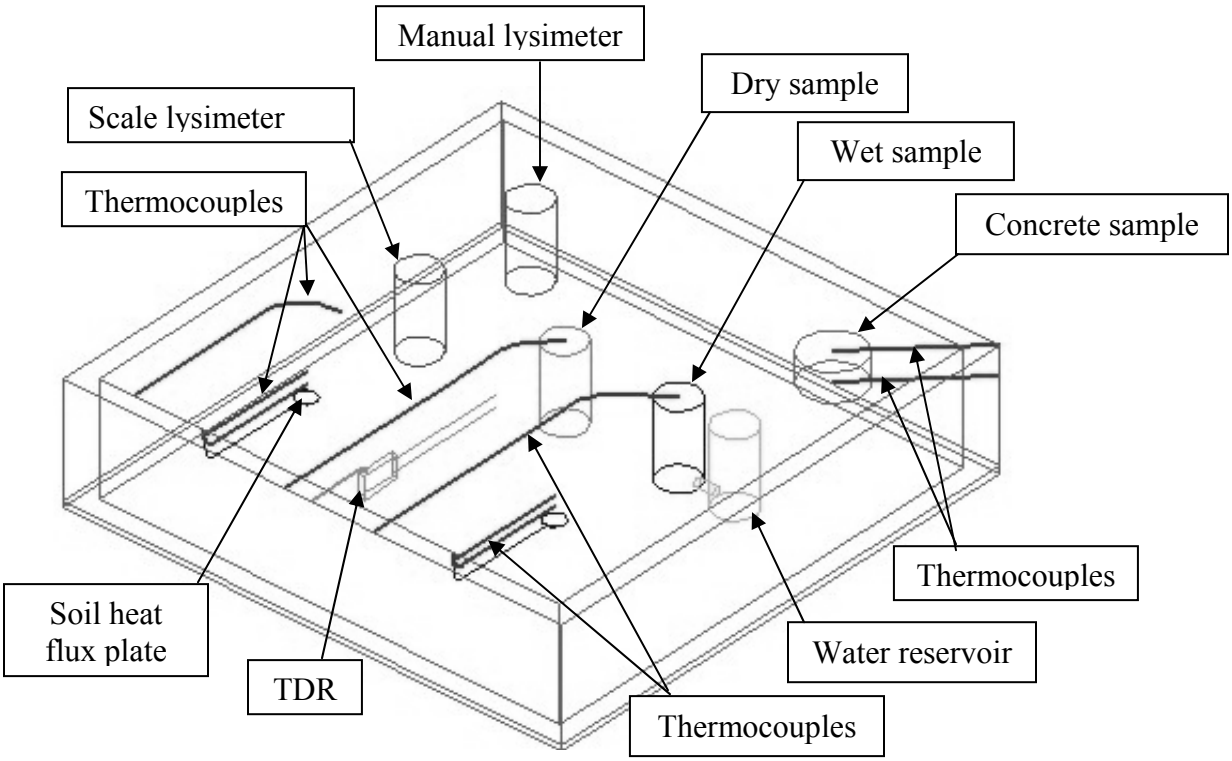

Figure 2. Three-dimensional layout of the experiment showing the placement of sensors below the surface.

samples are contained in plastic disposable cylinder molds manufactured by M.A. Industries, Inc., which insulate the samples from the surrounding soil and prevent moisture transfer between the samples and the surrounding soil. The use of plastic molds also reduces the transfer of heat vertically through the mold
itself, which can prematurely alter the temperature of the sample below the surface due to abrupt changes in air temperature. The scale lysimeter ambient sample is lined on the inside with a

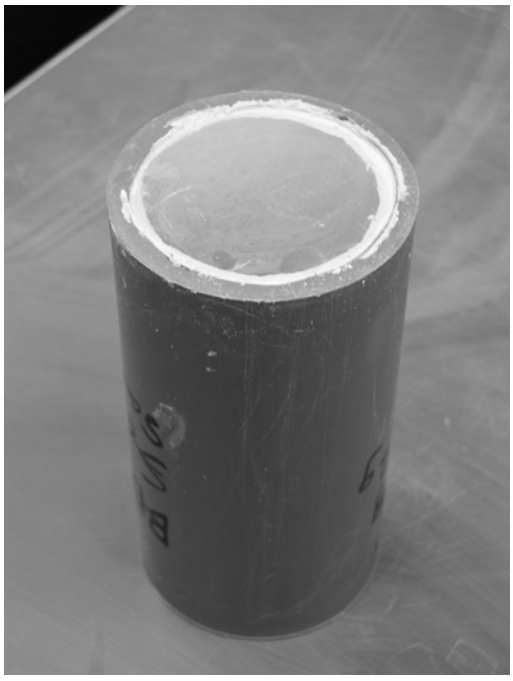

Figure 3. Copper disk inserted into the base of a plastic cylinder mold.

geofabric to enhance insulation to simulate surrounding soil. The dry sample, wet sample, and manual lysimeter ambient sample have copper-bottomed molds (see figure 3) to ensure vertical heat transfer between the sample and the underlying soil.

A concrete sample is located so that the center of the sample is 0.18 m from the western edge of the wooden box, and 0.18 m from the northern edge of the wooden box. The experiment is instrumented with various sensors that measure parameters (to be described later) that allow the calculation of net radiation (R_n), soil heat flux (G), sensible heat flux (H), and latent heat flux (LE). The simplified one-dimensional energy balance can be represented by the following equation:

$$R_n = G + H + LE \qquad (1)$$

The simplified one-dimensional energy balance allows for the accounting of energy flux at the soil surface, allowing LE to be accurately estimated using calculated values of R_n, G, and H.

2. Calculating the Components of the Energy Balance

Net Radiation (R_n)

Net radiation is calculated by measuring the incoming and outgoing short-wave radiation, air temperature, and dew point. Two LI-200SA pyranometer sensors measure the incoming and outgoing radiations, one upright (incoming short-wave radiation) and the other inverted (outgoing short-wave radiation). These two sensors are joined together at their bases and positioned so that the sensor face of the inverted pyranometer is 17 cm over the northeast quadrant of the box. LI-COR Biosciences calibrated the pyranometers on June 10, 2003. The air temperature and relative humidity are measured at 1.5 m above the surface of the soil using a Model CS500 temperature and relative humidity probe. The CS500 sensor chip was replaced at 10:10 A.M. on June 21, 2004.

R_n is calculated using the following equation from G. Y. Qiu et al. (1998):

$$R_n = R_s(1-\alpha) + \Delta R_l \qquad (2)$$

where R_s is the incoming short-wave radiation (W/m^2), α is the soil albedo, or reflectivity of the soil surface, and ΔR_l is the net long-wave radiation (W/m^2). The albedo is calculated using the following equation:

$$\alpha = \frac{R_r}{R_s} \qquad (3)$$

where R_r is the reflected short-wave radiation (W/m^2). The following empirical equation was developed by Matthias et al. (1999) to correct albedo for small areas of soil:

$$\alpha = 1.10962 * \alpha_m + 0.00592 \qquad (4)$$

where α is the corrected albedo, and α_m is the calculated albedo from the pyranometer readings. Since the current experimental setup was modeled after the experiment performed by Matthias et al. (1999), a correlation between the corrected albedo for the current experiment, calculated following the procedure spelled out by Matthias et al. (1999), and equation (4) was established. The corrected albedo calculations for the experiment correlated well with equation (4), which is illustrated by figure 4.

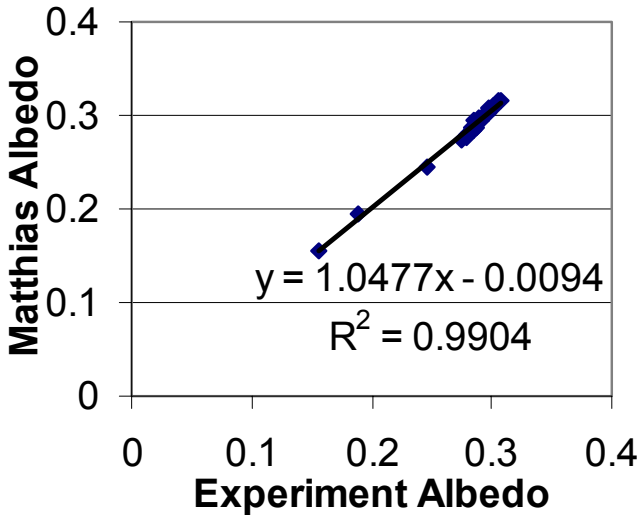

Figure 4. Plot of corrected albedos obtained from equation (4), developed by Matthias et al. (1999), against the albedos corrected for the experiment layout.

The net long-wave radiation, or the incoming atmospheric radiation minus the outgoing soil radiation, is calculated from measurements of air temperature and dew point made by the CS500 using the following equation from G.Y. Qiu et al. (1998):

$$\Delta R_l = \left(0.4 + 0.6\frac{R_s}{R_{so}}\right)\left(\varepsilon_a \sigma T_a^4 - \varepsilon_s \sigma T_s^4\right) \qquad (5)$$

where it has been assumed that R_{so}, the clear day solar radiation, is equal to R_s, σ is the Stefan-Boltzman constant (5.67×10^{-8} $Wm^{-2}K^{-4}$), T_a is the air temperature at 1.5 m above the soil surface (K), T_s is the ambient soil surface temperature (K), ε_s is the soil emissivity (0.925 Qiu et al 1998 p. 95). ε_a is the atmospheric emissivity calculated with the following equation from Campbell and Norman (1998):

$$\varepsilon_a = 1.72\left(\frac{e_a}{T_a}\right)^{\frac{1}{7}} \qquad (6)$$

where e_a is the vapor pressure (kPa) calculated from dew point measured at 1.5 m above the soil surface. Vapor pressure is automatically calculated by the CR7 using the relationships between dew point and vapor pressure given by Goff and Gratch (1946) and Weiss (1977)

Soil Heat Flux (G)

The soil heat flux at the surface is calculated by measuring the volumetric moisture content at 4 cm below the surface, two measurements of soil temperature at 2 cm below the surface, two measurements of soil temperature at 4 cm below the surface, and two measurements of soil heat flux at 8 cm below the surface. The volumetric moisture content is measured using a CS615 Water Content Reflectometer, also known as a Time Domain Reflectometer (TDR), the soil temperatures are measured using four type T thermocouples, and the soil heat flux is measured using two HFT3 soil heat flux plates (see figure 5). The distance between sets of thermocouples and HFT3 soil heat flux plates is 0.65 m.

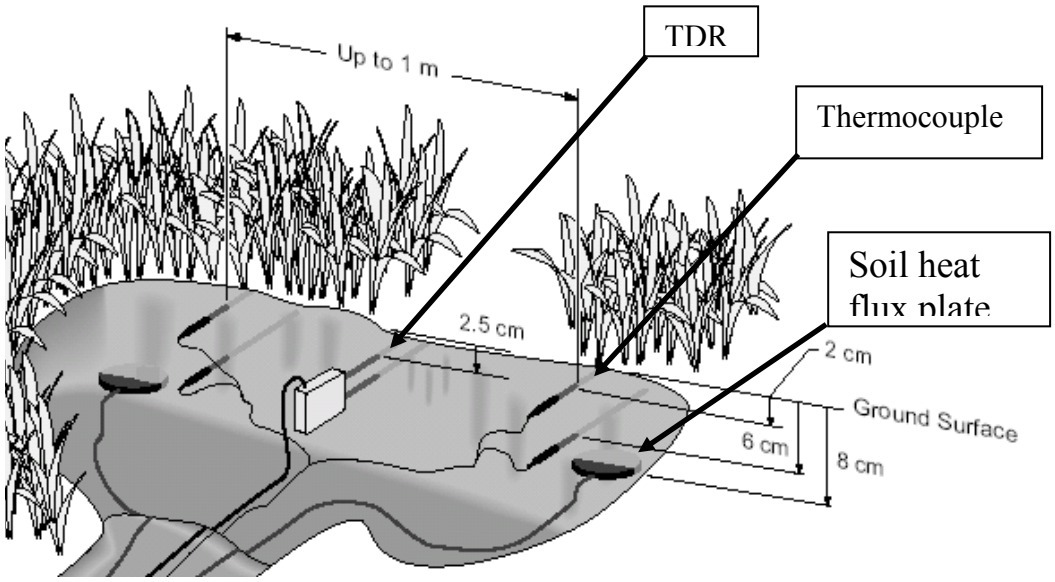

Figure 5. Configuration of soil heat flux plates, TDR, and thermocouples (figure taken from Campbell Scientific Inc. HFT3 Soil Heat Flux Plate Manual 1999).

The TDR was calibrated using point samples collected from the sand box, one at 11:45 A.M. on June 3, 2004, and two on June 21, 2004, one at 8:30 A.M. and the other at 1:00 P.M. A corer was used to extract the samples from the experiment taken at a depth of 2.5 cm to approximately 5.5 cm. Since the TDR readout is temperature sensitive, the TDR readout in milliseconds was adjusted for the temperature of the soil at the time the point sample was collected. The Campbell Scientific Inc. (CSI) CS615 Water Content Reflectometer Instruction Manual (1995) contains the temperature correction calculation used in this experiment. Figure 6 is a graph of the in situ TDR calibration.

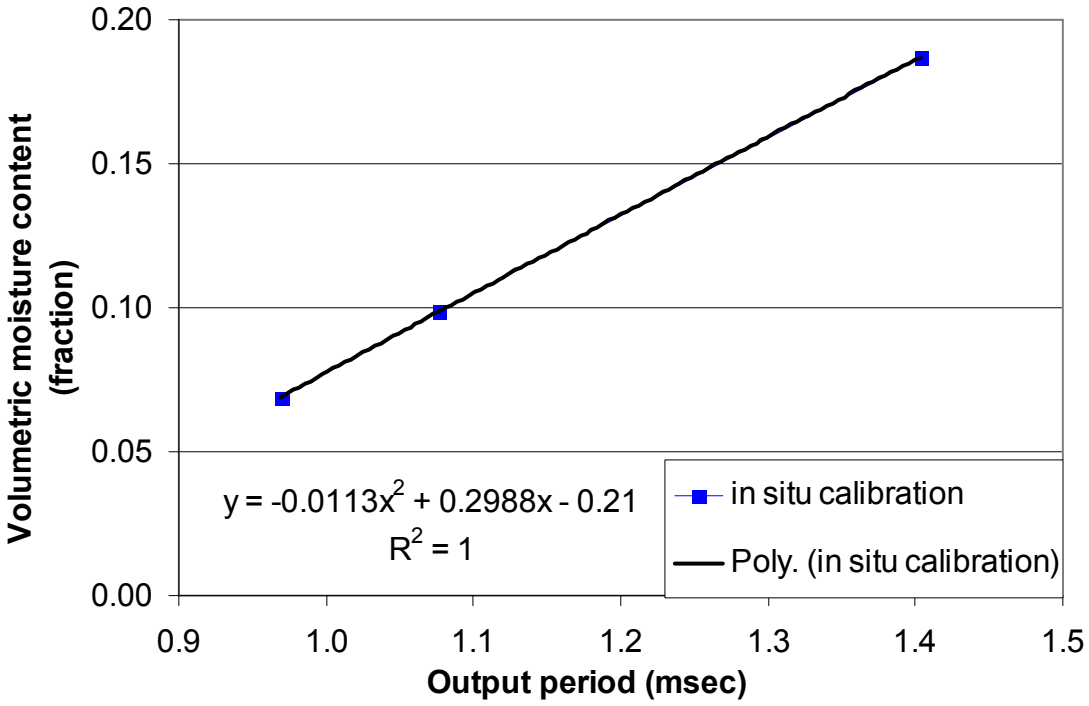

Figure 6. In situ TDR calibration.

The following equation, taken from the polynomial trend line in figure 6, was used to obtain the initial, uncorrected volumetric moisture content (θ_{vo}) from the TDR readout in milliseconds (TDR_{msec}):

$$\theta_{vo} = -.0113(TDR_{m\sec})^2 + .2988(TDR_{m\sec}) - .21 \qquad (7)$$

Following the procedure outlined in the CSI CS615 Water Content Reflectometer Instruction Manual (1995), the value for θ_{vo} is then inserted into the following equation to obtain the temperature coefficient ($Coef_{temp}$):

$$Coef_{temp} = -3.46 * 10^{-4} + 0.019\theta_{vo} - 0.045\theta_{vo}^2 \qquad (8)$$

The temperature coefficient is multiplied by the temperature at the TDR (T_{TDR}), which is averaged from the four thermocouples surrounding the TDR, minus 20 ºC to obtain the temperature correction (E_{temp}):

$$E_{temp} = (T_{TDR} - 20) * Coef_{temp} \qquad (9)$$

E_{temp} is subtracted from θ_{vo} in order to obtain the temperature corrected volumetric moisture content (θ_v):

$$\theta_v = \theta_{vo} - E_{temp} \qquad (10)$$

Figure 7 shows the diurnal pattern of uncorrected volumetric moisture content, temperature corrected volumetric moisture content, and the calculated heat capacity, which is a function of soil moisture content. As can be seen from the corrected volumetric moisture content in figure 7, there is a moisture content recovery period in the cooler morning hours, while the moisture content declines during the warmer daytime hours.

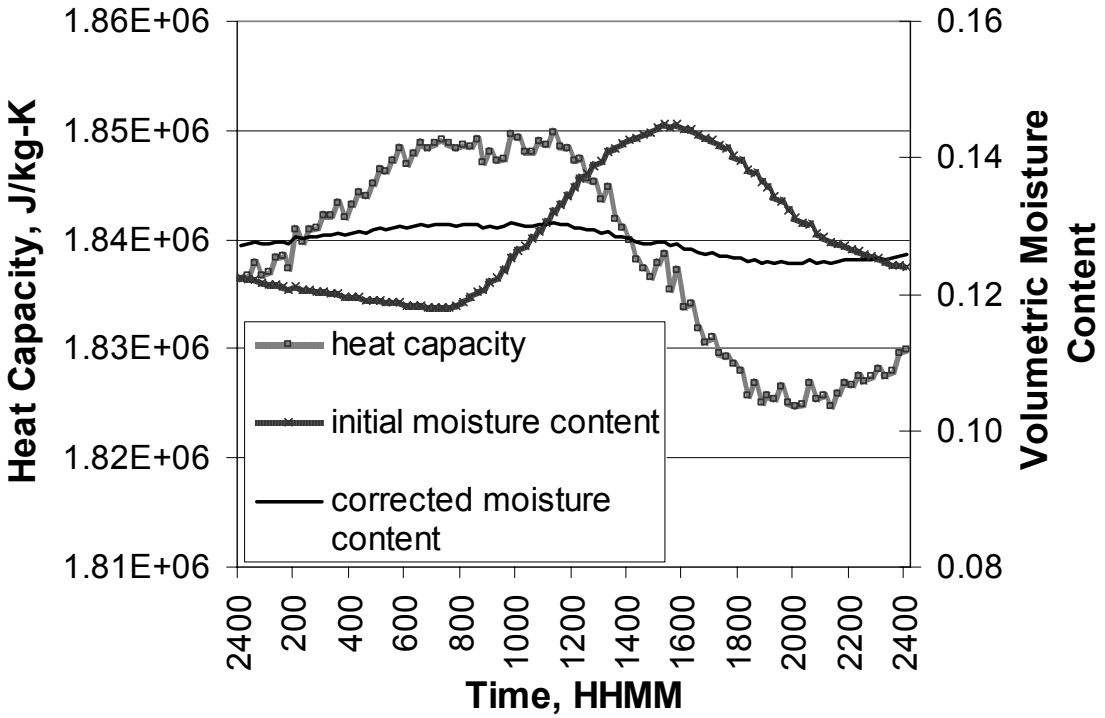

Figure 7. Diurnal variation of heat capacity, and uncorrected and temperature corrected volumetric moisture content on April 26, 2004. Time is given in military time where HH is the hours and MM is the minutes.

Radiation and Energy Balance Systems, Inc calibrated the heat flux plates on June 16, 2003. The type T thermocouples, which consist of one copper and one constantan wire are twisted and soldered together.

In order to calculate the soil heat flux at the surface (G), the measured heat flux at 8 cm below the surface (G_{8cm}) is added to the soil storage term (S):

$$G = G_{8cm} + S \qquad (11)$$

The storage term is calculated using the following equation:

$$S = \frac{\Delta T_s C_s d}{t} \qquad (12)$$

where ΔT_s is the change in the soil temperature over the output interval, or the time between measurements (t), d is the depth of the soil heat flux plates (8 cm), and C_s is the heat capacity of the soil. The heat capacity of the soil is calculated using the following equation:

$$C_s = \rho_d C_d + \theta_v \rho_w C_w \qquad (13)$$

where ρ_d is the dry density of the experiment soil (1.5 g/cm^3), C_d is the heat capacity of a dry mineral soil (840 J/kg*K, from the CSI HFT3 Soil Heat Flux Manual, 1999), ρ_w is the heat capacity of water (4200 J/kg-K, from Hillel p. 220 Table 12.1, 1998), and θ_v is the temperature corrected volumetric moisture content calculated from the TDR readout (equation 10).

Sensible Heat Flux (H)

The sensible heat flux is calculated from air temperature, ambient soil surface temperature, and wind speed measurements. The air temperature (T_a) is measured using a Model CS500 temperature and relative humidity probe at 1.5 m above the soil surface (see figure 8). The CS500 sensor chip was replaced at 10:10 A.M. on June 21, 2004. The ambient soil surface temperature (T_{amb}) is measured using a type T thermocouple located near the ambient soil sample buried as close to the surface as possible without exposing the thermocouple to direct sunlight. Alternatively, the ambient soil surface temperature was measured using the infrared temperature sensors, one located 0.15 m over the soil surface of the scale lysimeter ambient sample, and one located 0.15 m over the soil surface of the box near the scale lysimeter ambient sample (see figure 1). The wind speed (U) is measured using a Model 05103 Wind Monitor manufactured by RM Young, cabled for use with CR7 dataloggers, located at 1.8 m above the surface of the soil (see figure 8).
Sensible heat flux is calculated using the single layer or bulk resistance approach, in accordance with the following equation from Moran et al. (1994):

$$H = \frac{\rho C_p (T_{amb} - T_a)}{r_o + r_a + r_{ss}} \qquad (14)$$

where ρ is the density of air (1.2 kg/m^3), C_p is the specific heat of air (1010 J/kg-K), r_o is the structural resistance due to stratification of leaves over the surface (s/m)(zero in this experiment due to bare soil conditions), r_a is the aerodynamic resistance (s/m), r_{ss} is the "soil surface effect" resistance (s/m), and the other terms have been previously defined. r_a is calculated with the following equation which approximates the empirical data published by Rosenberg (1974, esp. Fig. 3.3, p.83):

$$r_a = 126 * U^{-0.96} \qquad (15)$$

r_{ss} is calculated with the following equation which approximates the empirical data published by Kustas et al. (1989):

$$r_{ss} = \left|3.24\left(T_{amb} - T_a\right)\right| \qquad (16)$$

Due to the fact that the empirical coefficients used in the resistance terms above were developed for situations differing from the current experiment, the data that has been collected over the summer are being analyzed in order to determine empirical coefficients for r_a and r_{ss} that will apply to the particular situation of the current experiment. Utilizing these empirical coefficients, sensible heat flux will be calculated accurately, allowing for the accurate estimation of latent heat flux, which can be verified by lysimetry.

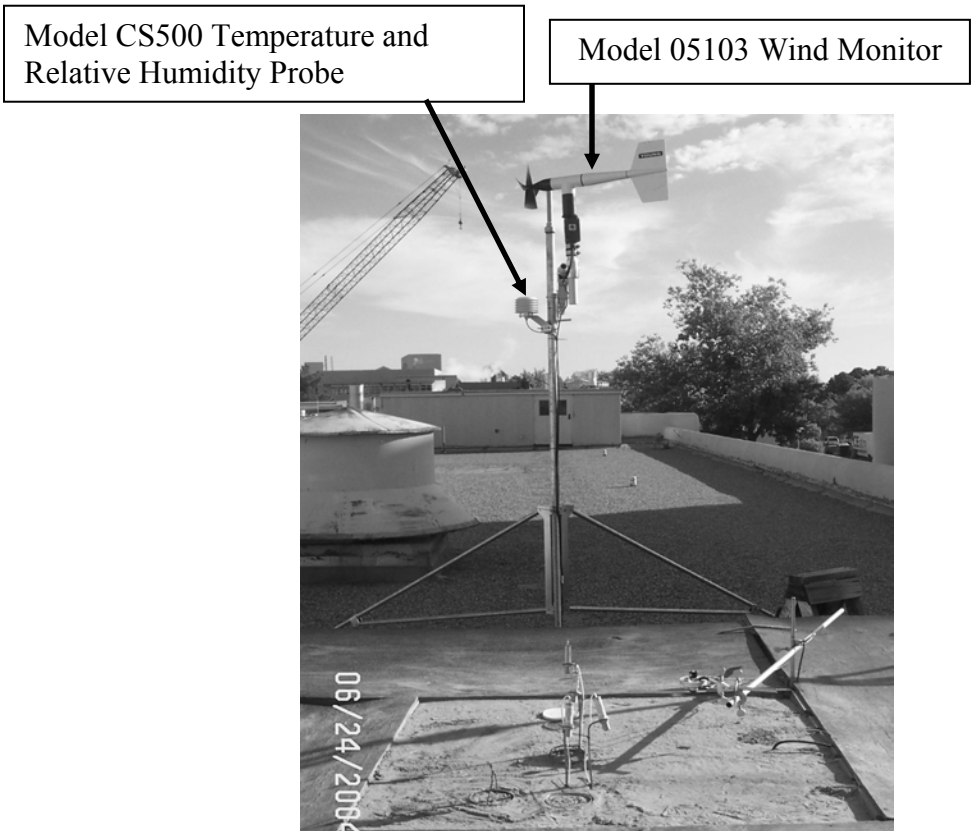

Figure 8. Simplified energy balance experiment – Tapy rooftop UNM

Latent Heat Flux (LE)

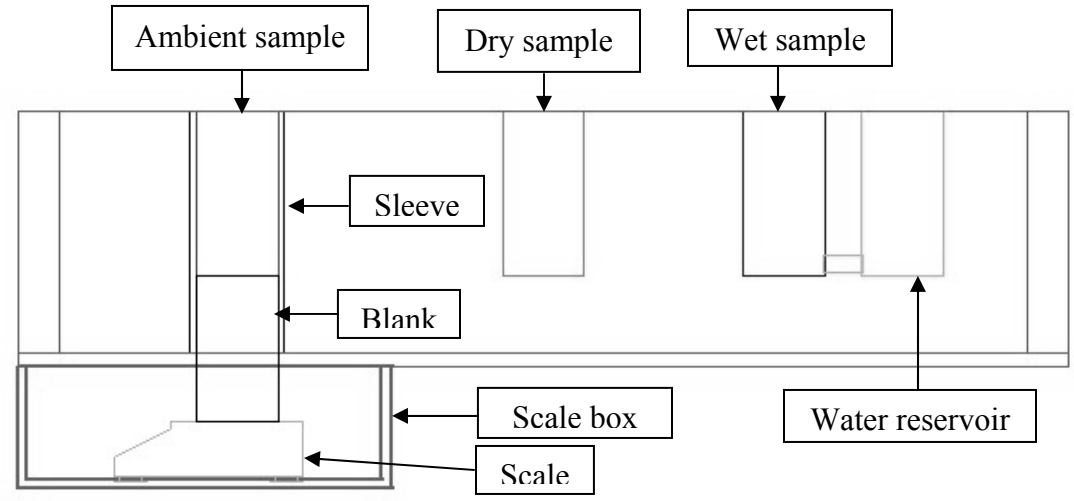

Figure 9. Scale lysimeter setup with respect to the samples in the experiment box – the right hand side of the drawing is the north side of the box.

Latent heat flux is calculated using a weighing lysimeter (scale lysimeter), where the mass of the ambient soil sample is weighed using a UX4200 Shimadzu Balance enclosed in a wooden box suspended underneath the experiment box (see figures 9 and 10). The UX4200 Shimadzu Balance is linked directly to a computer where the mass of the ambient sample is logged at one-minute intervals. A sleeve in the experiment box allows the ambient soil sample to sit on a spacer (blank) that spans the distance from the scale to the ambient sample so that the surface of the sample is at the same height as the experiment box soil surface. A manual lysimeter is also located in the box, with a plastic sleeve that allows it to be removed and weighed at least four times a day to verify that the scale lysimeter is accurately measuring evaporation.

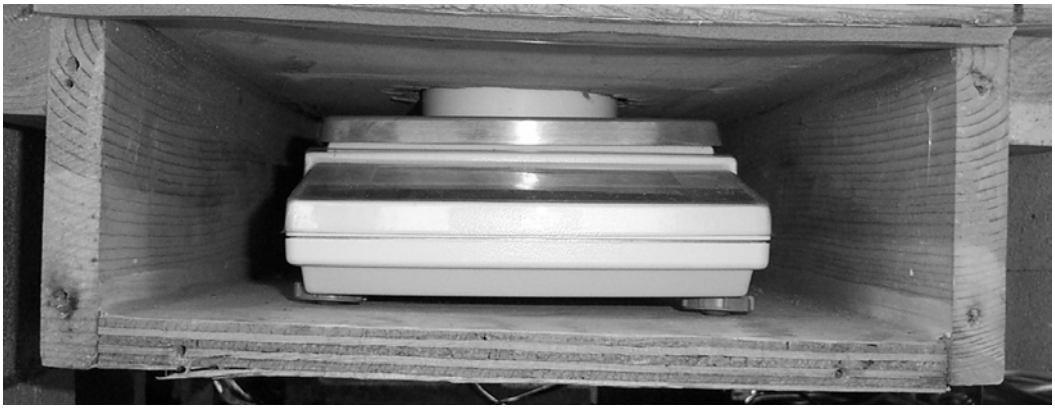

Figure 10. The UX4200 Shimadzu Balance located in a wooden box suspended beneath the experiment box, shown with the front cover removed.

The scale lysimeter measures the mass of the ambient soil sample at one-minute intervals. The readings are then averaged over the logging time interval of the CR7 datalogger to reduce wind

effects due to the exposed surface of the ambient soil sample. The following equation is then used to calculate the gravimetric evaporation rate (E) of the sample:

$$E = \frac{M_{small} - M_{current}}{A_s * t} \qquad (17)$$

where M_{small} is the smallest of the previous mass readings, $M_{current}$ is the current mass reading, A_s is the area of the ambient soil sample, and t is the logging period. The "SMALL" fuction in Excel has been used to ensure that evaporation is not accounted for twice due to variations in scale readings from wind effects by taking the smallest of the previous mass readings when calculating the evaporation rate. If the evaporation rate is less than zero, or if the previous reading is less than the current reading, the latent heat flux is set to zero. All of the previously mentioned measures ensure that evaporation is only accounted for once.

3. Data Analysis

The data that is downloaded from the CR7 datalogger and the scale is analyzed using an Excel workbook. The CR7 and the scale data are imported into worksheets in the workbook. This data is then referenced to worksheets that use the data to calculate net radiation, soil heat flux, sensible heat flux, and latent heat flux as described in the previous section. Graphs of surface temperatures, subsurface temperatures, albedo, and mass of the ambient sample are plotted to verify that the expected diurnal pattern for these values is followed, as shown on the following graphs:

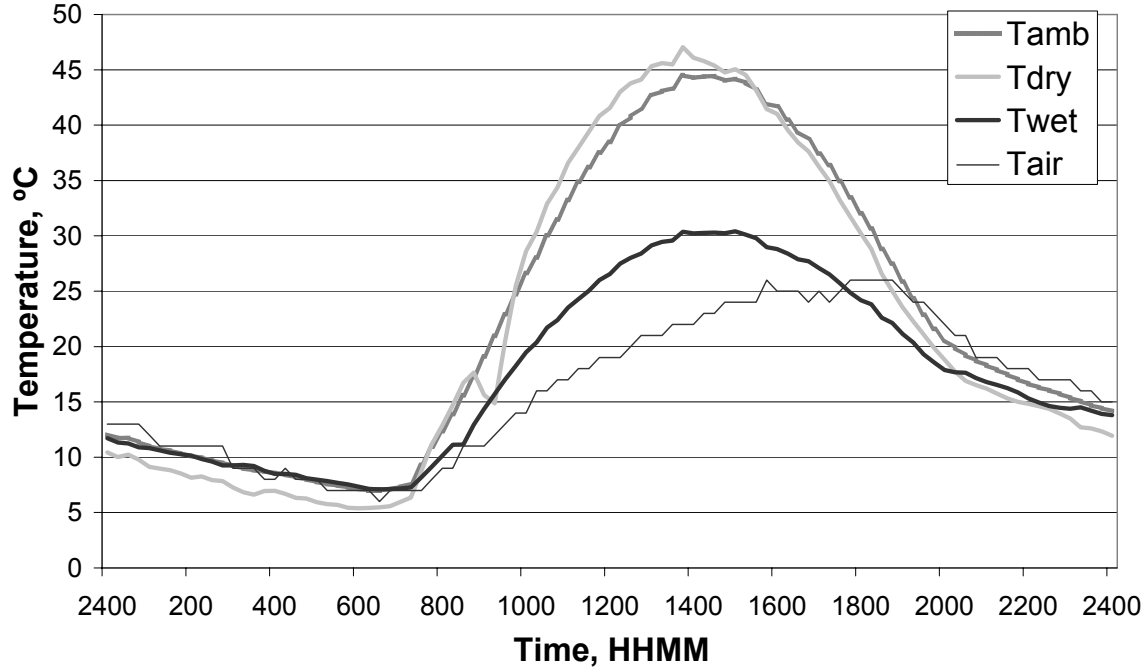

Figure 11. Surface temperatures measured with Type T thermocouples on April 26, 2004

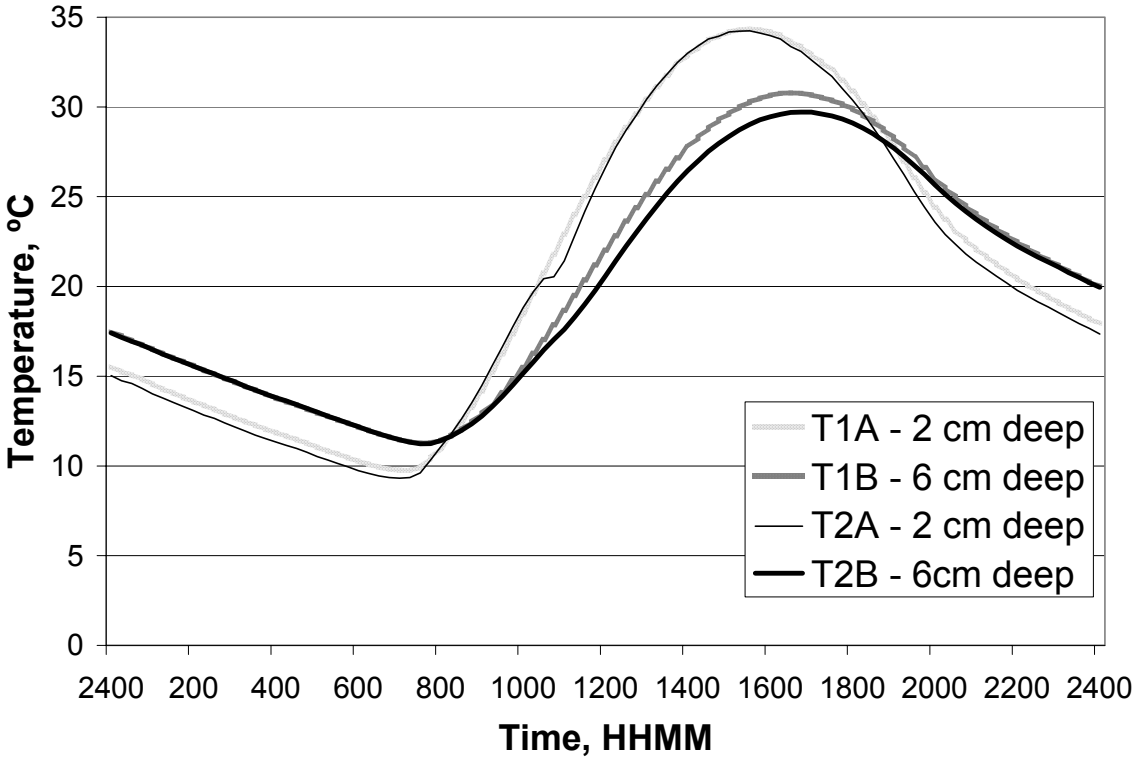

Figure 12. Subsurface temperatures on April 26. 2004

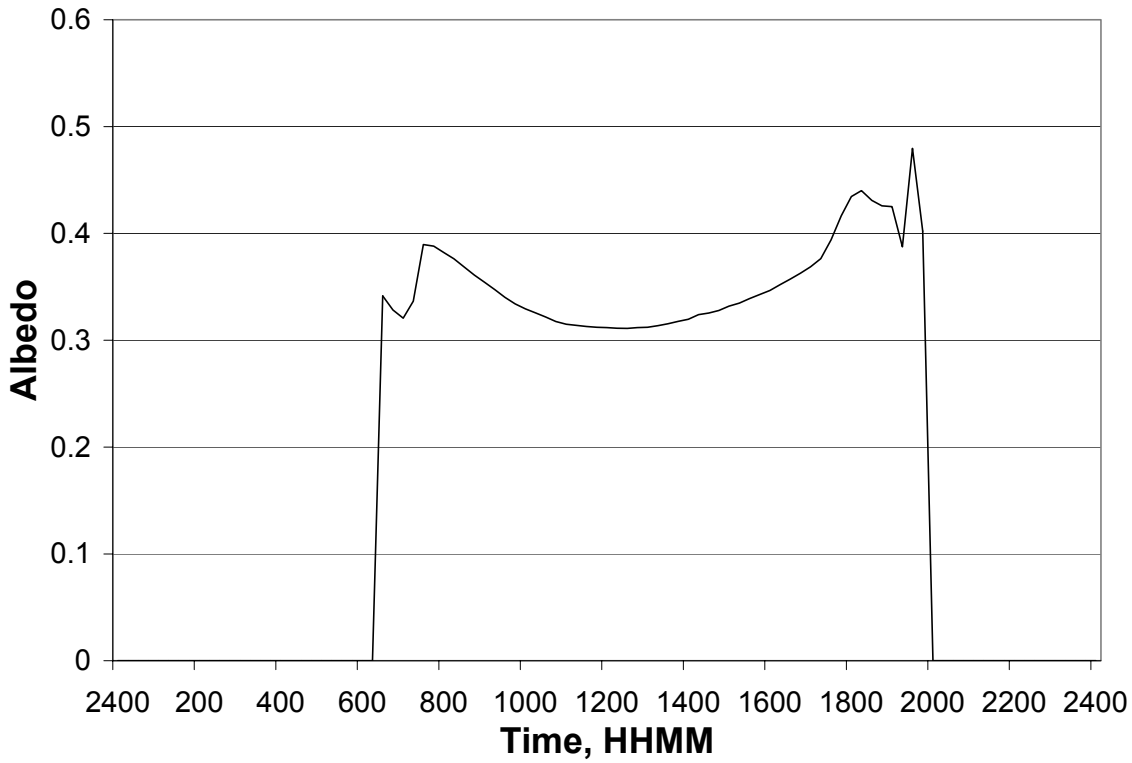

Figure 13. Albedo measurements on April 26, 2004

As can be seen in figure 11, the temperature of the dry sample (T_{dry}) is the highest temperature during the day, and is also the coolest temperature at night, as is to be expected due to its lower heat capacity, while the temperature of the wet sample (T_{wet}) remains the coolest during the day, while it is the highest overnight. The temperature of the ambient, or drying sample (T_{amb}) is located between T_{dry} and T_{wet}, with its relative location dependent on its moisture content. In figure 12, it can be seen that during the day, the temperatures taken at 2cm below the surface (T_{1A} and T_{2A}) are higher than the temperatures taken at 6cm below the surface (T_{1B} and T_{2B}), while at night this relationship is reversed. This is caused by the fact that during the day, the heat is moving downward through the soil profile, while at night, when the net radiation is negligible; the heat begins to move upward through the soil profile. This diurnal subsurface temperature pattern is a direct indication of the soil heat flux in the soil profile. In figure 13, it can be observed that the albedo becomes non-zero shortly after 6:00 AM, or after sunrise, and returns to zero shortly after 10:00 PM, or after sunset. The diurnal pattern of albedo is a function of sun angle. Matthias et al. (2000) suggests that the minimized albedos at high sun angles (midday) is caused by light trapping by gaps between soil particles. It is also believed that higher albedo readings during early mornings and late evening hours is due to the increased contribution of diffuse radiation at times when the sun angle is low (Matthias et al. 2000). In figure 14, a plot of the recorded mass of the ambient sample scale lysimeter is plotted over time, where it can be seen that the rate of mass loss is the greatest during the warm daytime hours.

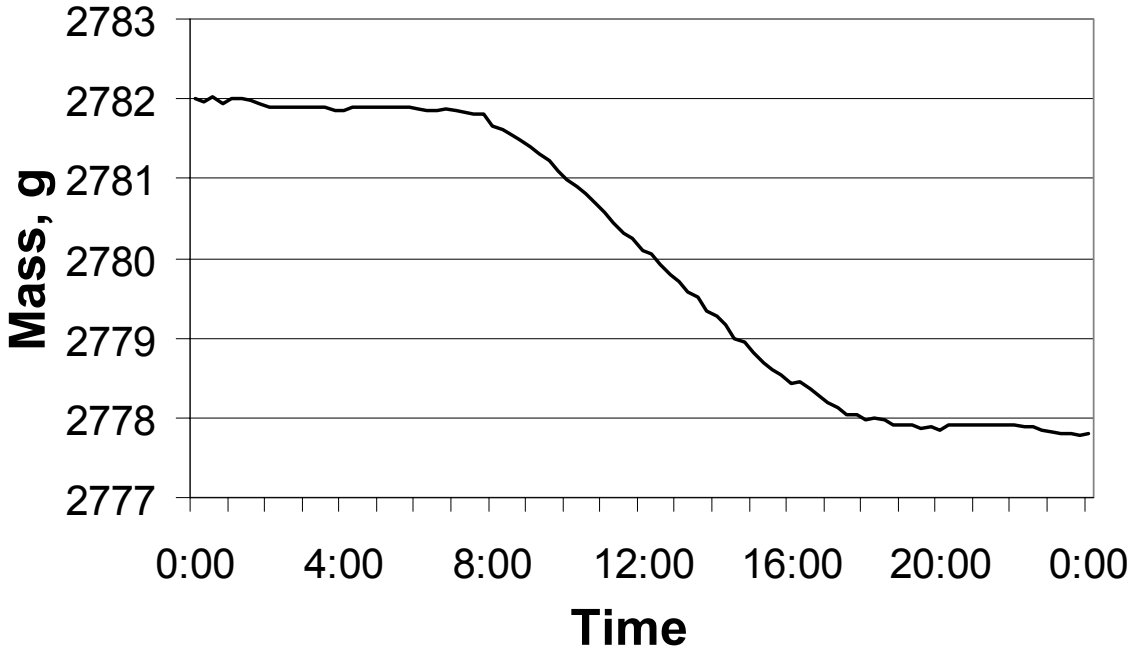

Figure 14. Scale readings measuring the mass of the ambient sample on April 26, 2004

To determine how well sensible heat flux is being estimated using the equation in the section on sensible heat flux (equation 14), the energy balance has been solved for the residual sensible heat flux (H_{res}) using the following equation:

$$H_{res} = R_n - G - LE \qquad (18)$$

The residual sensible heat flux from the energy balance is then plotted against the calculated sensible heat flux (described in the previous section). The results of such a plot can be seen on the following graph:

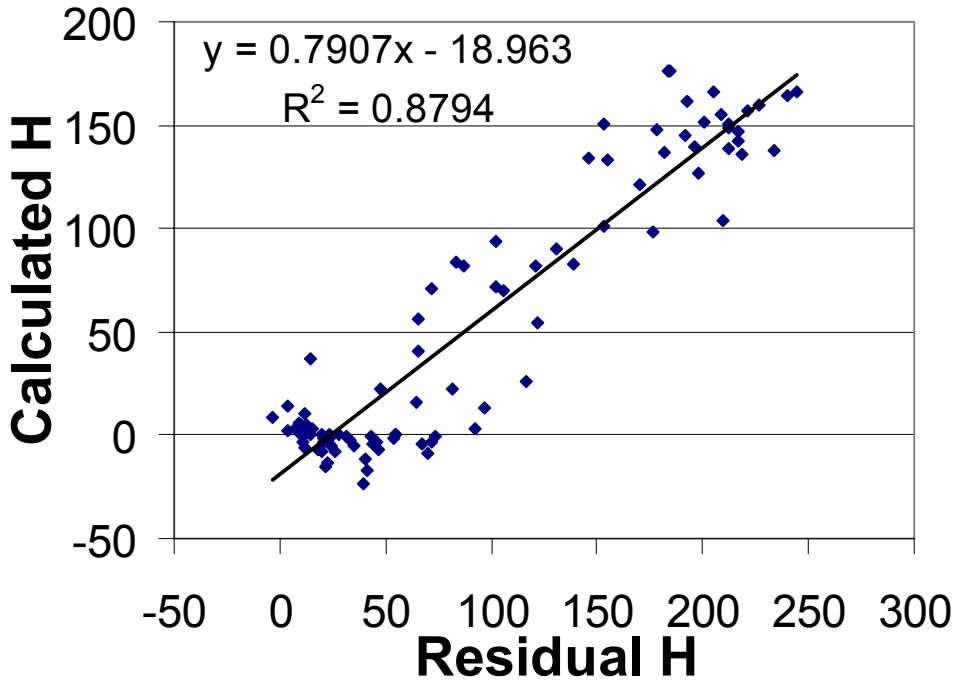

Figure 15. Calculated sensible heat flux versus the residual sensible heat flux on April 26, 2004

Since the preceding graph was plotted with a calculated sensible heat flux that uses empirical coefficients for the resistance terms taken from studies done by Rosenberg (1974) and Kustas et al. (1989) (refer to sensible heat flux section), improvements may be possible for calculating sensible heat flux by developing empirical coefficients for the resistance terms using the data collected from the experiment.

The residual latent heat flux (LE_{res}) is calculated using the following equation:

$$LE_{res} = R_n - G - H \qquad (19)$$

The residual latent heat flux is then plotted versus calculated latent heat flux as seen in Figure 16. Once again, it is believed that the accuracy of estimating latent heat flux with the energy balance residual can be improved upon with the development of empirical coefficients for the resistance term used to calculate sensible heat flux. Once this is completed, the data can be more confidently used to develop a method to estimate evaporation using easily measured parameters in the field.

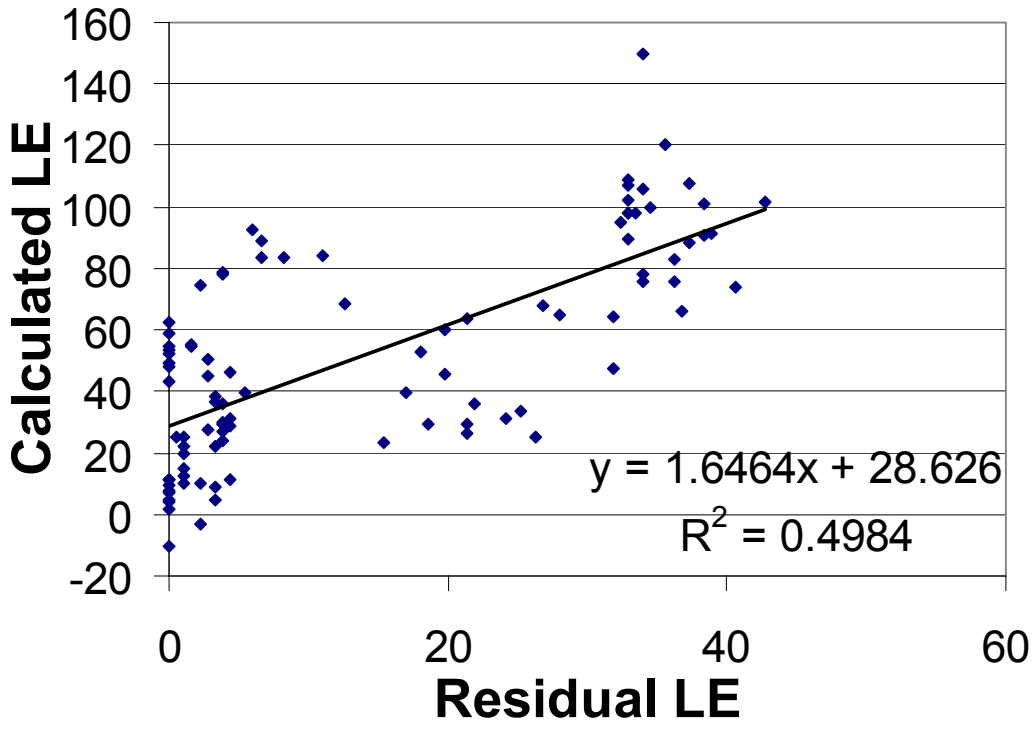

Figure 16. Calculated latent heat flux versus residual latent heat flux on April 26, 2004.

This completes the data analysis in the workbook, at which time a line graph of energy fluxes in the experiment can be plotted for an overall view of the energy balance (see figure 17).

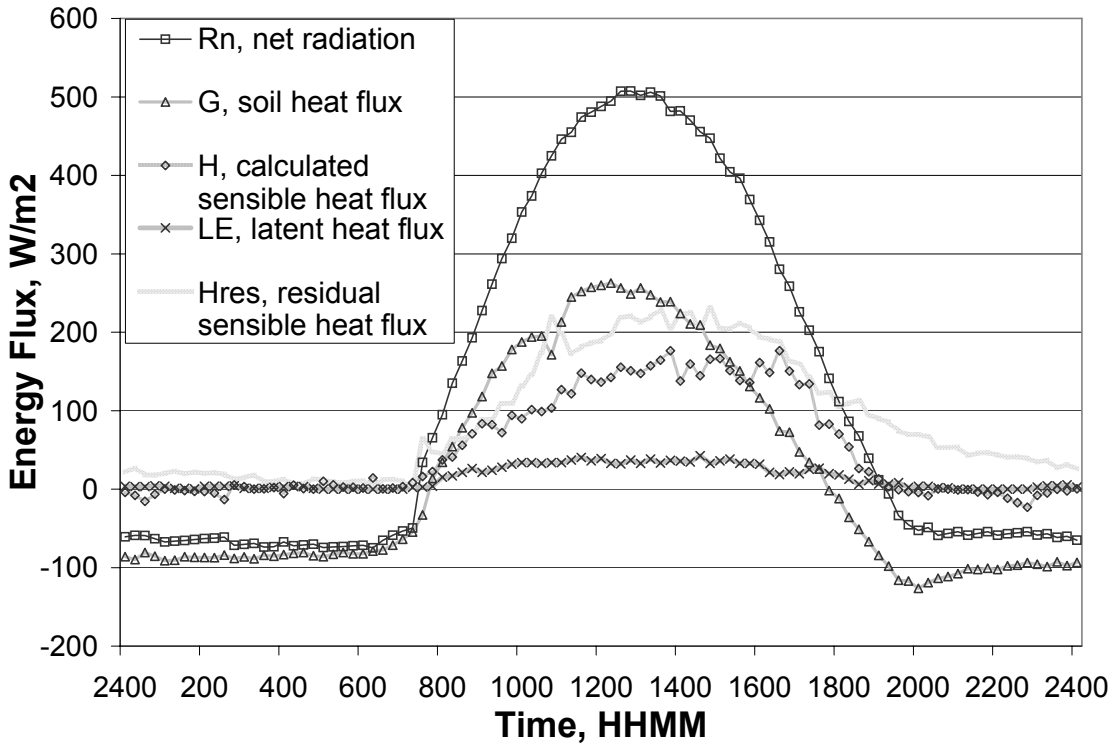

Figure 17. Energy flux for the experiment on April 26, 2004

4. Evaporation Estimation Methods

The overall goal of this research is to develop a method to estimate bare soil evaporation in the field using easily obtained parameters, such as surface temperatures through infrared thermometry, and meteorological data that can be obtained either from a weather station or online. The method that is being analyzed currently for use on this project is based on research conducted by Fox (1968) and Ben-Asher et al. (1983).

According to the research of Ben-Asher et al. (1983) and others, bare soil evaporation can be estimated from mid-day surface-soil temperatures and wind speed. In order to develop an equation relating mid-day surface-soil temperatures and wind speed to bare soil evaporation, Fox (1968) and others have made the following two assumptions for the energy balance denoted by A and B:

$$\begin{aligned} A &= \int_{t_1}^{t_2} \left(K_o \uparrow - K_d \uparrow + G_o - G_d\right) dt << \int_{t_1}^{t_2} LE dt \\ B &= T_{o,min} - T_{d,min} << T_{o,max} - T_{d,max} \end{aligned} \qquad (20)$$

where K represents short-wave radiation, with the upward pointing arrow signifying that this is outgoing short-wave radiation, G stands for soil heat flux, T stands for surface-soil temperature, the subscript ‘o’ stands for the dry soil, and the subscript ‘d’ stands for the ambient or drying soil.

For this experiment, assumption A was found to be true, while assumption B was not. It was observed that for the seven days in early July that were analyzed, the minimum temperature difference between dry and ambient soil was not negligible when compared to the maximum temperature difference between these two soils. This phenomenon is what is to be expected, since the moisture content of the soil, the deciding factor in the heat capacity of a particular soil, will govern to what extent the soil can retain or lose heat. Since the dry soil has a lower heat capacity than the ambient sample, it is unable to retain as much heat during the cooler nighttime hours. This has led to the realization that the simplifying assumptions may need to be examined more closely, with the probable elimination of assumption B.

Using the simplifying assumptions previously mentioned, the energy balance can be reduced to the following form:

$$\int_{t_1}^{t_2} LE dt = S(T_{o,max} - T_{d,max}) \qquad (21)$$

where S is the coefficient of proportionality obtained by integrating the energy balance after simplification using the previously mentioned assumptions. The equation for S is as follows:

$$S = 8.7\left(\rho c_p r_{tot}^{-1} + 4\varepsilon\sigma\overline{T}^3\right) \qquad (22)$$

where ρ is air density, c_p is specific heat of air, r_{tot} is the resistance term, ε is the atmospheric emmisivity, σ is the Stefan-Boltzmann constant, and $\overline{T}$ is the average instantaneous surface temperature, assumed to be constant. Ben Asher et al. (1983), whose research was conducted in December, assumed that evaporation at nighttime

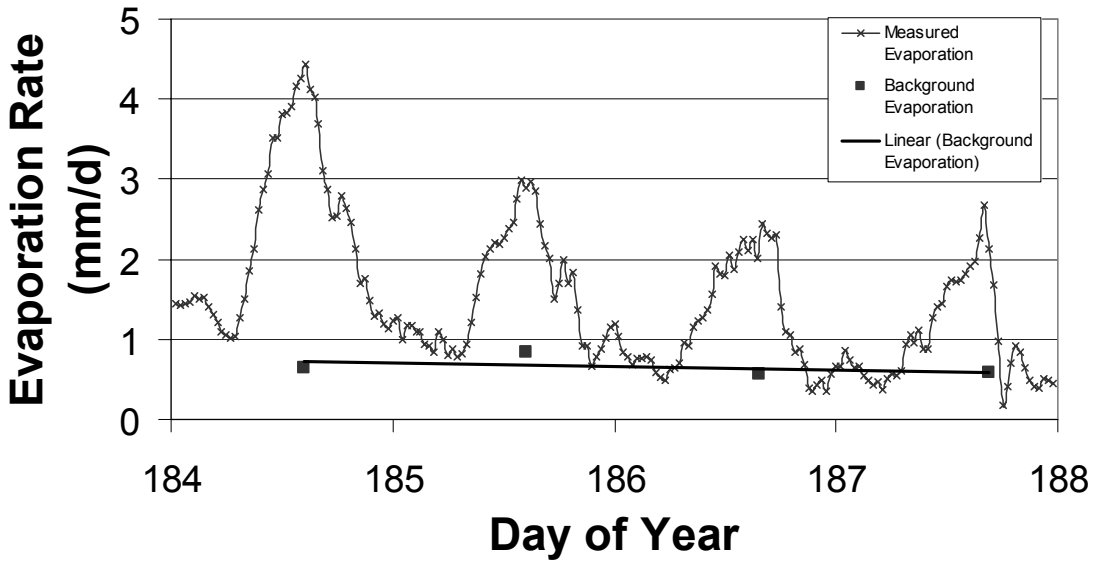

Figure 18. Evaporation rate versus time from July 2 until July 5, 2004

dropped to zero. However, for this experiment, for which data has been collected during the spring and summer months up to this point, it was observed that evaporation did not drop to zero during the nighttime hours, which can be seen in figure 18. A reduction in evaporation rate can be seen over the four days due to the fact that this was a dry-down period after wetting, in which the evaporation rate declines as the available water is reduced.

In order to indirectly estimate nighttime evaporation, an empirical model was developed that relates the difference between the twenty-four hour minimum surface-soil temperatures for the ambient sample and the dry sample to the minimum evaporation rate during the night (see figure 19). The following equation taken from the trend line fit in figure 19 relates minimum nighttime evaporation (E_{min}), in mm/d, to the temperature difference between the dry ($T_{o,min}$) and ambient ($T_{d,min}$) soil in K:

$$E_{min} = 0.2198\left(T_{d,min} - T_{o,min}\right) + 0.1466 \qquad (23)$$

Given the R-squared value of 0.9045, it is believed that there is a strong correlation for this data. Research was initiated during the summer of 2004 to establish a physical model for this empirical relationship, with further research in this area planned for the future.

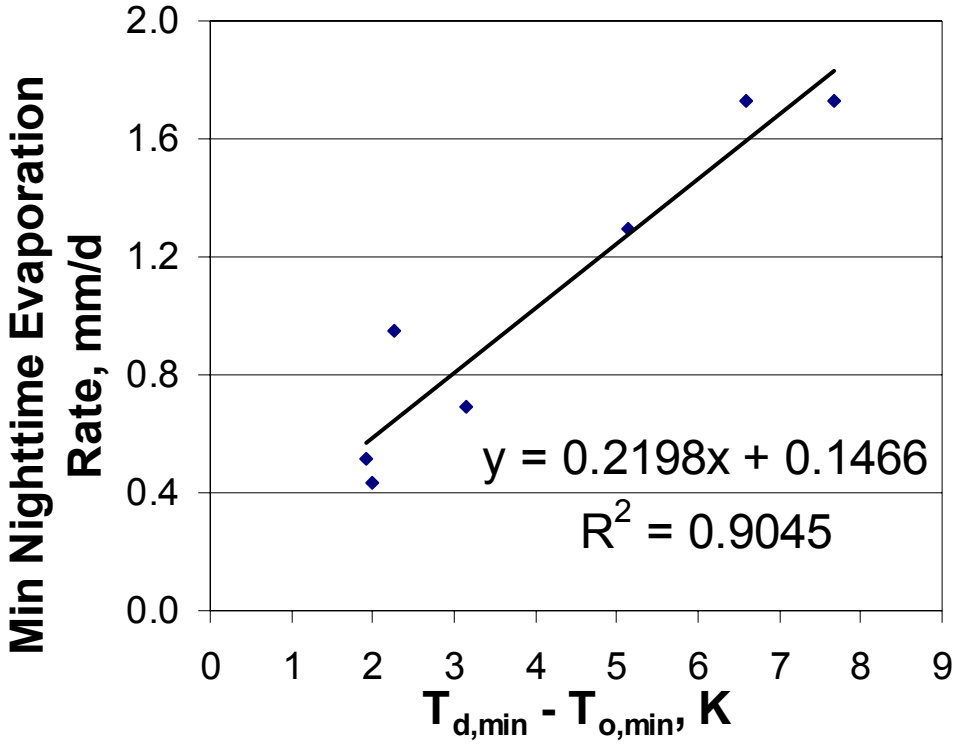

Figure 19. Trend line fit of seven days of data in early July 2004, relating minimum nighttime temperature difference between the dry (subscript o) and the drying sample (subscript d) to minimum observed nighttime evaporation rate.

Considering the minimum nighttime evaporation as a continuous "background evaporation", and adding this to the estimated evaporation using the method developed by Ben-Asher et al. (1983), the estimated values for evaporation correlated well with the actual evaporation determined by lysimetry, as seen in figure 20 and Table 1.

.

As seen in Table 1, for the seven days that were analyzed, the simplified energy balance method overestimated actual evaporation by 6.2% (0.12 mm/d) with a standard deviation of 12.9 (0.45 mm/d). The magnitude of this error is comparable to the error that Ben-Asher et al. (1983) found, where the simplified energy balance underestimated by an average of 15%. It is planned to extend this method to more data in the future at a cooler time of the year when background evaporation may become nonexistent or negligible.

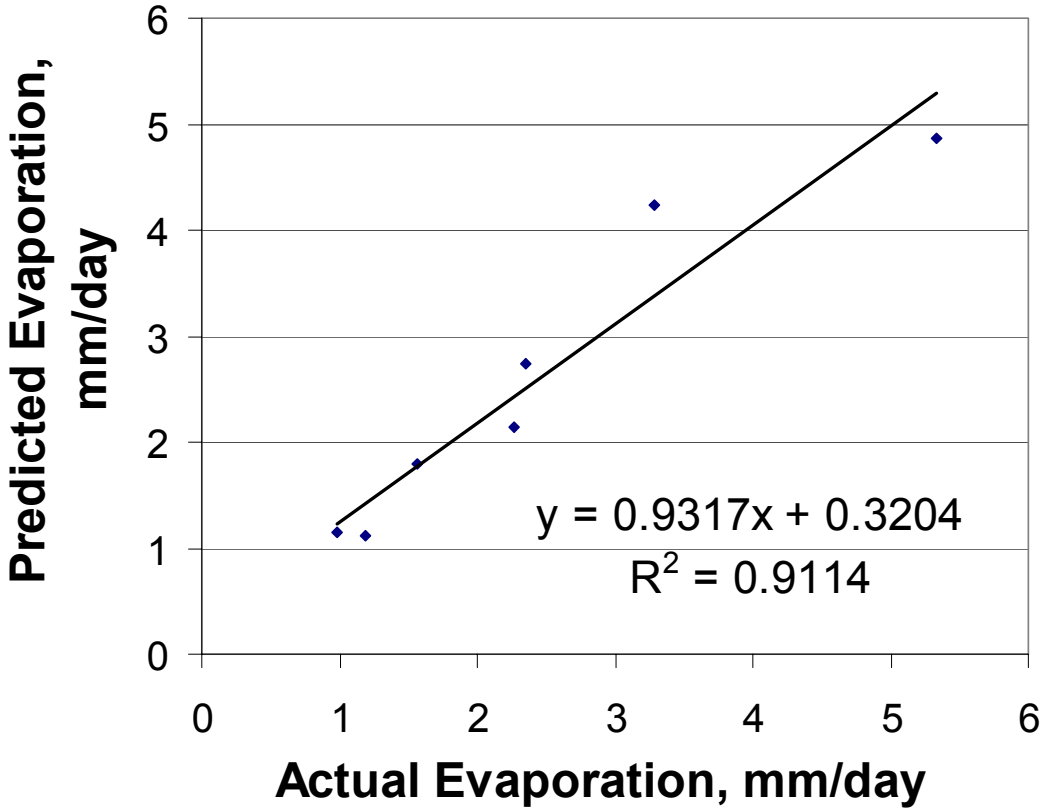

Figure 20. Predicted evaporation versus actual evaporation using data collected on seven days in early July.

Day of Year	measured evaporation (mm/d)	predicted evaporation (mm/d)	difference (mm/d)	difference (%)
184	2.27	2.14	-0.13	-5.95
185	1.56	1.79	0.23	12.85
186	1.19	1.12	-0.07	-5.98
187	0.98	1.16	0.18	15.31
189	3.29	4.24	0.95	22.33
192	5.33	4.86	-0.47	-9.66
193	2.35	2.75	0.40	14.40
		average difference	0.12	6.20
		standard deviation	0.45	12.90

Table 1. Comparison of measured or actual evaporation versus predicted evaporation for data collected on seven days in early July

5. Conclusions/Future Plans

It is planned to finish the data analysis for the data that has been collected up to this point. Once this is completed, an energy balance including all of the available data sets will be compiled into a single energy balance, allowing the identification of the data that is worth analyzing further in the evaporation estimation method described earlier. Possible reasons for excluding data from the previously mentioned analysis includes erratic winds, monsoonal rainfall, interspersed clouds

and full sun, which causes erratic fluctuations in net radiation, or equipment failure. The experiment on the rooftop will continue through the fall.

The simplified one-dimensional energy balance has proven to be an invaluable tool in determining a relationship between easily measured parameters in the field and bare-soil evaporation. The results that the data analysis is producing are showing that the sensible heat flux can be accurately calculated using the temperature gradient above the surface of the soil and wind speed. This also means that the latent heat flux can be accurately estimated using calculated values for net radiation, soil heat flux, and sensible heat flux. Although initiating the experiment on the roof top of Tapy Hall has proven useful in the debugging of the experiment, and the data that is being collected appears to be useful in determining a relationship for evaporation, it is felt that the experiment should be relocated to a more natural environment, where the conditions will more closely resemble field conditions. It is felt that the rooftop may introduce unwanted turbulence directly over the surface of the experiment box during windy conditions. It is difficult to measure the impact that this turbulence has on the energy balance, since wind speed is being measured at 1.8m above the surface. The experimental configuration is also creating strong edge effects, where the internal boundary layer located over the soil surface can not fully develop due to a lack of fetch, or distance where the surface conditions are constant (Schmugge and André, 1991). It is also felt that the current experimental configuration may have a strong 'oasis effect', where advective sensible heat contributes to the incoming energy to the system (Schmugge and André, 1991). This is particularly apparent after wetting the experiment, and has to do with the fact that the evaporating water from the soil surface cools the surface, while the surrounding dry rooftop remains relatively warmer (see figure 21). This temperature gradient makes it possible for additional energy, on top of the net radiation, to enter the system as advective sensible heat from the surrounding air. This advective heat flux

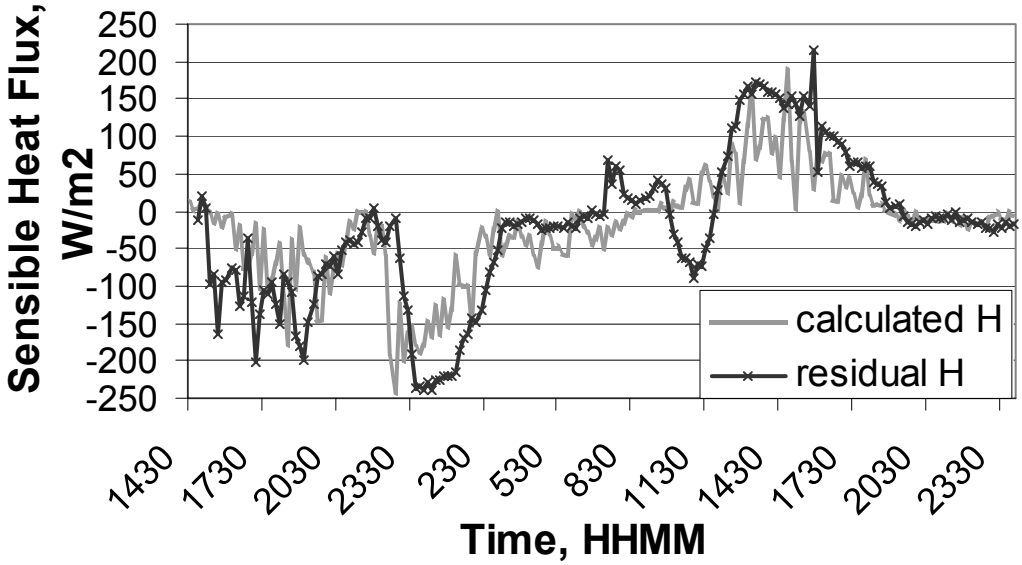

Figure 21. Calculated sensible heat flux and residual sensible heat flux for July 30 at 2:30 PM until midnight July 31, 2004, where the negative values of sensible heat flux denote advective sensible heat flux due to the wetting of the soil with approximately 1 cm of water at around 2:20 PM July 30, 2004.

has proven to be difficult to measure. It has been proposed to look into moving the experiment to the Atrisco site located along the west bank of the Río Grande, also known as the Bosque Lab. The experiment would be surrounded by bosque soil at this location, increasing the fetch, and reducing the effects of advective sensible heat.

Acknowledgements

- Bureau of Reclamation
- Principal Investigators: Dr. John Stormont & Dr. Julie Coonrod
- University of New Mexico
- National Science Foundation Research Assistants: Kelly A. Krellner, Pennsylvania State University & Daniel B. Wright, University of Michigan

References

Ben-Asher, J., Matthias, A.D. & Warrick, A.W. (1983): Assesment of evaporation from bare soil by infrared thermometry. *Soil Sci. Soc. Am. J.*, **47**: 185-191.

Campbell, G.S., & Norman, J.M. (1998): An introduction to environmental biophysics, second edition. Edward Brothers Inc., Ann Arbor, MI.

Fox, Michael J. (1968): A technique to determine evaporation from dry stream beds. *J. Appl. Meteorol.* **7**: 697-701.

Goff, J.A. & Gratch, S. (1946): Low-pressure properties of water from –160º to 212ºF. *Trans. Amer. Soc. Heat. Vent. Eng*., **51**: 125-164.

Hillel, Daniel (1998): Environmental Soil Physics. Academic Press, San Diego, CA.

Kustas, W.P., Choudhury, B.J., Moran, M.S., Reginato, R.J., Jackson, R.D., Gay, L.W. & Weaver, H.L. (1989): Determination of sensible heat flux over sparse canopy using thermal infrared data. *Agric. For. Meteorol.,* **44**: 197-216.

Matthias, A. D., Post, D.F., Accioly, L., Fimbres, A., Sano, E.E. & Batchily, A.K. (1999): Measurement of albedos for small areas of soil. *Soil Sci.* **164**: 293-301.

Moran, M.S., Kustas, W.P., Vidal, A., Stannard, D.I., Blanford, J.H. & Nichols, W.D. (1994): Use of ground-based remotely sensed data for surface energy balance evaluation of a semiarid rangeland. *Water Resour. Res.,* **30**: 1339-1349.

Qiu, G.Y., Yano, T. & Momii, K. (1998): An improved methodology to measure evaporation from bare soil based on comparison of surface temperatures with a dry soil. *J. Hydrol*., **210**: 93-105.

Rosenberg, Norman J. (1974): Microclimate: the biological environment. John Wiley and Sons, Inc. New York.

Schmugge, T.J., André, Jean-Claude (1991): Land surface evaporation: Measurement and Parameterization. Edward Brothers Inc., Ann Arbor, MI.

Weiss, A., (1977): Algorithms for the calculation of moist air properties on a hand calculator. Amer. Soc. Ag. Eng., **20**: 1133-1136.